USGS
science for a changing world

Coastal Circulation and Water-Column Properties in the National Park of American Samoa, February–July 2015

By Curt D. Storlazzi, Olivia M. Cheriton, Kurt J. Rosenberger, Joshua B. Logan, and Timothy B. Clark

Open-File Report 2017–1060

U.S. Department of the Interior
U.S. Geological Survey

Cover image. Underwater photograph showing corals in Tāfeu Cove, National Park of American Samoa, north shore of Tutuila Island, American Samoa.

U.S. Department of the Interior
RYAN K. ZINKE, Secretary

U.S. Geological Survey
William H. Werkheiser, Acting Director

U.S. Geological Survey, Reston, Virginia: 2017

Suggested citation:
Storlazzi, C.D., Cheriton, O.M., Rosenberger, K.J., Logan, J.B., and Clark, T.B., 2017, Coastal circulation and water-column properties in the National Park of American Samoa, February–July 2015: U.S. Geological Survey Open-File Report 2017–1060, 104 p., https://doi.org/10.3133/ofr20171060.

ISSN 2331-1258 (online)

Contents

Figures

Tables

Conversion Factors

U.S. customary units to International System of Units

Multiply	By	To obtain
	Length	
inch (in.)	2.54	centimeter (cm)
inch (in.)	25.4	millimeter (mm)
foot (ft)	0.3048	meter (m)
mile (mi)	1.609	kilometer (km)
mile, nautical (nmi)	1.852	kilometer (km)
yard (yd)	0.9144	meter (m)
	Area	
square foot (ft^2)	929.0	square centimeter (cm^2)
square foot (ft^2)	0.09290	square meter (m^2)
square inch (in^2)	6.452	square centimeter (cm^2)
section (640 acres or 1 square mile)	259.0	square hectometer (hm^2)
square mile (mi^2)	259.0	hectare (ha)
square mile (mi^2)	2.590	square kilometer (km^2)
	Volume	
ounce, fluid (fl. oz)	0.02957	liter (L)
gallon (gal)	0.003785	cubic meter (m^3)
gallon (gal)	3.785	cubic decimeter (dm^3)
million gallons (Mgal)	3,785	cubic meter (m^3)
cubic foot (ft^3)	0.02832	cubic meter (m^3)
cubic yard (yd^3)	0.7646	cubic meter (m^3)
cubic mile (mi^3)	4.168	cubic kilometer (km^3)
acre-foot (acre-ft)	1,233	cubic meter (m^3)
acre-foot (acre-ft)	0.001233	cubic hectometer (hm^3)
	Mass	
ounce, avoirdupois (oz)	28.35	gram (g)
pound, avoirdupois (lb)	0.4536	kilogram (kg)
ton, short (2,000 lb)	0.9072	metric ton (t)
ton, long (2,240 lb)	1.016	metric ton (t)

Temperature in degrees Celsius (°C) may be converted to degrees Fahrenheit (°F) as follows:

$$°F = (1.8 \times °C) + 32.$$

Temperature in degrees Fahrenheit (°F) may be converted to degrees Celsius (°C) as follows:

$$°C = (°F - 32) / 1.8.$$

Coastal Circulation and Water-Column Properties in the National Park of American Samoa, February–July 2015

By Curt D. Storlazzi,[1] Olivia M. Cheriton,[1] Kurt J. Rosenberger,[1] Joshua B. Logan,[1] and Timothy B. Clark[2]

Abstract

There is little information on the oceanography in the National Park of American Samoa (NPSA). The transport pathways for potentially harmful constituents of land-derived runoff, as well as larvae and other planktonic organisms, are driven by nearshore circulation patterns. To evaluate the processes affecting coral reef ecosystem health, it is first necessary to understand the oceanographic processes driving nearshore circulation, residence times, exposure rates, and transport pathways. Information on how the NPSA's natural resources may be affected by anthropogenic sources of pollution, sediment runoff, larval transport, or modifications to the marine protected areas is critical to NPSA resource managers for understanding and ultimately managing coastal and marine resources. To address this need, U.S. Geological Survey and U.S. National Park Service researchers conducted a collaborative study in 2015 to determine coastal circulation patterns and water-column properties along north-central Tutuila, American Samoa, in an area focused on NPSA's Tutuila Unit and its coral reef ecosystem. The continuous measurements of waves, currents, tides, and water-column properties from these instrument deployments over 150 days, coupled with available meteorological measurements of wind and rainfall, provide information on nearshore circulation and the variability in these hydrodynamic properties for NPSA's Tutuila Unit. In general, circulation was strongly driven by regional winds at longer (greater than day) timescales and by tides at shorter (less than day) timescales. Flows were primarily directed along shore, with current speeds faster offshore to the north and slower closer to shore, especially in embayments. Water-column properties exhibit strong seasonality coupled to the shift from non-trade wind season to trade wind season. During the non-trade wind season that was characterized by variable winds and larger waves in the NPSA, waters were warmer, slightly more saline, relatively less optically clear, and more stratified. When winds shifted to a more consistent trade wind pattern in the austral fall, the waters cooled and became less stratified because of decreased insolation. There are consistent spatial patterns in water column characteristics—Waters were warmer and less saline near the surface and closer to shore, especially in embayments, which tended to be more turbid, less clear, and characterized by higher chlorophyll than waters offshore. Water residence times were shorter farther offshore and longer closer to shore and in embayments, but varied spatially because of different forcing. Warmer, lower salinity, higher chlorophyll, and more turbid waters in embayments tend to reside in those locations for much greater durations, resulting in greater exposure of embayment ecosystems to those waters. This is in contrast with waters farther offshore, where the combination of shorter residence times and cooler, higher salinity water results in less exposure to land runoff. Understanding coastal circulation patterns and water-column properties in NPSA's waters along north-

[1]U.S. Geological Survey.
[2]U.S. National Park Service, National Park of American Samoa.

central Tutuila may help to better understand how meteorological and oceanographic processes, at the regional and local scale, affect coral reef health and sustainability in this region.

Introduction

Flow in and around coral reefs affects a number of physical, chemical, and biological processes that influence the health and sustainability of coral reef ecosystems. These processes range from the residence time of sediment and contaminants to nutrient uptake and larval retention and dispersal. As currents approach a coast they diverge to flow around reef structures, causing high horizontal and vertical shear. This can result in either rapid advection of material in localized jets, or retention of material in eddies that form in the lee of bathymetric features. The high complexity and diversity within and between reefs, in conjunction with past technical restrictions, has limited our understanding of the nature of flow and the resulting flux of physical, chemical, and biological material in these fragile ecosystems.

Sediment, nutrients, and other pollutants from a variety of land-based activities adversely impact many coral reef ecosystems in the United States and around the world. These pollutants are transported in surface water runoff, groundwater seepage, and atmospheric fallout into coastal waters, and there is compelling evidence that pollutant sources have increased globally as a result of human-induced changes to watersheds. On Tutuila in American Samoa, and elsewhere on United States islands in the Pacific and Caribbean, significant changes in drainage basins resulting from agriculture, feral grazing, fires, and urbanization have altered the character and volume of land-based pollution released to coral reefs. Runoff (and associated sediment, nutrients, and contaminants often absorbed to it) and deposition on coral reefs are recognized to potentially have significant effects on coral health. There is little information on the spatial variability of such processes at the National Park of American Samoa (NPSA). Nearshore circulation patterns drive transport pathways for potentially harmful runoff constituents, as well as larvae and other planktonic organisms. Thus, to evaluate the processes affecting reef health, it is first necessary to understand the oceanographic processes driving nearshore circulation, residence times, exposure rates, and transport pathways. Information on how NPSA natural resources may be impacted by anthropogenic sources of pollution, sediment runoff, larval transport, or modifications to the marine protected areas is critical to NPSA resource managers for understanding and ultimately managing coastal and marine resources.

Project Objectives

In 2015, U.S. Geological Survey (USGS) and U.S. National Park Service (NPS) researchers began a collaborative study to determine coastal circulation patterns and water-column properties along north-central Tutuila, in an area focused on NPSA's Tutuila Unit and its coral reef ecosystem. The continuous measurements of waves, currents, tides, and water-column properties (temperature and salinity) from these instrument deployments, coupled with available meteorological measurements of wind and rainfall, provide information on nearshore circulation and the variability in these hydrodynamic properties for NPSA's Tutuila Unit. These data will complement ongoing and future water quality efforts along north-central Tutuila and in NPSA that will provide baseline information to determine impacts resulting from management and (or) climate change.

The field experiment included collection of continuous oceanographic data, as well as spatially extensive shipboard surveys and drifter deployments in NPSA from February through July 2015. The goals of the experiment were to understand controls on flow patterns and water-column properties in the NPSA. To do this, the USGS and NPS set out to complete the following tasks:

A. Measure temporal variability in wave heights, wave periods, wave directions, current speeds, current directions, temperature, and salinity.
B. Measure spatial variability in current speeds, current directions, temperature, salinity, chlorophyll, turbidity, and light transmission.
C. Track pathways of Lagrangian ocean surface current drifters to understand transport pathways of buoyant surface material (coral larvae, debris, search-and rescue, and so on).
D. Compile modeled deep-water wave height, wave period, and wave direction data and locally measured wind speed, wind direction, rainfall, and barometric pressure.
E. Determine the influence of oceanographic and meteorological forcing on circulation patterns and water-column properties along north-central Tutuila and in NPSA waters.

Study Area

This study was located along the north-central coast of the island of Tutuila, American Samoa, in the Samoan Archipelago (fig. 1). Tutuila lies between 14.1° S. and 14.3° S. and between 170.5° W. and 170.9° W., and has an area of 199 square kilometers (km^2). It is the easternmost island in American Samoa and is the only populated U.S. territory in the Southern Hemisphere (National Park Service, 2015). The northern part of the island is dominated by forested volcanic coastline that rises more than 960 meters (m) above sea level and is punctuated by embayments. The south-central part of the island is dominated by a coastal plain covered in forest and grassland; this is also the most heavily populated area of the island. A coral reef surrounds most of the island, except where rivers discharge into bays. The territory of American Samoa is described by the Central Intelligence Agency (2015) as having a tropical marine climate, with an average annual rainfall of about 3,000 millimeters (mm). The wet season runs from November through April, with the remaining months constituting the dry season, and little annual variation in temperature. On longer time scales, rainfall is correlated with El Niño-Southern Oscillation (ENSO), with El Niños resulting in drier than average conditions. The greatest frequency of typhoons occurs from December through March; on average, one tropical cyclone passes within 500 kilometer (km) of American Samoa each year.

U.S. Army Corps of Engineers Wave Information Studies wind and wave hindcast data for Tutuila (Coastal and Hydraulic Laboratory, 2015) for the period from 1980 to 2011 show dominance of southeast trade winds on general wind and wave climate for the study area. Winds are predominantly out of the east-southeast at speeds of 5–7 meters per second (m/s); similarly, waves are primarily out of the east-southeast and have mean heights of about 1.5–1.9 m with mean periods of 8 seconds (s). Although the mean wind and wave climate is dominated by southeast trade winds, the influence of Southern Ocean swell during the austral winter as well as cyclones passing close to American Samoa during the austral summer is evident in the directional distribution of large waves. Whereas their frequency of occurrence is low, the direction of the fastest wind speeds is more uniformly distributed than the mean speeds dominated by the trade winds. The tides off Tutuila are described by the Center for Operational Oceanographic Products and Services (2015) as microtidal and semidiurnal, with two uneven high tides and low tides each day; the mean tidal range is 0.79 m and the diurnal tidal range is 0.85 m. Mean sea levels are generally highest (+0.011 m) during the austral winter in July and lowest (−0.013 m) during the austral summer in January.

The seafloor in NPSA's Tutuila unit was mapped by the National Oceanic and Atmospheric Administration (NOAA) National Centers for Coastal Ocean Science (2005) and was characterized as a limited aggregate reef with low to moderate (10 to <50 percent) coral coverage. Using their classifications, the habitat consists of a macroalgae-covered (10 to <50 percent) reef flat, coral-covered

(10 to <50 percent) fore reef, and turf-covered (10 to <50 percent) upper insular shelf with interspersed patches of unconsolidated sediment.

Operations

This section provides information about the personnel, equipment, and field operations used during the study. See tables 1–5 for complete listings of instrument and deployment information.

Equipment and Data Review

Acoustic Doppler Current Profilers—Five upward-looking acoustic Doppler current profilers (ADCP) were mounted on MiniPROBEs along the 20-m isobath in the NPSA, between Fagasa and Afono Bays (fig. 1). They were used to measure current velocity in 25 1.0-m vertical bins from 2.2 m above the seafloor up to the surface; these velocity profiles were collected for 120 s every 20 minutes (min). Four ADCPs (all but the one at the Central site) also recorded directional wave data, collecting 1,200 measurements at a rate of 2 hertz (Hz) every 2 hours (hr) to allow calculation of tides (m), significant wave height (m), dominant wave period (s), mean wave direction (°True), and directional spread (°). Sensor locations are listed in tables 1 and 2; complete sensor and processing information is listed in appendix 1.

Conductivity and Temperature Sensors—Eight conductivity and temperature (CT) sensors collected and averaged four samples every 3 min to measure water temperature (°C) and conductivity (Siemens per meter [S/m]), from which salinity in practical salinity units (PSU) was calculated. The rapid sampling rate was chosen to resolve higher frequency processes such as internal waves and ephemeral fronts. Five CT sensors were mounted on the MiniPROBEs, at the same depths as the ADCPs. The other three CT sensors, which were pumped, were installed about 2 m below the surface on the West, Central, and East moorings. The sensor locations are listed in table 1; complete sensor and processing information is listed in appendix 2.

Temperature Loggers—Twenty-four temperature loggers (TL) collected water temperature (°C) measurements every 2 min at different depths throughout the water column at the West, Central, and East moorings. Each mooring had eight TLs, with pairs placed at four different depths. The TL pairs were programmed such that the second logger began data collection a few hours before the first stopped (because of memory limitations). Data from these loggers provided information on vertical thermal structure and stratification in the NPSA study area. The TL depths and locations are listed in tables 1 and 2; and detailed logger and processing information is in appendix 2.

Vessel-mounted Acoustic Doppler Current Profiler Surveys—Surveys of water column current speeds and directions were conducted by using a downward-looking 600 kilohertz (kHz) vessel-mounted acoustic Doppler current profiler (VM-ADCP) mounted to the port side of the *R/V Moana*. The data were collected in 1-m bins from the surface down to the seabed every second and averaged every 30 s. Bottom tracking by the VM-ADCP and a boat-mounted differential global positional systems (GPS) (DGPS) were used to accurately determine the location, magnitude, and direction of currents throughout the water column. Data were collected along 9 primary and 4 secondary cross-shore transects between Fagasa and Vatia bays (fig. 1) each day from 18–21 February 2015 (2015 Year Days [YD] 49–52). The order of transects were reversed each day to minimize the influence of tidal stage and diurnal sea-breeze forcing. In addition to the ADCP measurements, measurements of wind speed and direction were obtained on the survey vessel at 1-s intervals with an ultrasonic anemometer mounted above the cabin, about 3 m above the sea surface. The VM-ADCP transect locations are listed in table 3; and instrument and processing information is in appendix 1.

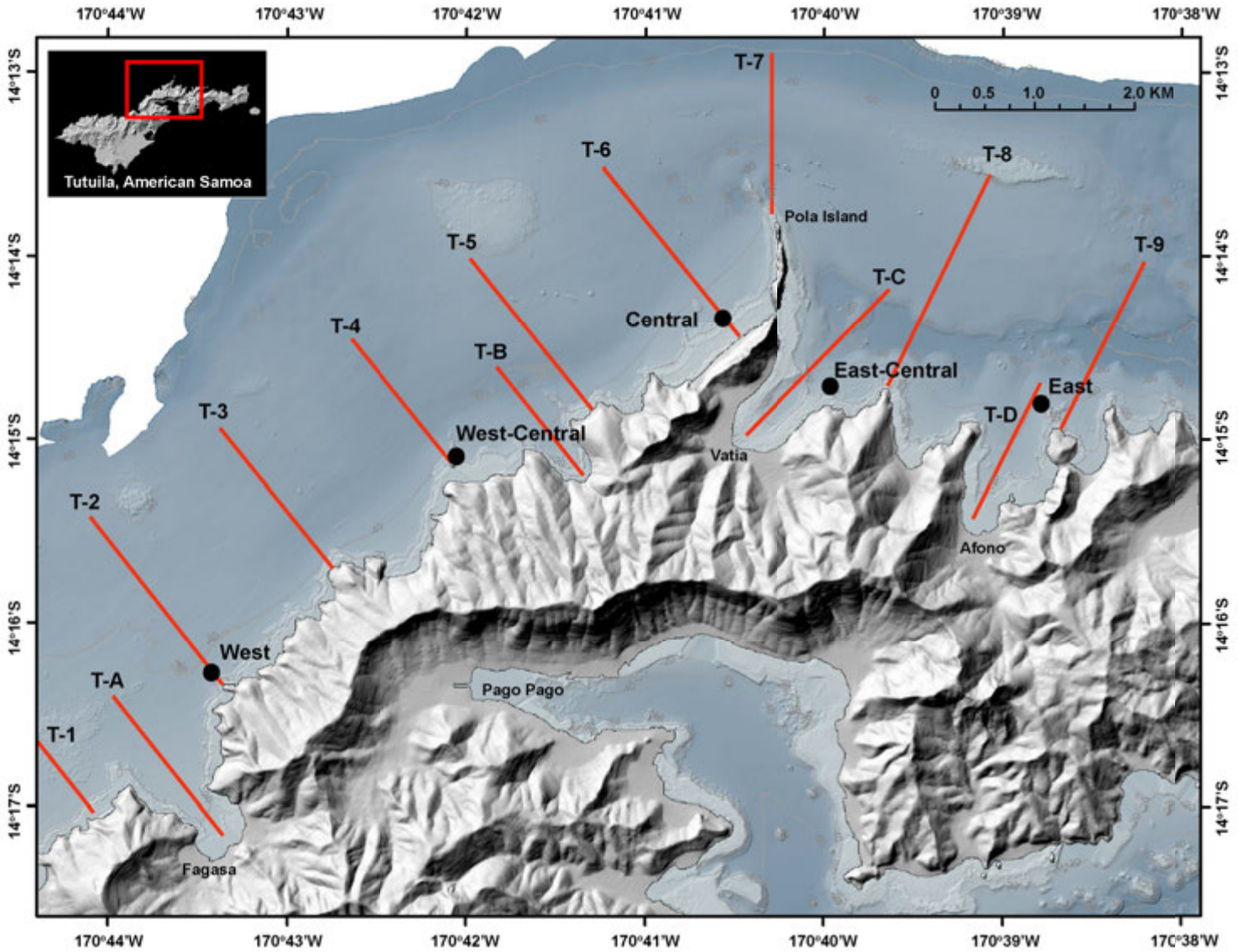

Figure 1. Map of American Samoa and locations of measurements made in the National Park of American Samoa (NPSA) coastal region. Black dots denote locations of time-series bottom-mounted instrument packages and moorings. Red lines denote transects along which vessel-mounted acoustic Doppler current profiler (VM-ADCP) data were collected; water column profiler measurements were generally made at the beginning and end of each VM-ADCP transect. The 20-meter isobaths are shown for reference.

Table 1. Instrument package location information.

Site name	Latitude (decimal degrees)	Longitude (decimal degrees)
West mooring	−14.27146	−170.72364
West MiniPROBE	−14.27146	−170.72352
West-Central MiniPROBE	−14.25071	−170.70124
Central mooring	−14.23907	−170.67587
Central MiniPROBE	−14.23906	−170.67573
East-Central MiniPROBE	−14.24540	−170.66578
East mooring	−14.24695	−170.64598
East MiniPROBE	−14.24697	−170.64623

Table 2. Instrument package sensors.

[kHz, kilohertz]

Site name	Depth (in meters)	Sensors
West mooring	2	Seabird SBE-37SMP Microcat conductivity-temperature sensor
	7	Onset HOBO temperature logger
	12	Onset HOBO temperature logger
	18	Onset HOBO temperature logger
	23	Onset HOBO temperature logger
West MiniPROBE	18	RDI 600 kHz Monitor acoustic Doppler current profiler
	18	Seabird SBE-37SM Microcat conductivity-temperature sensor
West-Central MiniPROBE	20	RDI 600 kHz Monitor acoustic Doppler current profiler
	20	Seabird SBE-37SM Microcat conductivity-temperature sensor
Central mooring	2	Seabird SBE-37SMP Microcat conductivity-temperature sensor
	6	Onset HOBO temperature logger
	12	Onset HOBO temperature logger
	17	Onset HOBO temperature logger
	23	Onset HOBO temperature logger
Central MiniPROBE	22	RDI 600 kHz Monitor acoustic Doppler current profiler
	22	Seabird SBE-37SM Microcat conductivity-temperature sensor
East-Central MiniPROBE	20	RDI 600 kHz Monitor acoustic Doppler current profiler
	20	Seabird SBE-37SM Microcat conductivity-temperature sensor
East mooring	4	Seabird SBE-37SMP Microcat conductivity-temperature sensor
	7	Onset HOBO temperature logger
	13	Onset HOBO temperature logger
	19	Onset HOBO temperature logger
	24	Onset HOBO temperature logger
East MiniPROBE	22	RDI 600 kHz Monitor acoustic Doppler current profiler
	22	Seabird SBE-37SM Microcat conductivity-temperature sensor

Table 3. Vessel-mounted acoustic Doppler current profiler (VM-ADCP) transects.

Transect	Location	Starting latitude (decimal degrees)	Starting longitude (decimal degrees)	End latitude (decimal degrees)	End longitude (decimal degrees)
T1	Outside-West	−14.2833	−170.7344	−14.2664	−170.749
TA	Fagasa	−14.2857	−170.7228	−14.2737	−170.7328
T2	West	−14.2719	−170.7231	−14.2566	−170.7351
T3	--	−14.2606	−170.7125	−14.2488	−170.7232
T4	West-Central	−14.2530	−170.7005	−14.2388	−170.7106
TB	Tafeu	−14.2527	−170.6896	−14.2435	−170.6972
T5	--	−14.2466	−170.6886	−14.2331	−170.6998
T6	Central	−14.2394	−170.6758	−14.2238	−170.6862
T7	Pola Island	−14.2287	−170.6715	−14.2146	−170.6715
TC	Vatia	−14.2493	−170.6739	−14.2360	−170.6605
T8	East-Central	−14.2449	−170.6608	−14.2258	−170.6511
TD	Afono	−14.2568	−170.6524	−14.2448	−170.6465
T9	East	−14.2484	−170.6444	−14.2338	−170.6369

Table 4. Water column profiler (WCP) cast location and depth information.
[VM-ADCP, vessel-mounted acoustic Doppler current profiler]

Cast #	Location by VM-ADCP transect	Latitude (decimal degrees)	Longitude (decimal degrees)	Approx. depth (in meters)
1	TA inshore Fagasa	−14.2857	−170.7228	15
2	T1 inshore	−14.2833	−170.7344	11
3	T1 offshore	−14.2664	−170.7490	41
4	T2 inshore	−14.2719	−170.7231	30
5	T2 offshore	−14.2566	−170.7351	42
6	T3 inshore	−14.2606	−170.7125	22
7	T3 offshore	−14.2488	−170.7232	39
8	T4 inshore	−14.253	−170.7005	14
9	T4 offshore	−14.2388	−170.7106	39
10	TB inshore Tafeu	−14.2527	−170.6896	9
11	T5 inshore	−14.2466	−170.6886	28
12	T5 offshore	−14.2331	−170.6998	40
13	T6 inshore	−14.2394	−170.6758	7
14	T6 offshore	−14.2238	−170.6862	40
15	T7 inshore	−14.2287	−170.6715	19
16	T7 offshore	−14.2146	−170.6715	43
17	TC inshore Vatia	−14.2493	−170.6739	7
18	T8 inshore	−14.2449	−170.6608	19
19	T8 offshore	−14.2258	−170.6511	37
20	T9 inshore	−14.2484	−170.6444	10
21	T9 offshore	−14.2338	−170.6369	43
22	TD inshore Afono	−14.2568	−170.6524	9

Table 5. Drifter deployment information.

[°, degrees; dd, day; hh, hour; m, month; mm, minute; SST, Samoa Standard Time; yyyy, year]

Deploy date (m/dd/yyyy) (Year Day)	Drifter	Deploy time (SST)	Deploy location (°)	Recovery date (m/dd/yyyy)	Recover time (SST)	Recovery location (°)	Total time (hh:mm)
4/14/2015 (104)	10	10:05	−14.28550 −170.72359	4/15/2015	10:24	−14.24548 −170.71095	24:19
4/14/2015 (104)	4	10:19	−14.25893 −170.70638	4/15/2015	10:31	−14.23315 −170.69267	24:12
4/14/2015 (104)	3	10:34	−14.25188 −170.65070	4/15/2015	10:43	ONSHORE	24:09
4/14/2015 (104)	1	10:41	−14.24582 −170.66965	4/15/2015	11:22	−14.20147 −170.67960	24:41
5/26/2015 (146)	10	10:56	−14.28584 −170.72363	5/27/2015	12:16	−14.19030 −170.69061	25:20
5/26/2015 (146)	3	11:10	−14.26104 −170.70586	5/27/2015	11:36	−14.24631 −170.69519	24:26
5/26/2015 (146)	4	11:18	−14.25231 −170.69006	5/27/2015	--	ONSHORE	
5/26/2015 (146)	1	11:30	−14.23789 −170.67429	5/27/2015	12:29	−14.16590 −170.67383	24:59
5/28/2015 (148)	10	11:01	−14.28482 −170.72388	5/29/2015	9:05	−14.24894 −170.71375	22:04
5/28/2015 (148)	3	11:13	−14.25962 −170.70447	5/29/2015	9:47	−14.19000 −170.65701	22:34
5/28/2015 (148)	1	11:22	−14.25259 −170.68991	5/29/2015	10:02	−14.17521 −170.67580	22:49
6/2/2015 (153)	4	10:20	−14.28548 −170.72389	6/3/2015	10:10	−14.24443 −170.68117	23:50
6/2/2015 (153)	10	10:25	−14.25981 −170.70537	6/3/2015	--	ONSHORE	
6/2/2015 (153)	1	10:34	−14.25212 −170.68944	6/3/2015	10:33	−14.21122 −170.73808	23:35
6/2/2015 (153)	3	10:46	−14.24813 −170.67180	6/3/2015	11:27	−14.20759 −170.70377	24:41
6/8/2015 (159)	3	11:16	−14.28572 −170.72362	6/9/2015	12:38	−14.23190 −170.71083	25:22
6/8/2015 (159)	10	11:32	−14.26015 −170.70490	6/9/2015	12:24	−14.25248 −170.70218	24:56
6/8/2015 (159)	1	11:39	−14.25243 −170.68971	6/9/2015	13:00	−14.16369 −170.65782	25:22
6/9/2015 (160)	1	13:22	−14.24684 −170.67067	6/10/2015	12:37	−14.20247 −170.70264	23:15

Deploy date (m/dd/yyyy) (Year Day)	Drifter	Deploy time (SST)	Deploy location (°)	Recovery date (m/dd/yyyy)	Recover time (SST)	Recovery location (°)	Total time (hh:mm)
6/9/2015 (160)	3	13:32	−14.25218 −170.69025	6/10/2015	13:00	−14.17717 −170.68108	23:38
6/9/2015 (160)	10	13:36	−14.26042 −170.70496	6/10/2015	12:17	−14.25251 −170.70702	22:41
6/9/2015 (160)	4	13:43	−14.28379 −170.72426	6/10/2015	12:01	−14.25008 −170.74982	22:42
6/10/2015 (161)	1	14:04	−14.28471 −170.70612	6/11/2015	11:45	−14.27226 −170.72331	21:41
6/10/2015 (161)	4	13:55	−14.26089 −170.70612	6/11/2015	11:32	−14.26297 −170.70658	21:37
6/10/2015 (161)	10	13:48	−14.25254 −170.68997	6/11/2015	11:12	−14.21360 −170.67670	21:24
6/16/2015 (167)	1	10:59	−14.25983 −170.70515	6/17/2015	15:46	−14.20919 −170.64552	28:47
6/16/2015 (167)	4	10:47	−14.28551 −170.72337	6/17/2015	16:01	−14.22573 −170.59648	29:14
6/22/2015 (173)	10	11:11	−14.28380 −170.72473	6/23/2015	10:29	−14.56292 −170.72203	23:18
6/22/2015 (173)	4	11:16	−14.25955 −170.70445	6/23/2015	10:45	−14.24607 −170.68658	23:29
7/6/2015 (187)	10	12:00	−14.28535 −170.72365	7/7/2015	15:40	−14.27429 −170.77713	27:40
7/6/2015 (187)	1	14:40	−14.25292 −170.65128	7/7/2015	13:19	−14.23453 −170.70759	22:39
7/6/2015 (187)	4	14:55	−14.24638 −170.66989	7/7/2015	12:55	−14.24365 −170.69180	22:00
7/6/2015 (187)	3	15:11	−14.25976 −170.70493	7/7/2015	12:23	−14.24994 −170.69839	21:12
7/7/2015 (188)	3	12:30	−14.25190 −170.69055	7/8/2015	14:18	−14.26318 −170.67001	25:48
7/7/2015 (188)	4	14:20	−14.24675 −170.67012	7/8/2015	-	ONSHORE	
7/7/2015 (188)	10	16:07	−14.28536 −170.72386	7/8/2015	14:37	−14.27779 −170.77859	22:30
7/7/2015 (188)	1	15:38	−14.25903 −170.70477	7/8/2015	14:53	−14.27378 −170.72795	23:15

Water Column Profiler—Surveys of water-column properties (WCP) were made by using a water column conductivity/temperature/depth profiler with optical backscatter, transmissometer, and chlorophyll (fluorescence) sensors sampling at 4 Hz to collect vertical profiles of water temperature (°C), salinity (PSU), light transmission (m), optical backscatter (NTU), and fluorescence (milligrams per cubic meter [mg/m^3]) in 0.25-m vertical bins. The cast location and depth information is listed in table 4; complete sensor information and individual cast acquisition logs are listed in appendixes 3 and 4. The profile surveys were conducted between Fagasa and Afono Bays and were repeated during the two different seasons (February/wet summer and July/dry winter).

Lagrangian Surface Current Drifters—Satellite-tracked, DGPS-equipped, Lagrangian Surface Current Drifters (LSCDs) were deployed over 12 weeks between 14 April and 7 July 2015 (YD 104–190), at various locations within and offshore of the NPSA study area to track surface currents. The LSCDs internally logged their location every 1 min and transmitted their positions to satellites every 5 min. The LSCDs were drogued at a depth centered around 1.0 m below sea level. The LSCDs were deployed by way of the *M/V Poge* and recovered the same day or the following day by the *M/V Poge*, refurbished, and prepared for release at a future date. Details of each drifter deployment including locations, times, distances, and velocities are shown in table 5.

Miscellaneous Data Sources—Navigation equipment for deployment, recovery, and survey operations included hand-held Wide Area Augmentation System (WAAS)-equipped GPS units and a computer with positioning and mapping software. The positioning and mapping software enabled real-time GPS position data to be combined with images of previously collected high-resolution shaded-relief bathymetry, 5-m isobaths, and aerial photographs of terrestrial parts of maps. Meteorological data from the American Samoa Observatory (SMO) weather station were obtained from the NOAA Earth System Research Laboratory (ESRL; http://www.esrl.noaa.gov/).

Research Platform and Field Operations

Instrument deployments and recoveries were conducted by using the *R/V Moana* and the *R/V Poge*. Vessel operations, including mobilization and demobilization, were based out of Pago Pago Harbor and Fagasa Bay. The *R/V Moana* starboard quarterdeck was adapted for instrument deployment and recovery operations, which included the use of a hand winch and an overhead davit. The instruments were deployed by attaching a removable bridle to the instrument package with a connecting line through the davit and down to the winch. The instruments were lowered to within a few meters of the seafloor, where scuba divers attached a lift bag and detached the lifting line. The divers then moved the instrument package into position for anchoring. Vessel-mounted ADCP surveys were performed using the *R/V Moana*. The water column profiler casts were conducted by hand from the *R/V Moana*. The driver's station was outfitted with a laptop computer and GPS-enabled navigation system to provide the vessel captain with a graphic display of position information, speed, heading, and distance to the next location.

Data Acquisition and Quality

Data were acquired for 150 days during the period from 14 February through 14 July 2015 (YD 45–195). More than 3,231,000 temporal data points were recorded by the ADCPs, CTs, and TLs; more than 48,000 data points were recorded by the WCP. More than 950,000 and 50,000 spatial data points were recorded by the VM-ADCP and vessel-mounted wind sensor, respectively. Raw data were archived at https://doi.org/10.5066/F7RN362H and copies of the data were post-processed for analysis.

Mooring and water column profiler data generally appear to be of high quality. The ADCP on the West MiniPROBE stopped collecting data early, on 20 June 2015 (YD 171), 24 days before the end of the experiment. The near-surface CT sensors on the Central and East moorings failed to collect valid salinity data, most likely because of thermal stress on the instruments during storage at an NPS facility in Hawaii.

To determine the contributions of different forcing mechanisms to flow patterns, current data were constrained to periods when just the forcing mechanism of interest was dominant. For example, to identify the influence of winds (large waves) on flow patterns, a time period was identified without concurrent large waves (strong winds). To identify the contribution of tides to circulation patterns, the entire record was 10–28-hr band-pass filtered.

Results

Temporal Patterns

This section reviews data collected by the instruments and addresses the significance of the findings to better understand oceanographic conditions in the study area.

Oceanographic and Atmospheric Forcing

The study period, from February through July 2015, spanned the transition from the wet, rainy, non-trade wind season that normally runs from October through March to the trade wind season that normally runs from April through September. Winds recorded at the American Samoa Observatory on Cape Matatula on the northeastern tip of Tutuila show the transition from the non-trade wind to the trade wind seasons, which occurred in the austral fall between late March and late April 2015 (about YD 90–120; fig. 2). For the first 45 days of the study (YD 45–90) leading up to this transition, wind speeds were weak and directions were relatively variable. The transition to the trade wind season was marked by the start of stronger winds that were consistently out of the southeast. The strongest rainfall event occurred on 22 Apr 2015 (YD 112), with hourly precipitation rates reaching 43 millimeters per hour (mm/hr). Otherwise, rainfall remained relatively consistent throughout the study period, and only began to decline in late June (about YD 170). For the entire record, hourly precipitation had a mean ±1 standard deviation of 0.27±1.54 mm (table 6). Air temperature exhibited large diurnal fluctuations. Hourly averaged air temperature ranged from a low of 23.1 to a high of 34.1 °C, with a mean temperature ±1 standard deviation of 27.5±1.7 °C. In the trade wind season, the mean daily air temperature decreased slightly, and the diurnal range decreased as well (fig. 2).

Table 6. Meteorological statistics.

[All values were calculated for 2015 Year Days 45–195; wind direction is “coming from.” °, degrees; °C, degrees Celsius; mb, millibars; m/s, meters per second; mm/hr, millimeters per hour; SD, standard deviation]

Site name	Mean ±1 SD	Minimum	Maximum
Sea level barometric pressure (mb)	1,001.5 ± 2.2	994.9	1,007.2
Air temperature (°C)	27.5 ± 1.7	23.1	34.1
Precipitation (mm/hr)	0.27 ± 1.54	0	42.80
Wind speed (m/s)	6.04 ± 3.18	0	16.18
Wind direction (°)	133 ± 57	0	360

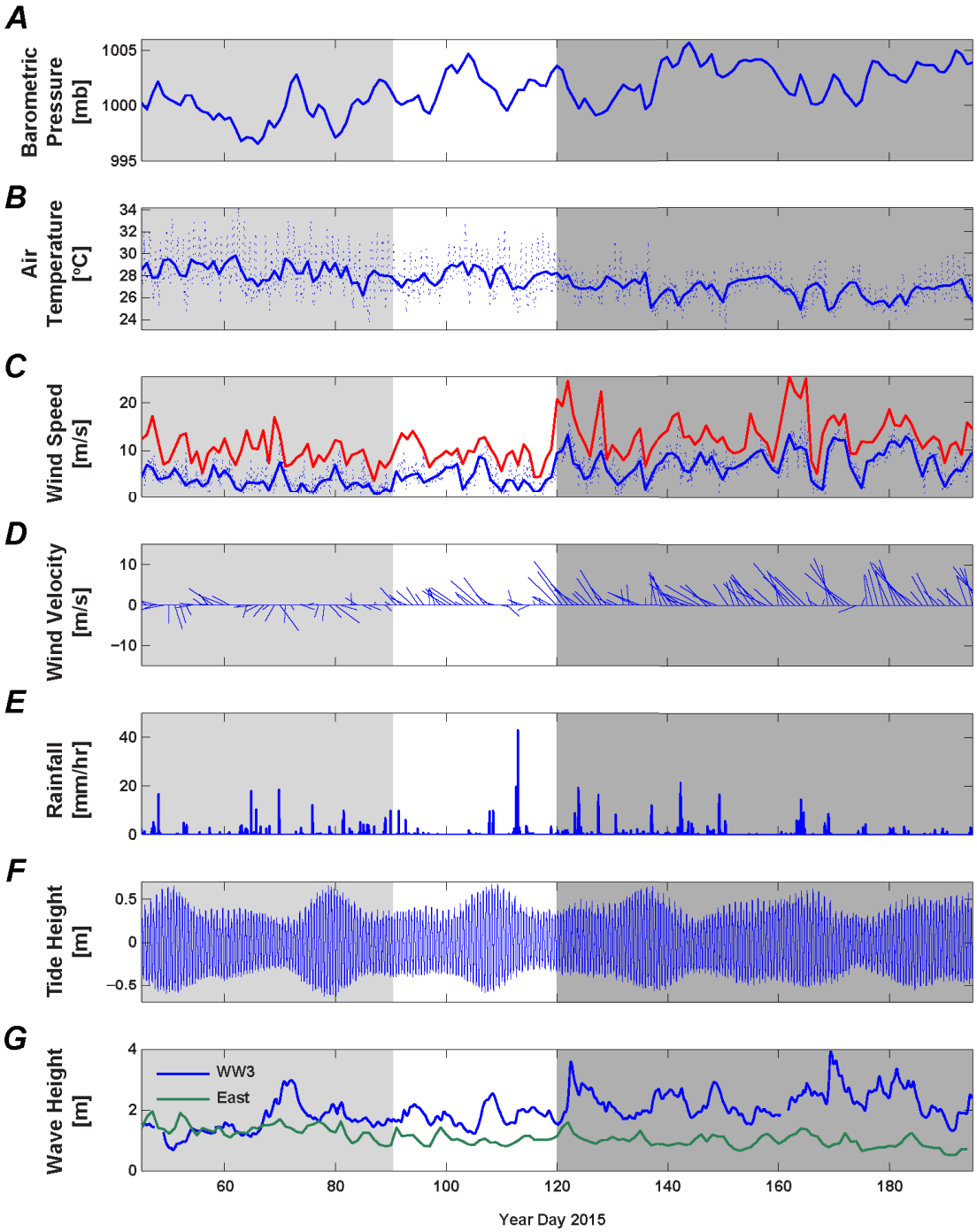

Figure 2. Time-series plots of meteorological and oceanographic forcing data collected during the study period. *A*, Barometric pressure, in millibars (mbar), from the Cape Matatula American Samoa Observatory (SMO). *B*, Air temperature, in degrees Celsius (°C), with hourly (dashed blue line) and daily-averaged (solid blue line) temperature from the SMO. *C*, Wind speed, in meters per second (m/s), with hourly (dashed blue line), daily-averaged (solid blue line), and maximum daily (solid red line) speeds from the SMO. *D*, Daily-averaged wind velocity, with direction indicating heading in degrees clockwise from true north, and speed in meters per second (m/s) from the SMO. *E*, Rainfall in millimeters per hour (mm/hr), from the SMO. *F*, Tidal height, in meters (m) relative to mean sea level, from the Central site. *G*, Daily-averaged significant wave height, in meters (m), from the WaveWatchIII (WW3) model (blue line) and the East site (green line).

Tides

The study period encompassed five complete spring-neap tidal cycles. Tides near NPSA are predominantly semidiurnal with two nearly even high tides and two nearly even low tides per day; thus, the tides change at a frequency of about 6 hr (fig. 2). The mean daily tidal range was about 0.83 m, whereas the minimum and maximum daily tidal ranges were 0.42 and 1.20 m during neap and spring tides, respectively. The highest high tide was +0.71 m and the lowest low tide was −0.67 m.

In addition to the surface tide, a strong internal tidal signal (for example, Storlazzi and others, 2003; 2013) was present in water column current velocity and temperature measurements. An internal tide is generated when surface tides drive flows over sloping bottom bathymetry, causing a vertical displacement of internal water column structure that occurs at tidal frequencies. The internal tidal signal within the NPSA study site is highly coherent with the surface tide (coherence=0.95 at the semidiurnal frequency, 12.5-hr period); the corresponding phase lag indicates that the internal tidal signal lags the surface tide by about 3 hr (for example, appendix 5).

Winds

Hourly wind speeds at the American Samoa Observatory ranged from 0.00 to 16.19 m/s, with a mean speed ±1 standard deviation of 6.04±3.18 m/s (fig. 2, table 6). Winds at this site did not exhibit diurnal patterns, indicating the predominant role of regional winds and minimal sea-breeze effects. Up until the shift to the trade wind season (using YD 95 as transition point), winds were variable, with a mean wind velocity of 4.21 m/s coming out of the southwest (243° from true North). During the trade wind season (about YD 95–195) the mean wind velocity was 7 m/s out of the southeast (143° from true north). The strongest winds occurred during the latter half of the study (May through July 2015, about YD 120–195) and were driven by sustained southeasterly trade winds.

Waves

Waves that affected the NPSA study area during the course of the experiment are shown in figs. 2–4, and statistics for each site are listed in table 7. Wave heights across all study sites ranged from less than a 1 to 2.6 m, with peak wave periods ranging from about 4 to 18 s. Waves approached the NPSA study area out of the northwest to northeast, in predominantly shore-normal directions (mean direction ranged from −17 to 21° from true north). In general, the East site consistently experienced the largest wave heights, and the West-Central site the smallest. Across all sites the wave patterns exhibited a seasonal shift from the non-trade wind to trade wind season. During the non-trade wind season, wave heights and periods were relatively consistent in magnitude across all sites, though wave heights tended to be greatest at the West, West-Central, and East sites. After the shift to the trade wind season, particularly after about mid-May 2015 (about YD 140), wave heights at the West and West-Central sites lessened by a factor of two, and peak wave periods were longer. In addition, the wave directional spread increased during the trade wind season, with more waves coming from the east, particularly at the West, West-Central, and East sites. Regional wave patterns, as determined by the WW3 model, were primarily directed out of the southeast to southwest. Because the NPSA study area is sheltered from wave patterns out of the south, nearshore wave patterns observed at the NPSA study sites were distinct from offshore, regional wave characteristics.

Table 7. Wave statistics.

[Wave direction is "coming from." °, degrees; m, meters; s, seconds; SD, standard deviation]

Site name	Parameter	Mean ±1 SD	Minimum	Maximum
West MiniPROBE	Height (m)	0.97 ± 0.32	0.37	2.30
	Period (s)	11.4 ± 2.6	5.0	19.3
	Direction (°)	343 ± 34	0	359
West-Central MiniPROBE	Height (m)	0.69 ± 0.27	0.22	2.11
	Period (s)	11.0 ± 2.3	6.1	18.0
	Direction (°)	342 ± 34	0	359
East-Central MiniPROBE	Height (m)	0.94 ± 0.22	0.36	1.90
	Period (s)	9.3 ± 2.0	4.3	16.8
	Direction (°)	29 ±16	0	359
East MiniPROBE	Height (m)	1.10 ± 0.31	0.00	2.60
	Period (s)	9.9 ± 2.4	4.4	18.0
	Direction (°)	21 ± 35	0	359

Currents

Mean surface and near-bed current velocities for each MiniPROBE site are listed in table 8. Current velocity magnitudes in the NPSA study area showed high spatial variability, with the fastest currents at the West-Central site and slowest at the East-Central site. Currents were primarily tidally driven, showing little seasonal variation in speed or direction. In addition, flow direction appeared to be strongly controlled by local shoreline curvature and bathymetric steepness. In general, flows were along isobath, with flood (rising) tides generally characterized by weak flows to the west, and ebb (falling) tides with strong flows to the east and northeast (figs. 5–6). During tidal ebb phases, near-surface currents were considerably stronger than those closer to the seabed. At West-Central and East sites there was a high amount of shear in the water column, with near-bed and near-surface currents often oppositely directed (appendix 6). In addition, some sites exhibited remarkably vigorous vertical velocities. The West-Central and East sites regularly experienced upwards and downwards vertical velocities exceeding 5 centimeters per second (cm/s), whereas the West, Central, and Central-East sites had relatively weak, net downward velocities. Shear and vertical velocity patterns suggest a high amount of bathymetric steering, likely resulting from the steep seabed slope where the instruments were deployed.

Because tides were the primary control of current velocities, there was little seasonal variation of current patterns between the large wave/non-trade wind and the strong trade wind season (figs. 7–8). Under strong trade wind forcing, the mean current direction at the West, West-Central, and Central sites was north-to-northeastward at the surface and north-to-northwestward at the seabed. East of Pola Island at the East-Central and East sites, trade wind-driven currents were weak and toward the east. Mean current patterns during large waves and weaker winds show little difference from the strong trade wind season, with the exception of the Central site, which has southward-directed (as opposed to northward) flow during larger waves and weaker winds.

The West-Central site experienced the greatest current speeds, with 35 percent of near-surface currents exceeding 0.3 m/s, and 4 percent exceeding 0.5 m/s (figs. 5–6, table 8, appendix 6). These strong currents were primarily directed to the northeast. Currents were also moderately strong at the West and the East sites, with 25 and 10 percent, respectively, of measured surface currents exceeding

0.2 m/s. Flows were weakest at the Central and East-Central sites, with only 3 percent of currents greater than 0.2 m/s at Central and 8 percent of currents greater than 0.1 m/s at the East-Central site.

Table 8. Mean surface (low depths) and near-bed (high depths) current velocities for each MiniPROBE site.
[Current direction is "going toward"; minimum speed recorded at each site was 0.00 meters per second (m/s); ° True, degrees from true north; m, meters; SD, standard deviation]

Site name	Depth (m)	Mean speed ±1 SD (m/s)	Mean direction (° True)	Maximum speed (m/s)
West MiniPROBE	4.3	0.15 ± 0.09	19°	0.50
	16.3	0.12 ± 0.07	39°	0.42
West-Central MiniPROBE	7.6	0.24 ± 0.14	207°	0.76
	17.6	0.11 ± 0.09	24°	0.61
Central MiniPROBE	3.2	0.10 ± 0.06	211°	0.46
	19.2	0.06 ± 0.03	77°	0.30
East-Central MiniPROBE	2.1	0.05 ± 0.03	38°	0.22
	17.1	0.04 ± 0.02	96°	0.19
East MiniPROBE	4.3	0.11 ± 0.07	259°	0.48
	16.3	0.06 ± 0.04	231°	0.31

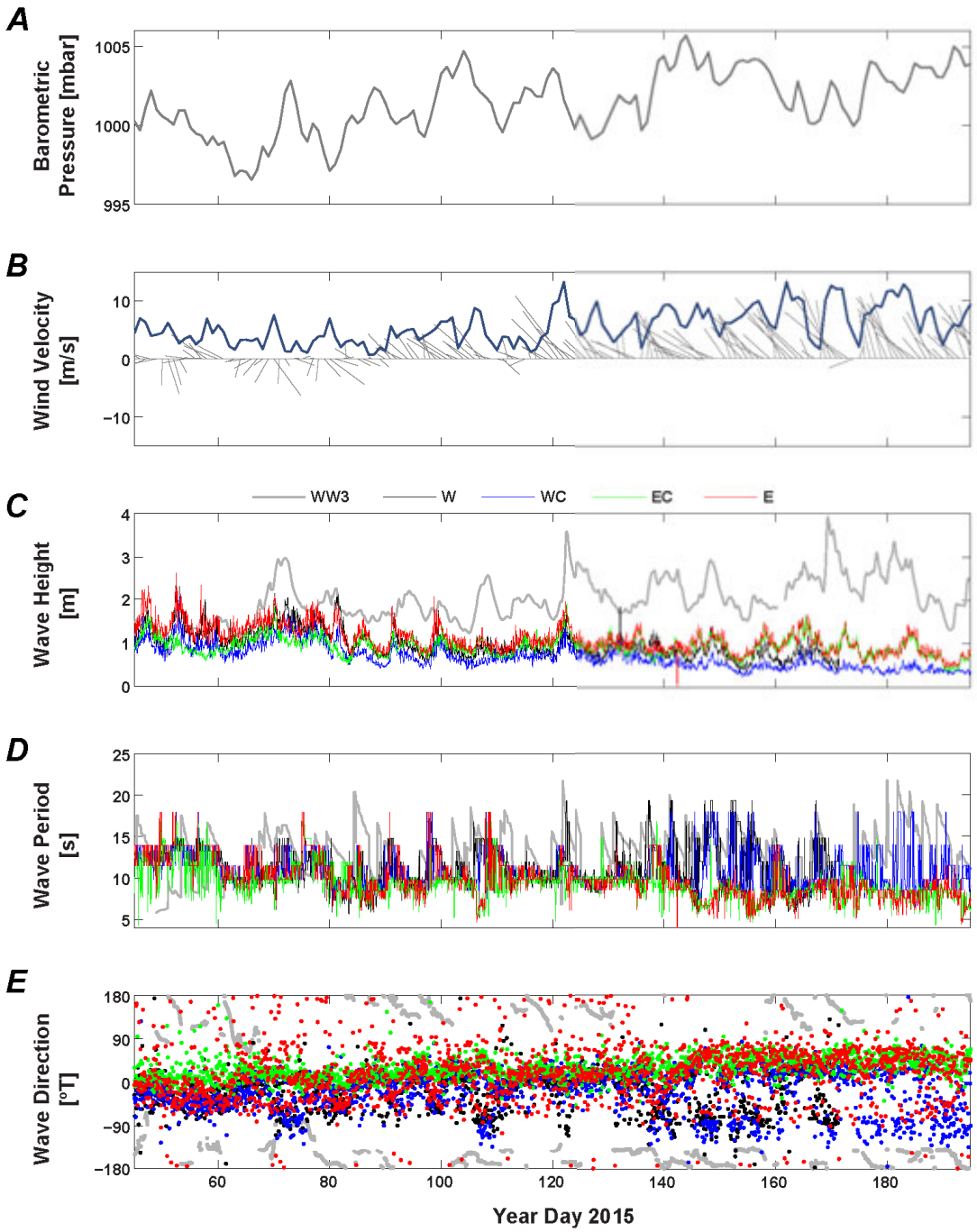

Figure 3. Time-series plots of daily averaged meteorological forcing from the Cape Matatula American Samoa Observatory (SMO) and wave parameters. *A*, Barometric pressure, in millibars (mbar), from the SMO. *B*, Wind velocity, with direction shown as heading in degrees clockwise from true north (gray lines), and speed (black line) in meters per second (m/s), from the SMO. *C*, Significant wave height, in meters (m), from the WaveWatchIII (WW3) model (gray line) and the mooring sites (colored lines). *D*, Peak wave period, in seconds (s), from the WaveWatchIII (WW3) model (gray line) and the mooring sites (colored lines). *E*, Peak wave direction, in degrees from true North (°T), from the WaveWatchIII (WW3) model (gray points) and the mooring sites (colored points). Colors for mooring sites in figures *C*–*E* are West site (black), West-Central site (blue), East-Central site (green), and East site (red).

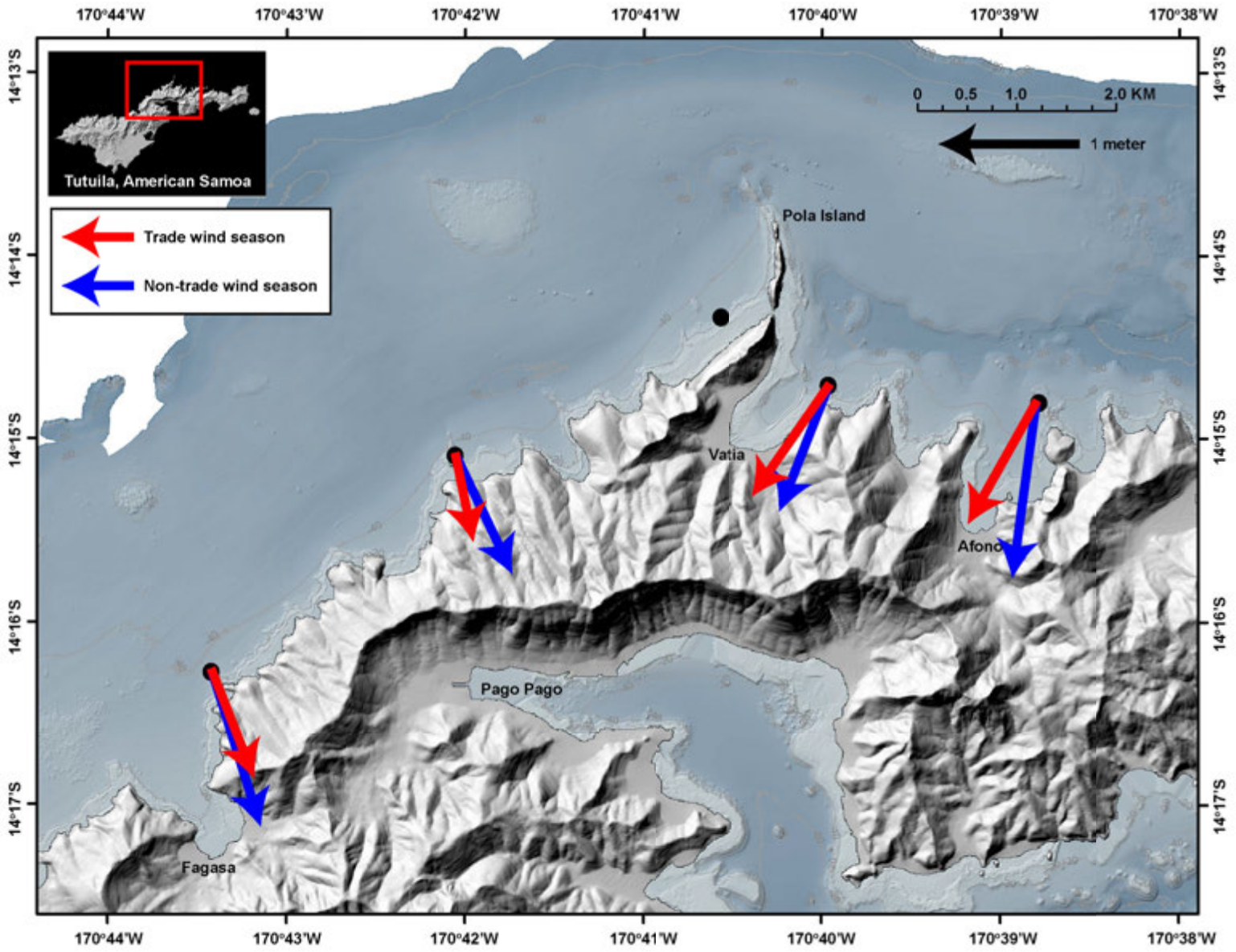

Figure 4. Map showing mean wave direction as heading ("going to") at each mooring site, in degrees from true north, and magnitude of significant wave height, in meters (m), from trade wind period (red arrows) and non-trade wind period (blue arrows).

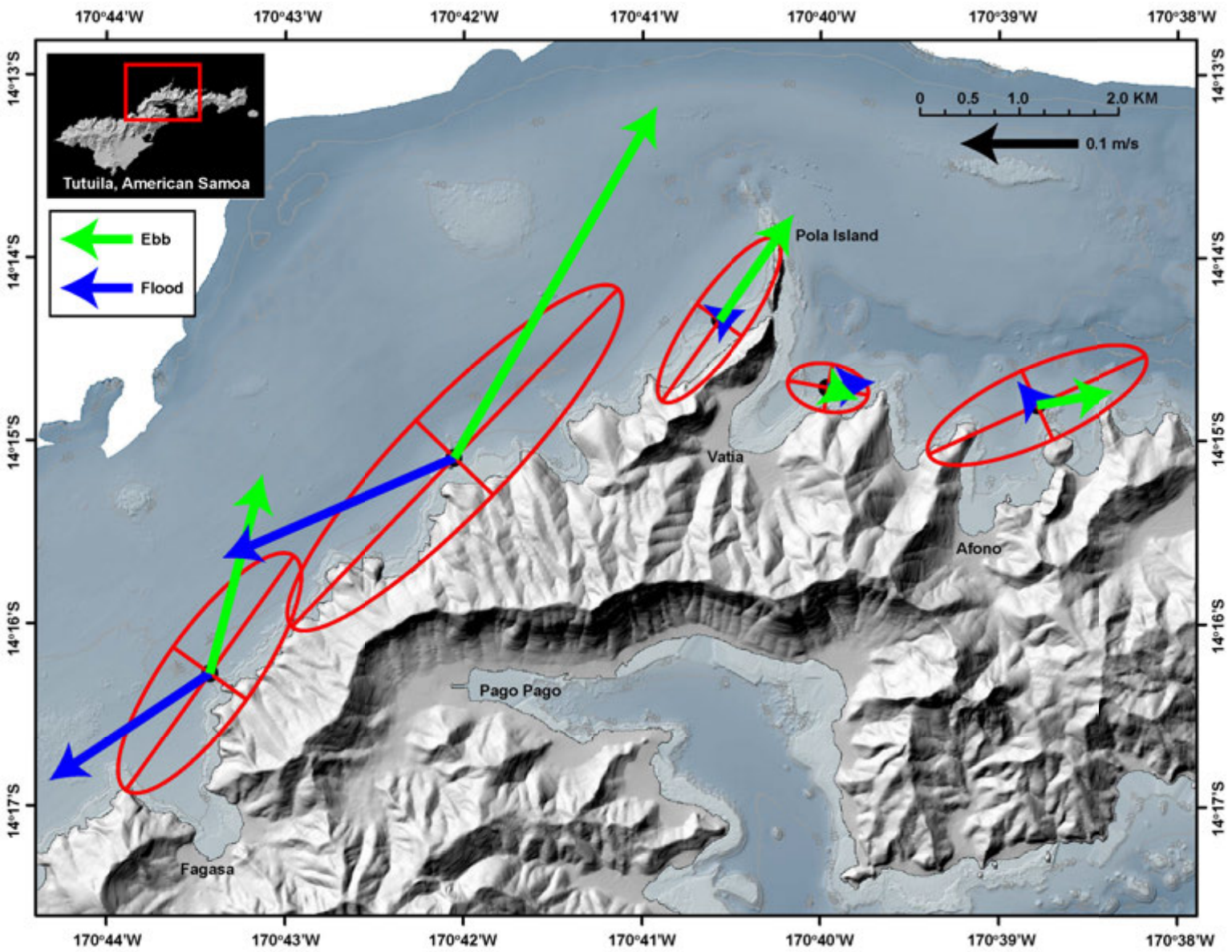

Figure 5. Map showing the mean (blue and green arrows) and variability (red ellipses) of near-surface current directions at each mooring site as heading ("going to"), in degrees from true north, and speeds in meters per second (m/s), during flood tides (blue arrows) and ebb tides (green arrows) during the 2015 experiment.

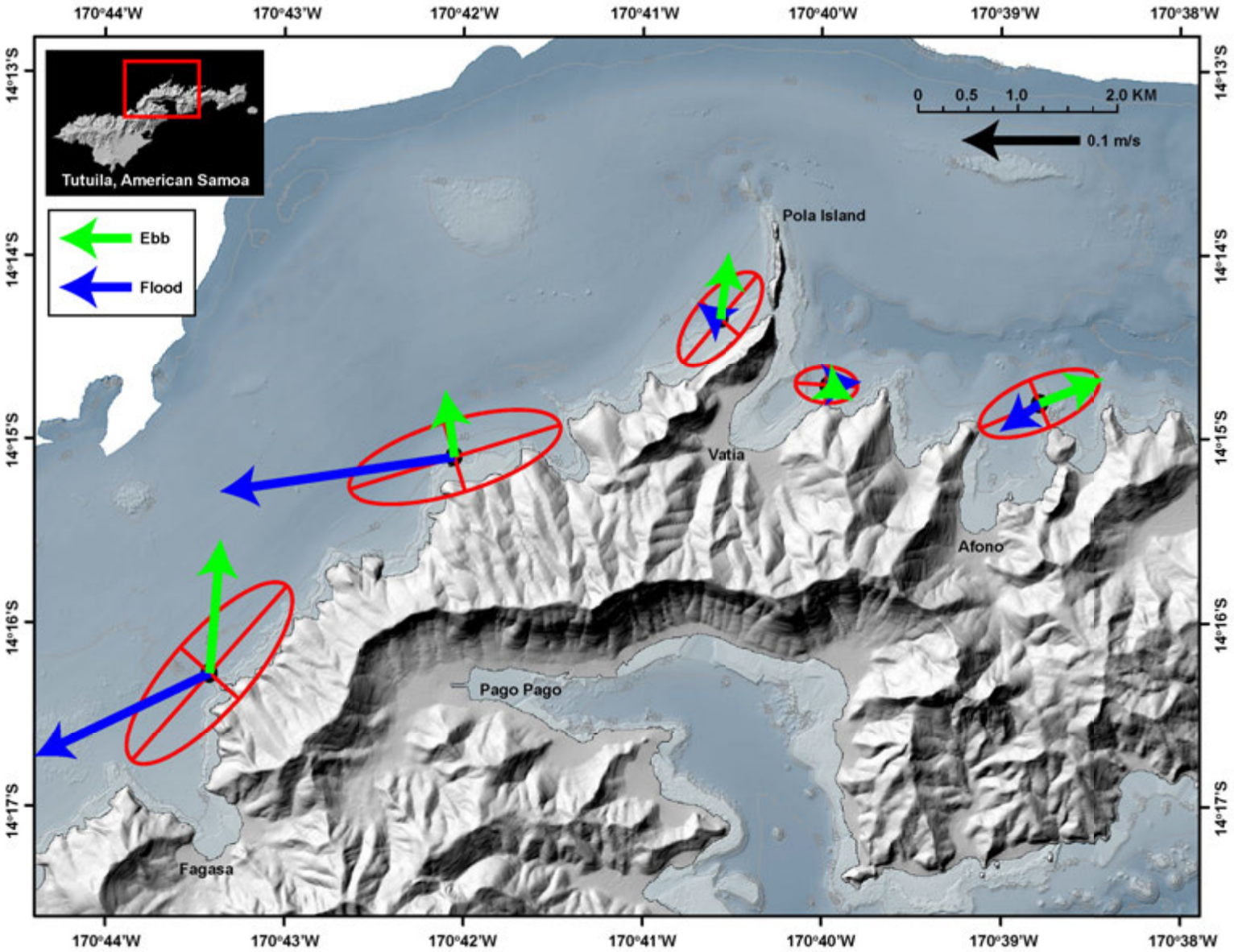

Figure 6. Map showing the mean (blue and green arrows) and variability (red ellipses) of near-bed current directions at each mooring site as heading ("going to"), in degrees from true north, and speeds in meters per second (m/s), during flood tides (blue arrows) and ebb tides (green arrows) during the 2015 experiment.

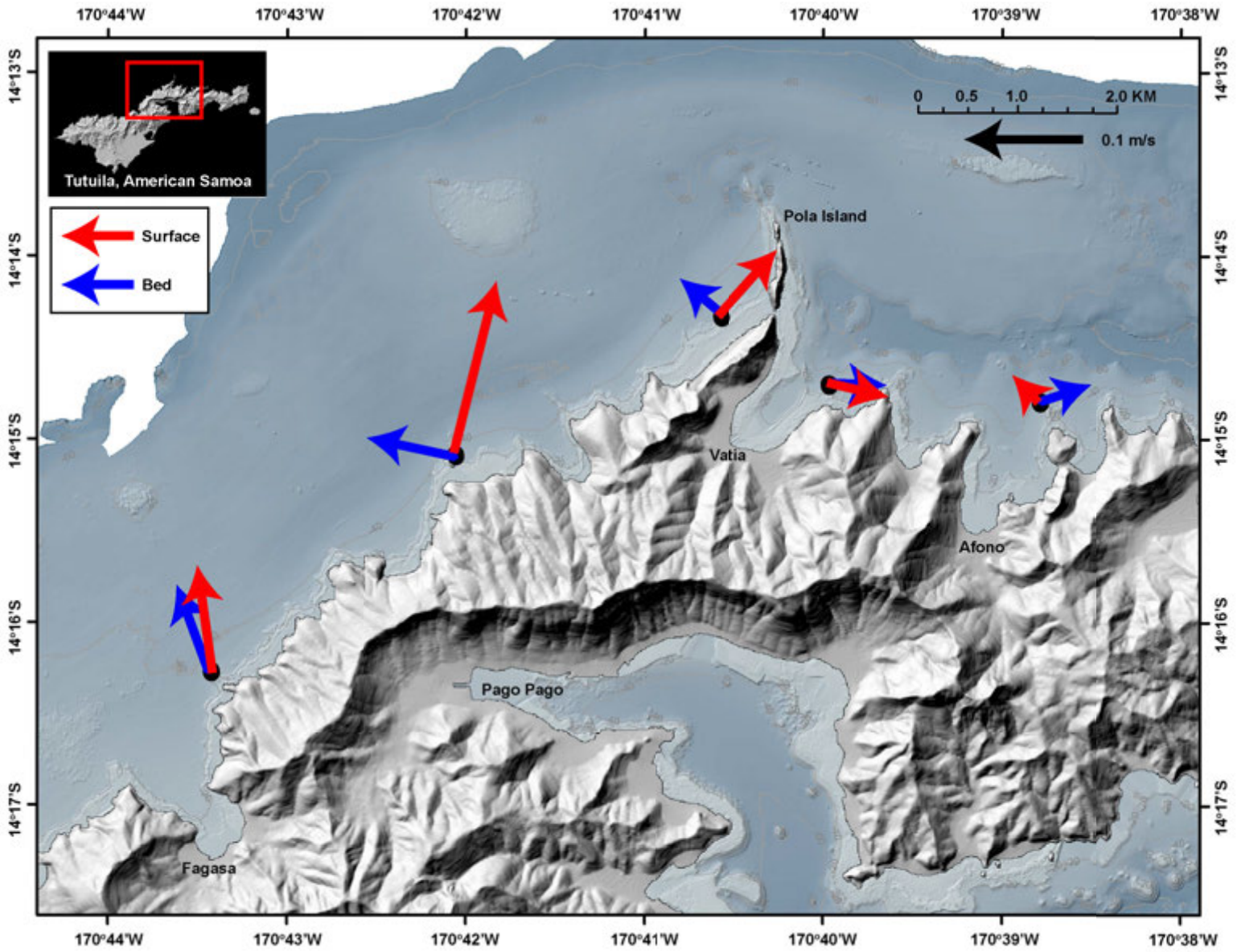

Figure 7. Map showing the mean near-surface (red arrows) and near-bed (blue arrows) current directions at each mooring site as heading ("going to"), in degrees from true north, and speeds in meters per second (m/s), during conditions dominated by southeasterly trade winds (2015 Year Day 160–166).

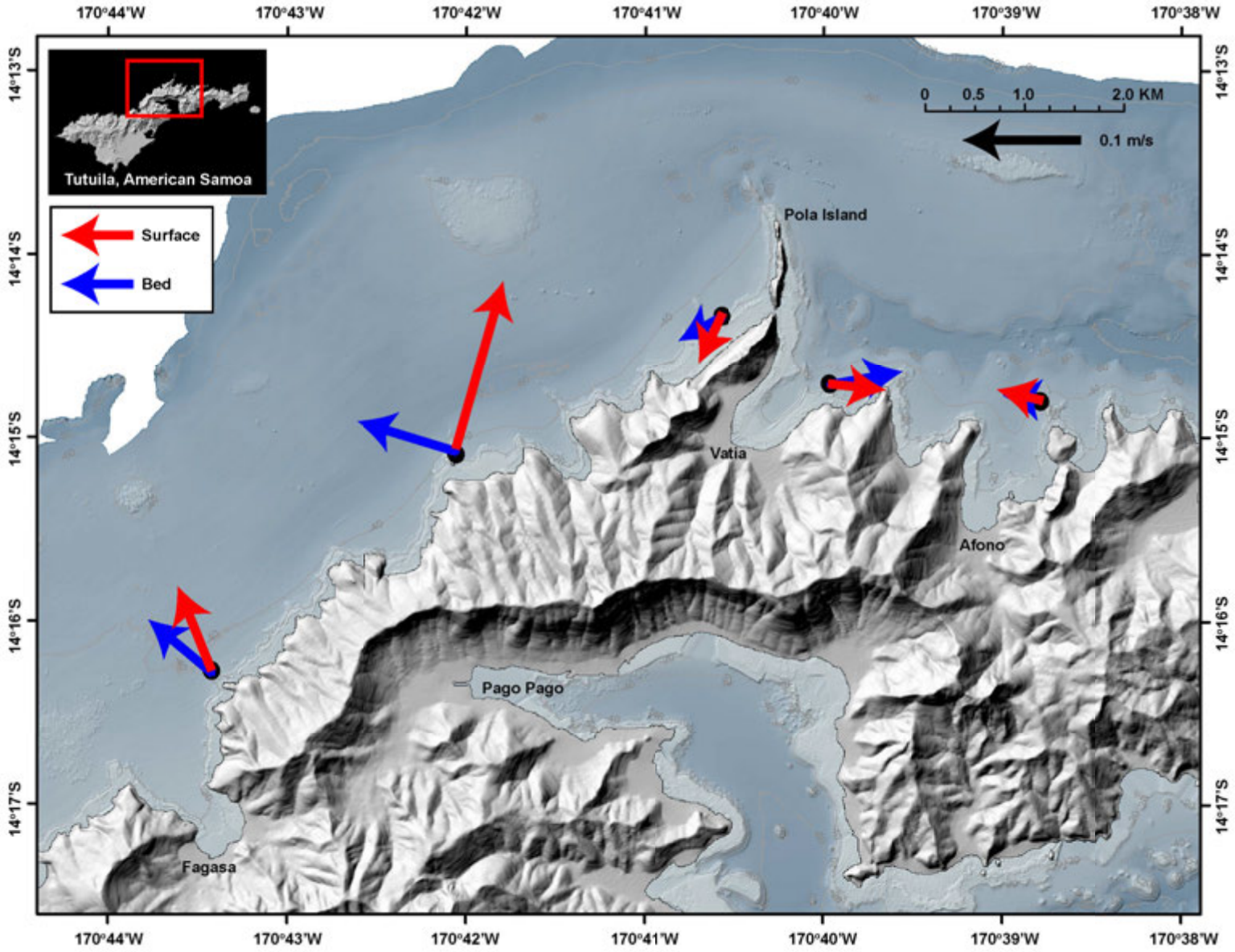

Figure 8. Map showing the mean near-surface (red arrows) and near-bed (blue arrows) current directions at each mooring site as heading ("going to"), in degrees from true north, and speeds in meters per second (m/s), during conditions dominated by large waves (2015 Year Day 50–56).

Water-Column Properties

The moored temperature loggers and CTs recorded variations in temperature (°C) and salinity (PSU) across a range of temporal scales.

Temperature—Near-bed water temperatures at the MiniPROBE sites ranged between 27.8 and 30.6 °C, with a mean temperature ±1 standard deviation of 29.2±0.6 °C (table 9, appendix 6). Near-surface temperatures recorded at the mooring sites ranged from 28.2 to 31.6 °C, with a mean temperature ±1 standard deviation of 29.8±0.4 °C. A similar seasonal temperature trend was found across all sites: during the non-trade wind period (about YD 45–90), temperatures were warmer, more variable, and vertical stratification was greater, whereas during the trade wind period, water temperatures cooled, exhibited less variability, and vertical stratification decreased (figs. 9–12). After onset of strong trade winds, temperature variability and vertical stratification decreased quickly from about 21 March 2015 (YD 80) to 10 April 2015 (YD 100), but overall cooling was more gradual, with temperature study period minimums not reached until about 9 July 2015 (YD 190). By this time, the mean near-bed temperature in the study area had decreased by 1.6 °C from that during the non-trade wind season. This cooling was relatively uniform across all study sites. The vertical chain of temperature loggers on each mooring revealed several interesting high-frequency processes during the stratified, non-trade wind season. Near-bottom temperatures fluctuated with internal tide movement, at a semidiurnal (about 12.4-hr) period, but near-surface temperatures fluctuated on a diurnal (24-hr) period, indicating the importance of surface heating to the upper water column and the influence of tidal dynamics in the lower water column. In addition, high-frequency (periods less than 1 hr) internal waves also occurred during the non-trade wind season, and produced large fluctuations in temperature throughout the water column at the mooring sites (fig. 13).

In general, the East site had the coolest temperatures, and water temperatures increased from east to west across the NPSA study area (figs. 11–12; appendix 6). Changes in wind patterns drove a fairly uniform water column response across all three mooring sites: winds out of the southeast led to cooling of near-bottom waters and upward movement of isotherms, and any wind relaxations or reversals led to warming and downward movement of isotherms (figs. 13–14). However, the timing of these water column responses was offset between sites, with the initial temperature change first occurring at the East site, then at Central, and lastly West. On average, upward-movement of isotherms (cooling) would first appear at the East site about 12 hr before the same cooling signature appeared at the West site. A similar time delay for water column warming of 12 hr was found between the East and West sites.

Table 9. Temperature statistics.

[°C, degrees Celsius; m, meters; SD, standard deviation]

Site name	Depth (m)	Mean ± 1 SD (°C)	Minimum (°C)	Maximum (°C)
West mooring	2	29.9 ± 0.4	28.8	31.6
West MiniPROBE	19	29.4 ± 0.6	27.9	30.6
West-Central MiniPROBE	20	29.3 ± 0.6	27.8	30.4
Central mooring	2	29.6 ± 0.5	28.2	31.5
Central MiniPROBE	22	29.3 ± 0.6	27.9	30.3
East-Central MiniPROBE	20	29.3 ± 0.6	28.0	30.3
East mooring	4	29.9 ± 0.2	29.2	30.9
East MiniPROBE	19	29.3 ± 0.6	27.9	30.3

Salinity—Near-bed salinity in the study area ranged between 31.6 and 35.4 PSU, with a mean salinity ±1 standard deviation of 34.4±0.3 PSU (table 10, appendix 6). Similar to temperature patterns, salinities decreased during the seasonal shift from the non-trade wind season to the trade wind season (figs. 9–11), with a mean decrease of 0.4 PSU from 21 March 2015 (YD 80) to 10 April 2015 (YD 100). Whereas the seasonal temperature shift occurred gradually, the salinity shift occurred more rapidly, with near-bed salinities reaching study period minimums by about 10 April 2015 (YD 100). Compared with temperature, the seasonal shift in salinity was less uniform across study sites, with the decrease in salinity occurring more rapidly at the Central site, and most gradually at the East site. The West site experienced the least seasonal change in near-bottom salinity. Near-surface salinities recorded at the West site declined by 0.5 PSU between 21 March 2015 (YD 80) and 10 April 2015 (YD 100), but also exhibited a slight increase starting after 10 April 2015 (YD 100).

Table 10. Salinity statistics.

[m, meters; NA, not available; PSU, practical salinity units; SD, standard deviation]

Site name	Depth (m)	Mean ±1 SD (PSU)	Minimum (PSU)	Maximum (PSU)
West mooring	2	34.6 ± 0.1	33.8	35.0
West MiniPROBE	19	34.4 ± 0.2	31.6	35.2
West-Central MiniPROBE	20	34.4 ± 0.3	33.3	35.4
Central mooring[1]	2	NA	NA	NA
Central MiniPROBE	22	34.2 ± 0.3	33.0	35.2
East-Central MiniPROBE	20	34.3 ± 0.3	33.4	35.2
East mooring[1]	4	NA	NA	NA
East MiniPROBE	19	34.6 ± 0.2	32.3	35.2

[1]Central and East mooring salinity measurements were fouled.

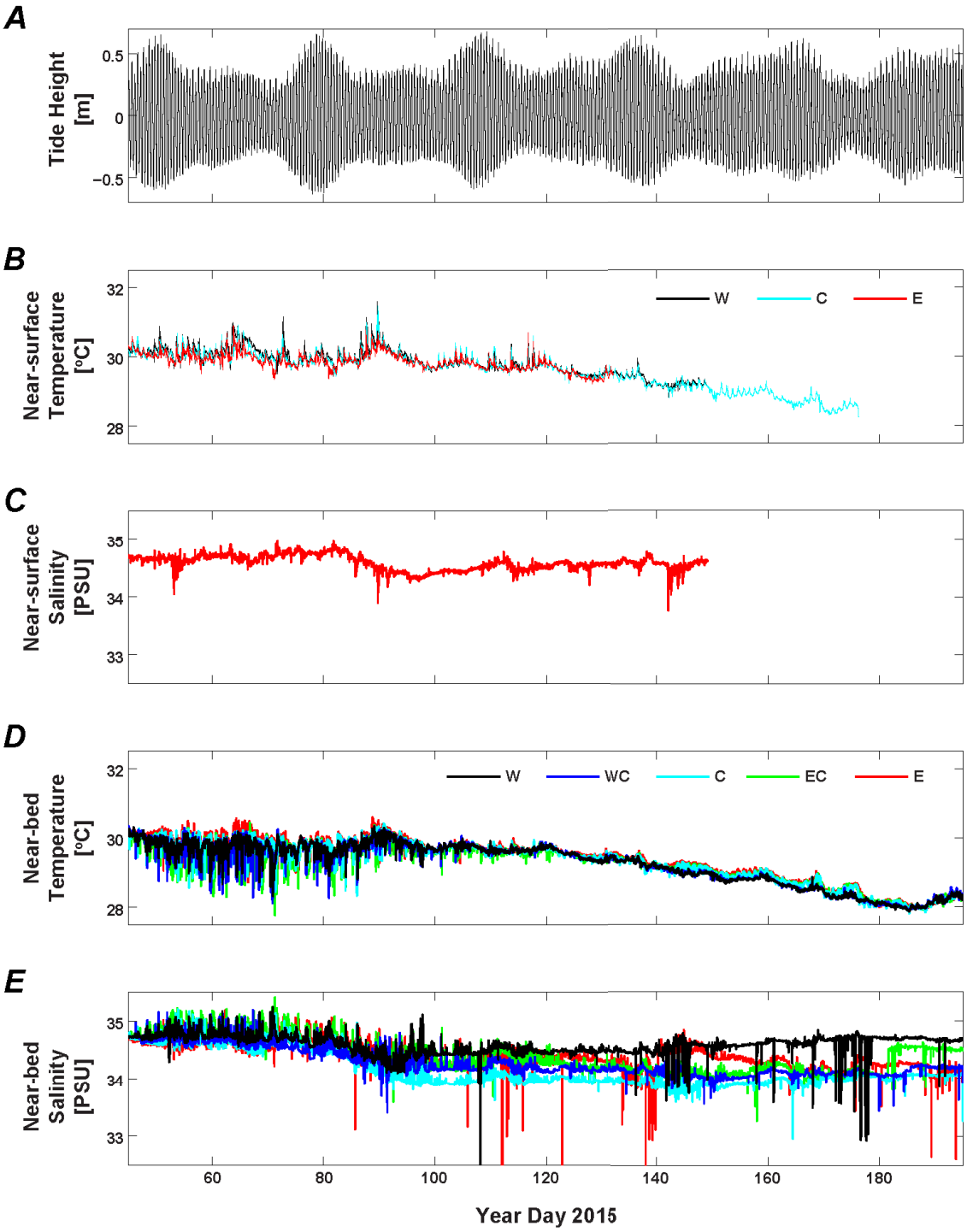

Figure 9. Time-series plots of nearshore temperature and salinity measurements. *A*, Tidal height, in meters (m), from the Central site. *B*, Near-surface temperature, in degrees Celsius (°C), measured at the mooring sites West (black line), Central (cyan line), and East (red line). *C*, Near-surface salinity, in Practical Salinity Units (PSU), measured at the East site. *D*, Near-bed temperature, in degrees Celsius (°C), measured at the MiniPROBE sites West (black line), West-Central (blue line), Central (cyan line), East-Central (green line), and East (red line). *E*, Near-bed salinity, in Practical Salinity Units (PSU), measured at the MiniPROBE sites West (black line), West-Central (blue line), Central (cyan line), East-Central (green line), and East (red line).

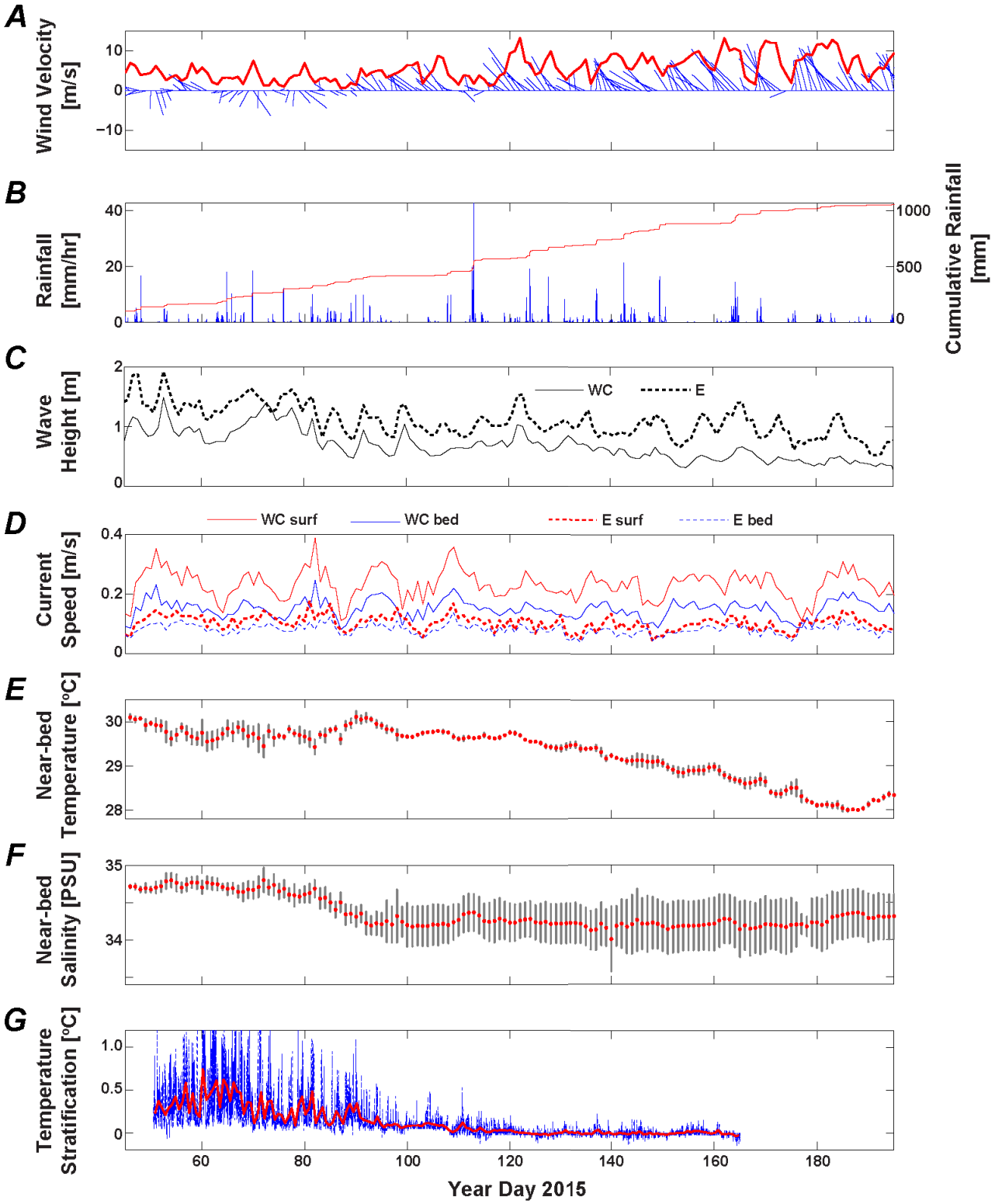
A
Wind Velocity [m/s]
10
0
−10
B
Rainfall [mm/hr]
40
20
0
1000
500
0
Cumulative Rainfall [mm]
C
Wave Height [m]
2
1
0
WC
E
D
Current Speed [m/s]
WC surf
WC bed
E surf
E bed
0.4
0.2
0
E
Near-bed Temperature [°C]
30
29
28
F
Near-bed Salinity [PSU]
35
34
G
Temperature Stratification [°C]
1.0
0.5
0
60
80
100
120
140
160
180
Year Day 2015

Figure 10. (previous page) Time-series plots of meteorological forcing from the Cape Matatula American Samoa Observatory (SMO) and oceanographic variability from the West-Central site. *A*, Daily-averaged wind velocity (blue lines), with direction shown as heading in degrees clockwise from true north and speed in meters per second (m/s), with daily-averaged wind speed (red line), in meters per second, from the SMO. *B*, Hourly (blue lines) and cumulative (red line) rainfall, in millimeters per hour (mm/hr), from the SMO. *C*, Daily-averaged significant wave height, in meters (m), from the West-Central (solid black line) and East (dashed black line) sites. *D*, Daily-averaged current speed, in meters per second (m/s), for West-Central near-surface (solid red line) and near-bed (dashed red line), and East near-surface (solid blue line) and near-bed (dashed blue line). *E*, Daily-averaged near-bed temperature (red dots) and daily temperature range (gray bars) in degrees Celsius (°C), across all mooring sites. *F*, Daily-averaged near-bed salinity (red dots) and daily salinity range (gray bars), in Practical Salinity Units (PSU), across all mooring sites. *G*, Difference between near-surface and near-bed temperatures, in degrees Celsius (°C), at the West site for both 3-minute (blue dashed line) and daily-averaged (solid red line) values.

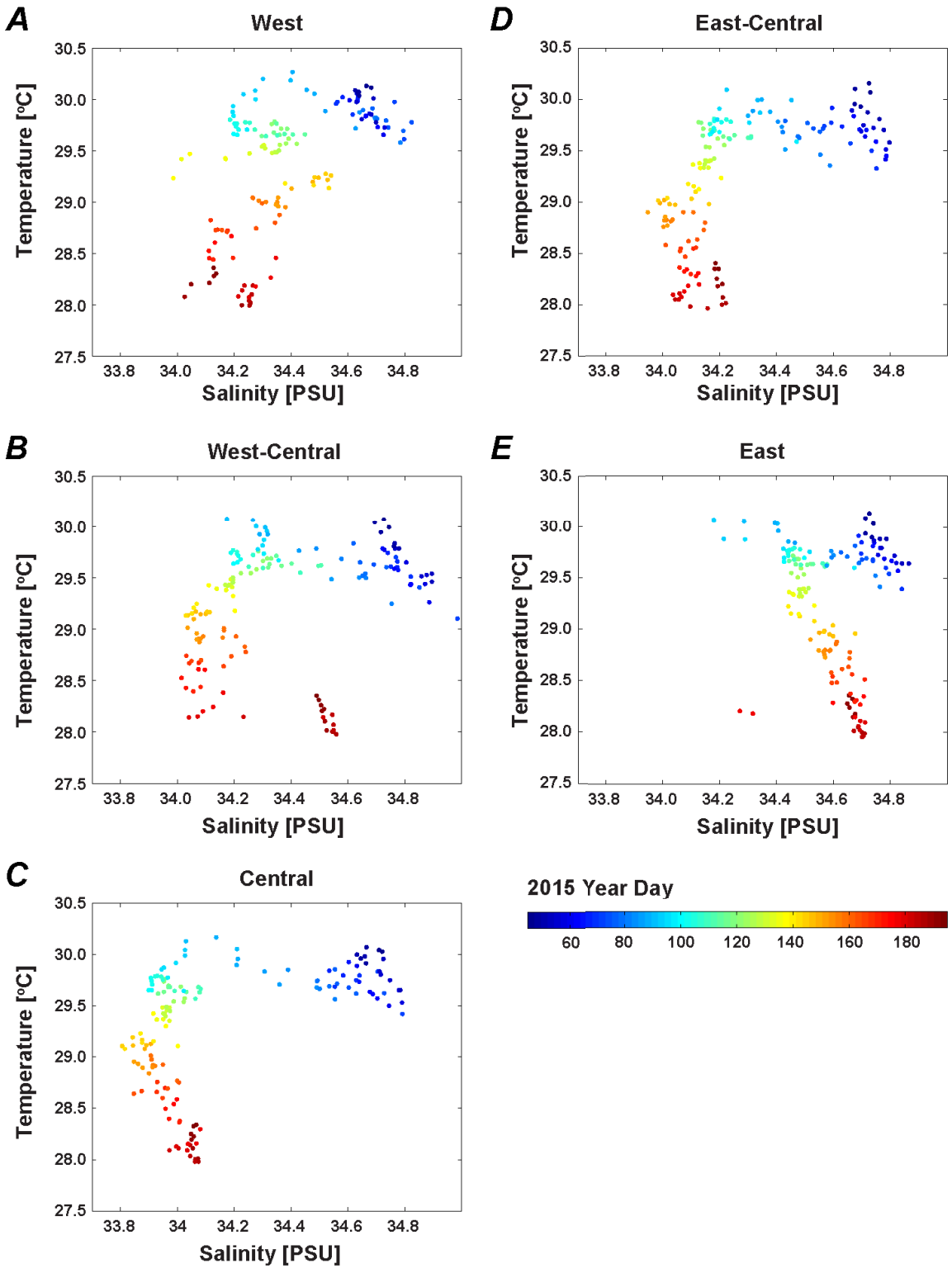

Figure 11. Scatter plots of temperature, in degrees Celsius (°C), versus salinity, in Practical Salinity Units (PSU), showing their relationship for each site using daily-averaged values. Color-coding is by 2015 Year Day.

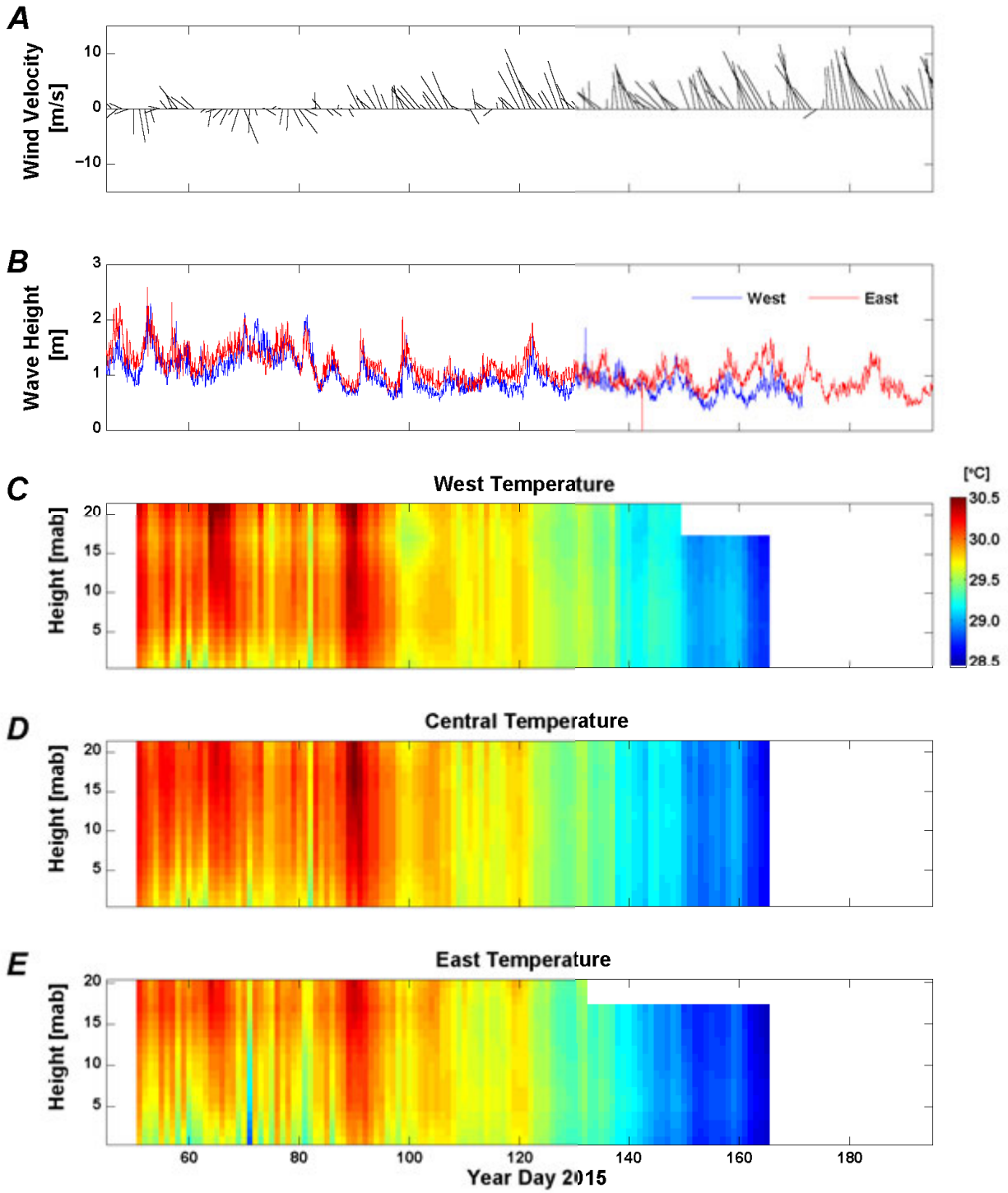

Figure 12. Time-series plots of nearshore vertical temperature. *A*, Daily-averaged wind velocity from the Cape Matatula American Samoa Observatory with direction shown as heading in degrees clockwise from true north and speed in meters per second (m/s). *B*, Significant wave height, in meters (m), from the West (blue line) and East (red line) sites. *C*, Daily-averaged temperature, in degrees Celsius (°C), at heights above the seabed (meters above bottom [mab]) for the West site. *D*, Daily-averaged temperature, in degrees Celsius (°C), at heights above the seabed (meters above bottom [mab]) for the Central site. *E*, Daily-averaged temperature, in degrees Celsius (°C), at heights above the seabed (meters above bottom [mab]) for the East site.

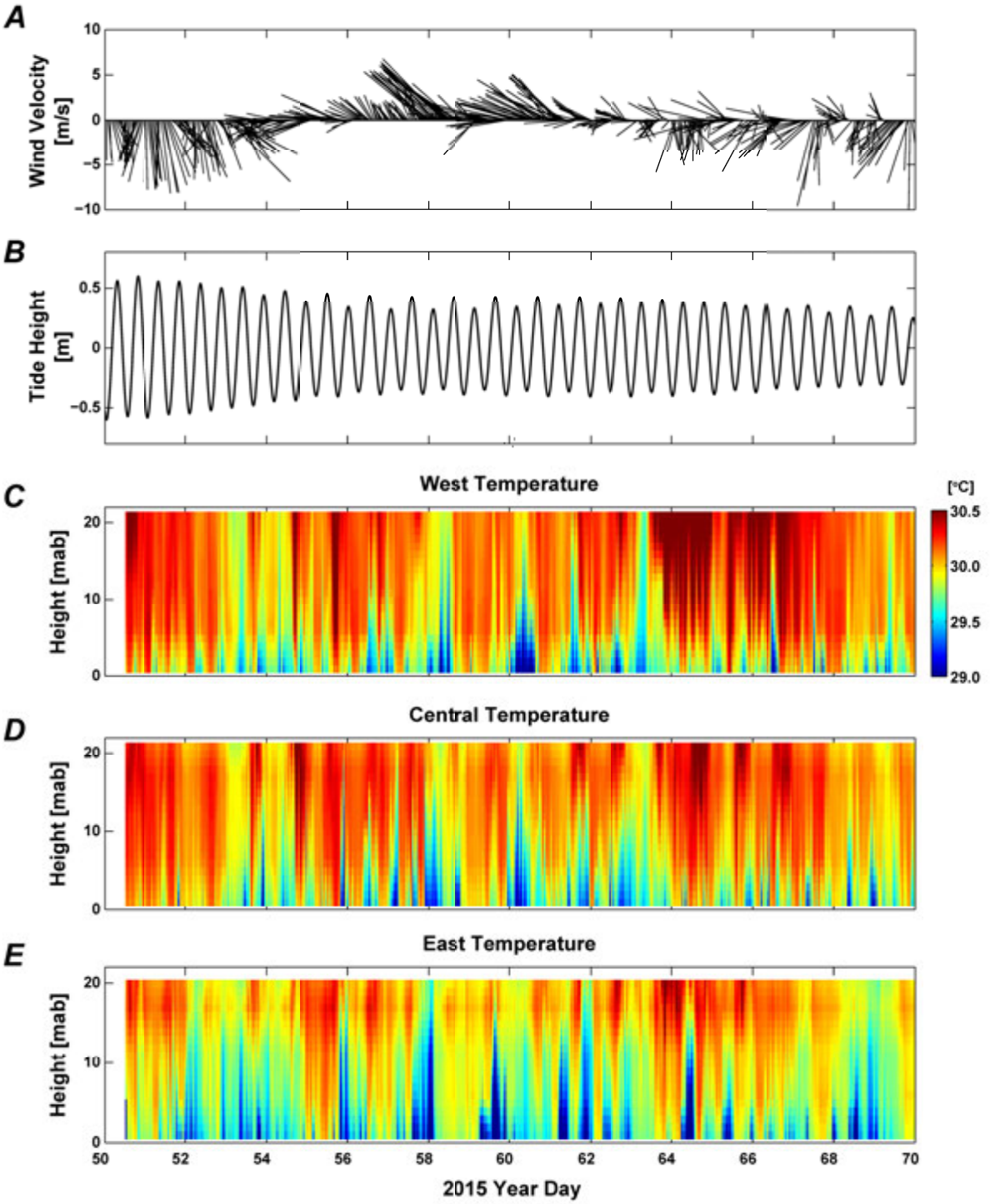

Figure 13. Time-series plots for a representative non-trade wind period (2015 Year Day 50–70) of nearshore vertical temperature. *A*, Daily-averaged wind velocity, with direction shown as heading in degrees clockwise from true north and speed in meters per second (m/s), from the Cape Matatula American Samoa Observatory. *B*, Tidal height, in meters (m), from the Central site. *C*, Temperature, in degrees Celsius (°C), at heights above the seabed (meters above bottom [mab]) for the West site. *D*, Temperature, in degrees Celsius (°C), at heights above the seabed (meters above bottom [mab]) for the Central site. *E*, Temperature, in degrees Celsius (°C), at heights above the seabed (meters above bottom [mab]) for the East site.

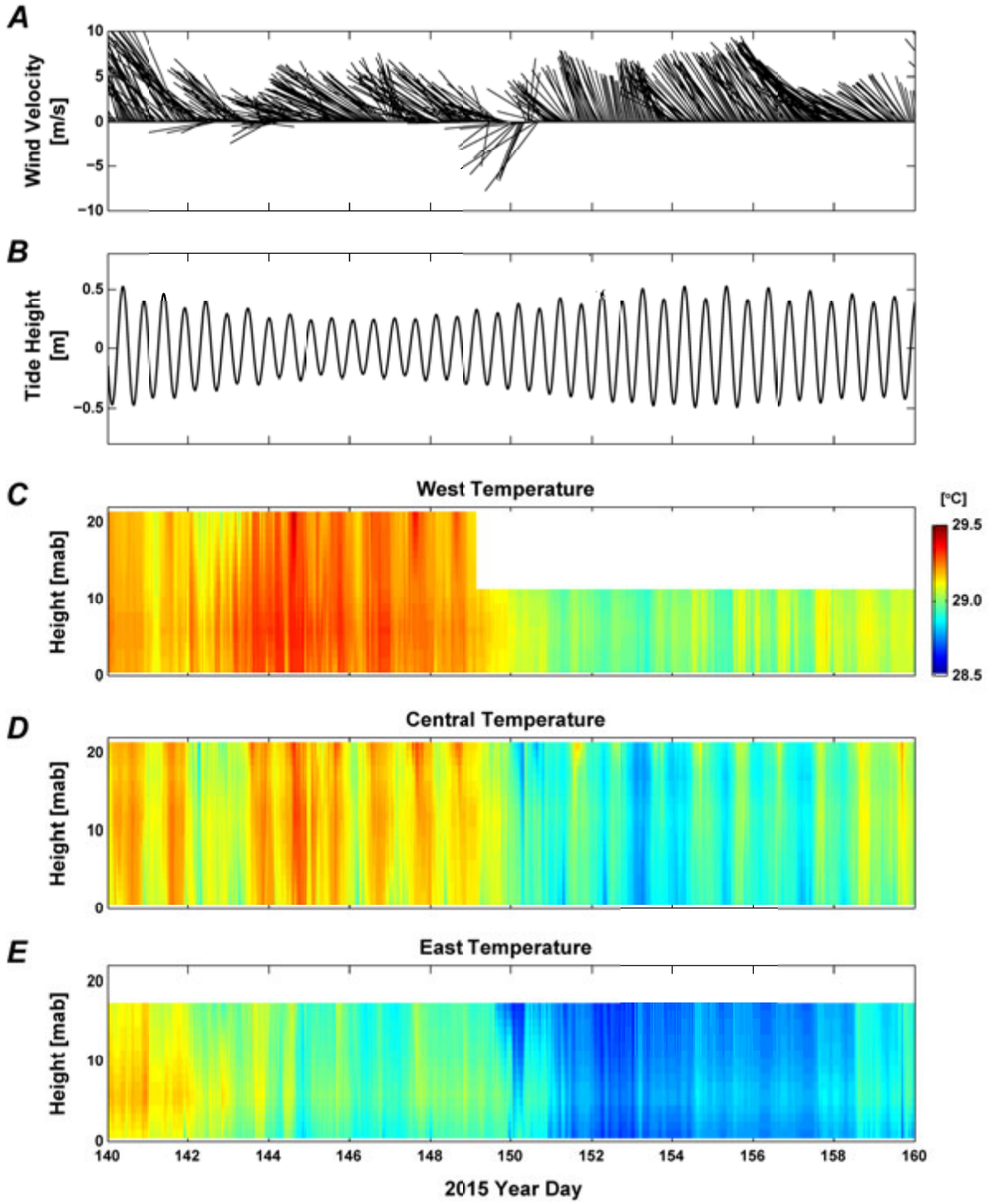

Figure 14. Time-series plots for a representative trade wind period (2015 Year Day 140–160) of nearshore vertical temperature. *A*, Daily-averaged wind velocity, with direction shown as heading in degrees clockwise from true north and speed in meters per second (m/s), from the Cape Matatula American Samoa Observatory. *B*, Tidal height, in meters (m), from the Central site. *C*, Temperature, in degrees Celsius (°C), at heights above the seabed (meters above bottom [mab]) for the West site. *D*, Temperature, in degrees Celsius (°C), at heights above the seabed (meters above bottom [mab]) for the Central site. *E*, Temperature, in degrees Celsius (°C), at heights above the seabed (meters above bottom [mab]) for the East site.

Spatial Patterns

Winds

During the week leading up to the February vessel surveys, winds were consistently northwestward (blowing out of the east-southeast), averaging 3–5 m/s (figs 2–3, appendix 7). Over the course of the 4-day survey period (17–20 February 2015; YD 48–51), wind speed stayed relatively constant (mean ±1 standard deviation of 4.7±0.9 m/s), but direction shifted; on 17–18 February 2015 (YD 48–49) winds were predominantly westward, rotating slightly from southwestward to northwestward, then on 19 February 2015 (YD 50) winds shifted to northerly (blowing out of the north), a direction that held through the end of the last survey on 20 February 2015 (YD 51). The high spatial resolution wind measurements made on the vessel during the VM-ADCP surveys reveal the amount to which terrestrial topography influences wind speed and direction over shelf waters (fig. 15). Winds were primarily alongshore, but the pattern on either side of Pola Island changed with the regional wind shift. With the easterly winds on 17–18 February 2015 (YD 48–49), the nearshore winds measured by the vessel survey found correspondingly easterly, alongshore winds to the west of Pola Island, whereas on the east side, winds were weak and more variable, though also on average directed to the west. Then, on the later survey days (19–20 February 2015; YD 50 and 51) after the regional winds shifted to a northerly direction, the region west of Pola Island still had easterly downcoast winds, but the east side of the Pola winds were stronger and more uniformly directed downcoast to the east. This may be the result of northerly winds being bifurcated by the steep topography of Pola Island. Closer to shore, the winds often rotated onshore, directed into the embayments and coastal valleys. In general, the winds were strongest in the eastern part of the study area, especially in the vicinity of Pola Island (likely because of topographic steering), and weaker to the west (because of sheltering by Pola Island); wind speeds were the lowest in the embayments.

Currents

VM-ADCP—Mean currents (averaged over all 4 sampling days) reveal several general spatial circulation patterns in and around the NPSA region; however, because of the low temporal coverage, these patterns may not dominate annual variability. The fastest mean current speeds were found closest to Pola Island, whereas the weakest were found furthest away (transect 1), indicating that Pola Island may strongly enhance and steer current velocities (fig. 16; appendix 8–9). In addition, across the survey area, mean currents were generally weaker closer to shore than farther offshore, and surface currents tended to be stronger than those observed near bottom, though the variability in the near-bottom currents was comparable to that of surface currents (fig. 17). Some exceptions to these general patterns were noted: on the western side of Fagasa Bay (transect 1), mean surface currents were weak and variable compared with the mean near-bottom flow. In addition, on the eastern edge of the survey area (transect 9) mean near-shore currents were comparable in magnitude to the mean of those measured farther offshore. Mean near-bottom flow over the survey area was predominantly weak and directed across shore, though whether this near-bottom flow was directed onshore or offshore varied spatially. Over the middle shelf region on the west side of Pola Island (transects 3–5), mean near-bottom flow was directed offshore, whereas the transects immediately adjacent (transects 2 and 6) measured relatively strong mean near-bottom flows that were oriented onshore. Off the tip of Pola Island, mean near-bottom flow was offshore along the entire transect (transect 7).

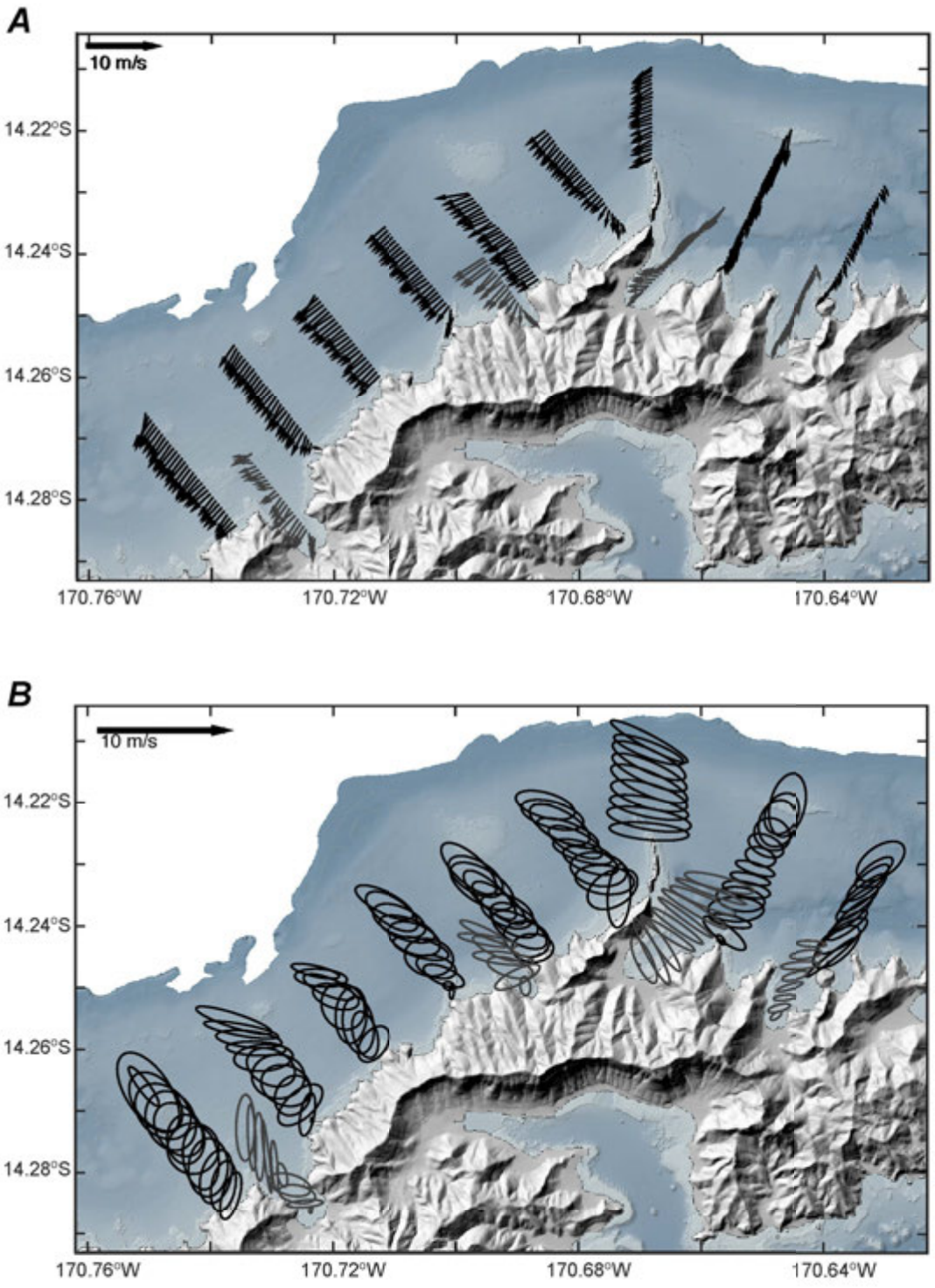

Figure 15. Maps showing spatial variability in surface winds during the vessel-mounted acoustic Doppler current profiler (VM-ADCP) surveys (2015 Year Day 48–51). *A*, Mean wind directions, with direction shown as heading ("going to") in degrees clockwise from true north, and speed in meters per second (m/s). *B*, Variability of wind direction, in degrees clockwise from true north, and speed in meters per second (m/s). Note that transects into embayments (gray arrows [*A*] and ellipses [*B*]) were only sampled on second and third days of VM-ADCP surveys, whereas other transects were surveyed all four days.

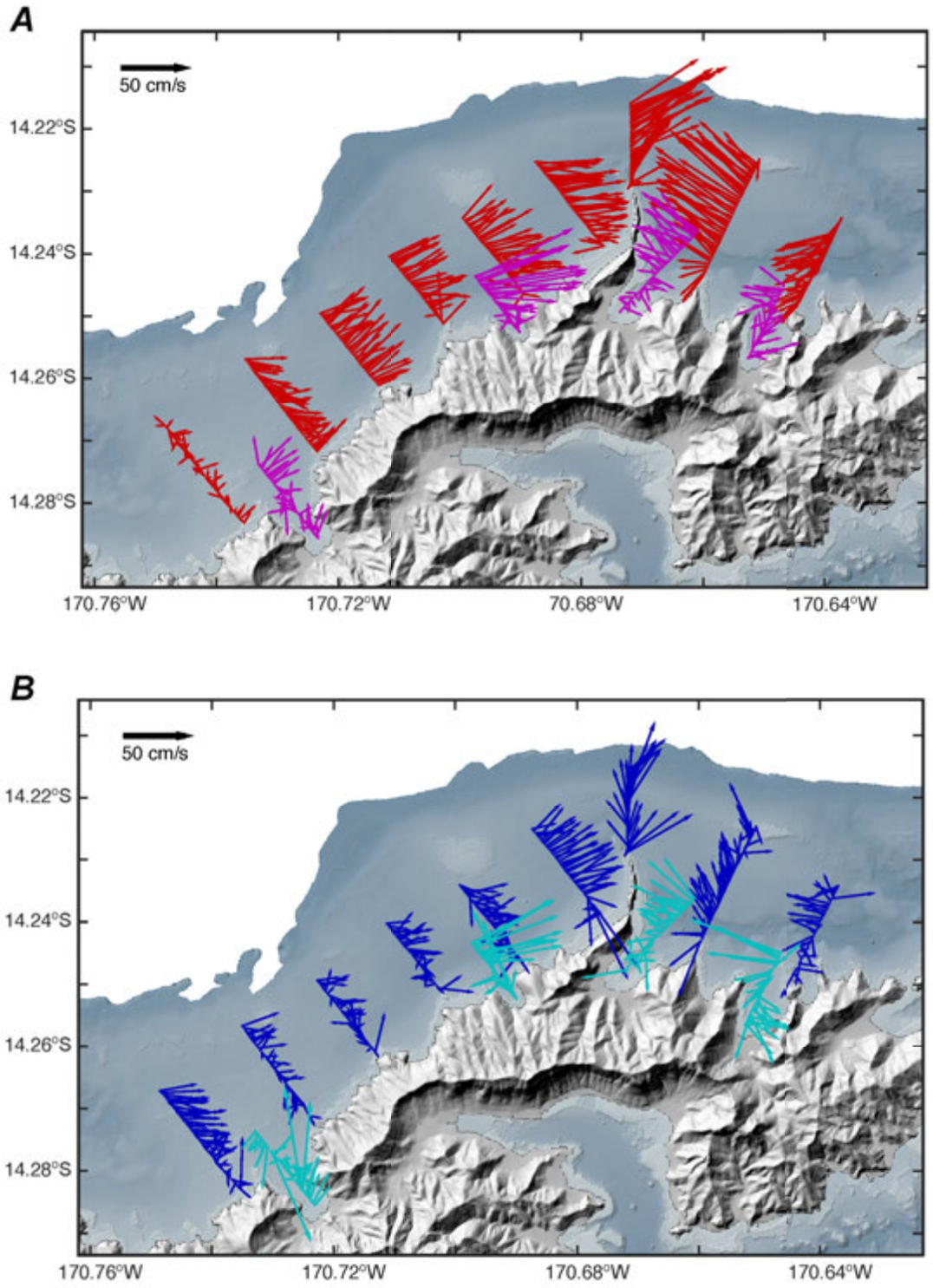

Figure 16. Maps showing mean current directions as heading ("going to"), in degrees from true north, and speeds, in centimeters per second (cm/s), during the vessel-mounted acoustic Doppler current profiler (VM-ADCP) surveys (2015 Year Day 48–51). *A*, Mean near-surface current directions and speeds (red and purple arrows). *B*, Mean near-seabed current directions and speeds (dark- and light-blue arrows). Note that transects into embayments (purple arrows [*A*] and light-blue arrows [*B*]) were only sampled on second and third days of VM-ADCP surveys, whereas other transects were surveyed all four days.

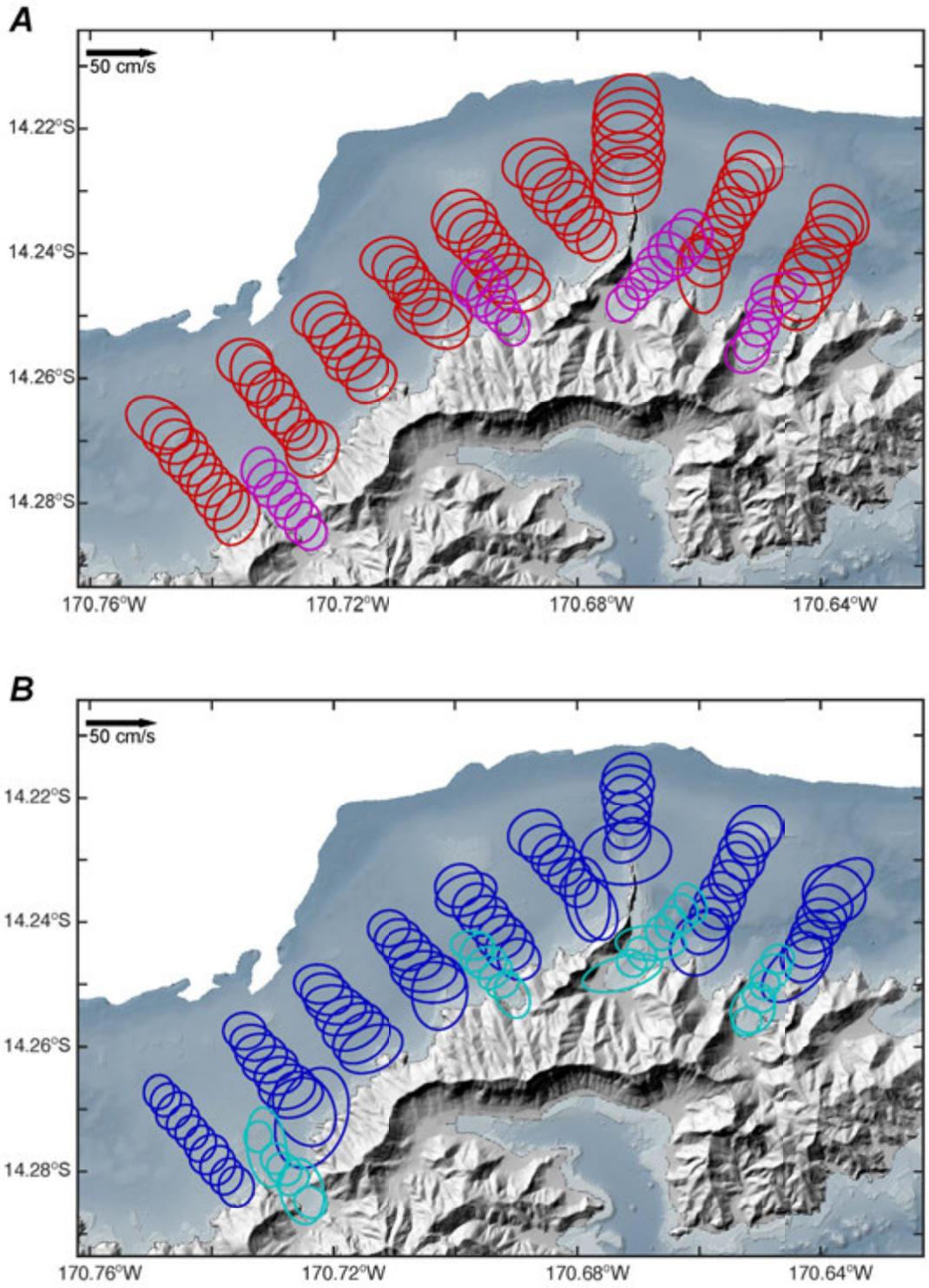

Figure 17. Maps showing variability of current directions as heading ("going to"), in degrees from true north, and speeds, in centimeters per second (cm/s), during the vessel-mounted acoustic Doppler current profiler (VM-ADCP) surveys (2015 Year Day 48–51). *A*, Near-surface current direction variability (red and purple ellipses). *B*, Near-seabed current direction variability (dark- and light-blue ellipses). Note that transects into embayments (purple ellipses [*A*] and light-blue ellipses [*B*]) were only sampled on second and third days of VM-ADCP surveys, whereas other transects were surveyed all four days.

In addition to steering, and possibly enhancing current speeds, the presence of the Pola Island topographical feature also appears to generate transient submesoscale (about 1 km) recirculating eddylike features. Although some variability occurred over the course of the survey, in general, with a predominant alongshore flow, in the lee of Pola Island, current patterns on the lee side of the Pola suggest the presence of a submesoscale clockwise eddy (fig. 16; appendix 9). The predominant alongshore flow observed during the surveys was to the northeast, with a recirculating flow pattern found on the east side of Pola Island. It is not clear if these clockwise eddy features are transient—growing and decaying on time scales according to tidal phase and (or) wind forcing patterns—or if they constitute a semipersistent feature that is present regardless of tidal stage or regional wind patterns. However, on 17 February 2015 (YD 48), with an alongshore flow that was predominantly to the west, a smaller scale clockwise recirculation cell was observed on the west side of Pola Island, with offshore currents flowing northeast, and currents closer to shore flowing southwest. The flow reversal occurred within a few hundred meters of the shoreline. It is not clear if this alongshore return flow is associated with the gap between Pola Island and the mainland. But the presence of this eddylike feature on the west and not the east side of the Pola suggests that these are likely transient features controlled by predominant current flow direction and wind patterns. These recirculating flow patterns held throughout the water column, though some rotation with depth occurred. As a result of this gyre, a complete reversal of flow was noted at the offshore end of transect 8 on two surveys, from southeastward flow offshore, to northwestward flow nearshore.

Nearshore local wind headings do not appear to correlate with current flow patterns in and around the NPSA study area. For the region west of Pola Island (transects 1–6), surface currents were predominantly eastward, with local winds directed oppositely to the west (fig. 15; appendix 7–9). The decoupling between local winds and current flow suggests that tides, bathymetry, and larger scale regional processes, such as offshore winds and waves, exert more influential control on current patterns in the study area.

LSCD—Thirty-six individual LSCDs were deployed over 12 weeks (14 April–9 July 2015; YD 104–190) at various locations within and offshore of the NPSA study area. A composite view of flow speeds during different tidal phases is displayed in figure 18; all individual drifter tracks and forcing during the deployments are shown in appendix 10. In general, flows were predominantly alongshore, except around slack tide; current speeds were greater (greater than 0.4 m/s) farther offshore and in the vicinity of Pola Island, as compared with close to shore and in the embayments (less than 0.1 m/s).

Water-Column Properties

Water column surveys that spanned the NPSA study area from Fagasa Bay east to Afono Bay were conducted at the beginning and end of the study (February and July, 2015; table 4, appendixes 4 and 11). These WCP surveys provide insight into the physical water column structure along the NPSA shoreline and are useful for putting time-series measurements made by the moorings and MiniPROBEs into regional context. Water-column properties measured by the water column profiler include temperature (°C), salinity (PSU), chlorophyll (mg/m^3), turbidity (NTU), and percent light transmission (percent) with depth.

Temperature—The greatest change in water-column properties between the non-trade wind season (February) and the trade wind season is decrease in water column temperature and lessening of stratification (fig. 19, appendix 11). During the non-trade wind season, surface waters, and those areas close to shore, are warm (greater than 30 °C), with cooler water present at depth in the outer shelf areas; this leads to enhanced vertical stratification. During the trade wind season, offshore and inshore (including embayments) areas showed relatively depth-uniform, cooler temperatures (about 28 °C), with little to no stratification.

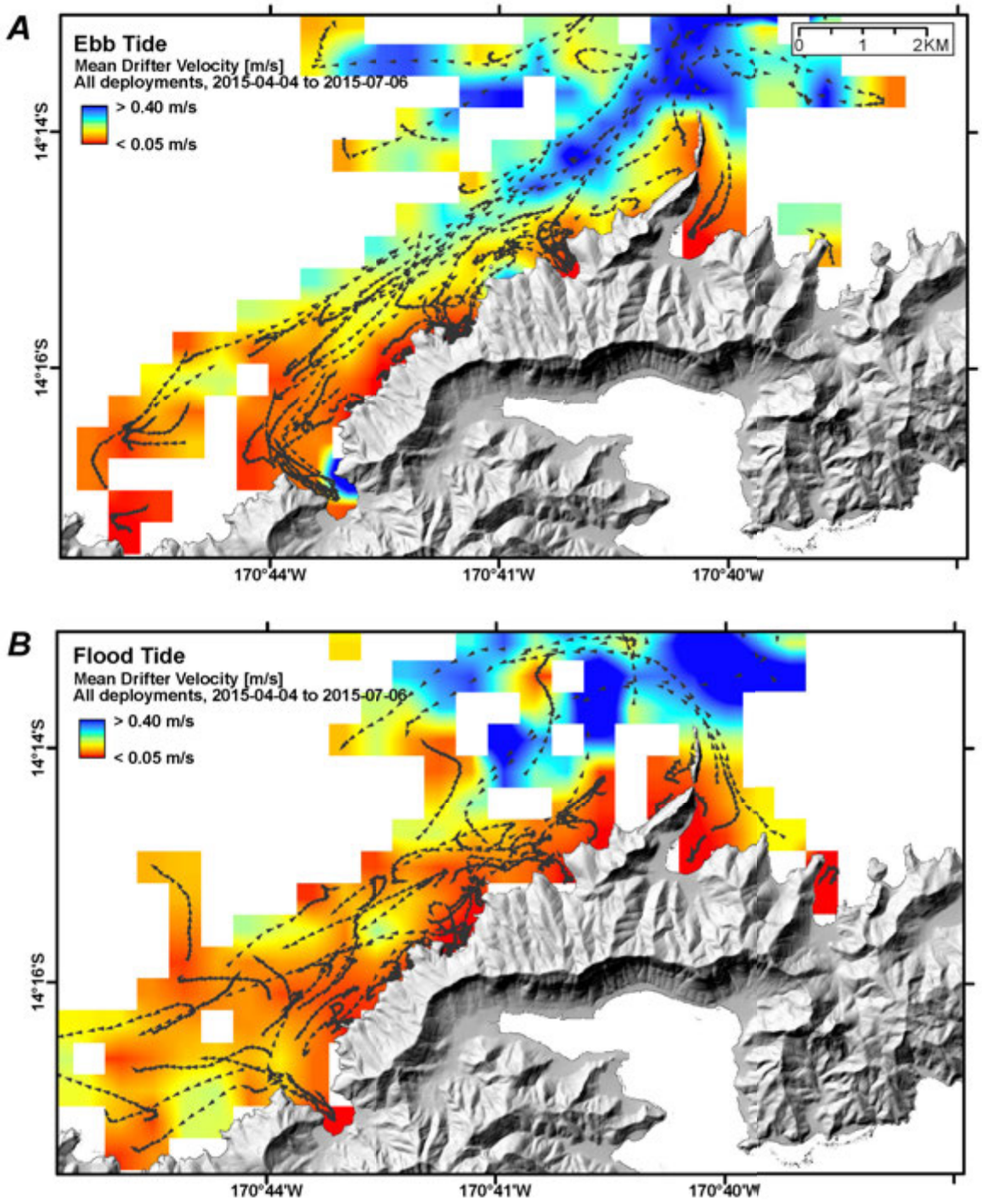

Figure 18. Maps showing Lagrangian Surface Current Drifters (LSCD) positions about every 15 minutes, mean current directions as heading ("going to"), in degrees from true north, and mean current speeds, in meters per second (m/s), during LSCD deployments (2015 Year Day 104–190). *A*, Current directions and speeds during falling (ebb) tides. *B*, Current directions and speeds during rising (flood) tides.

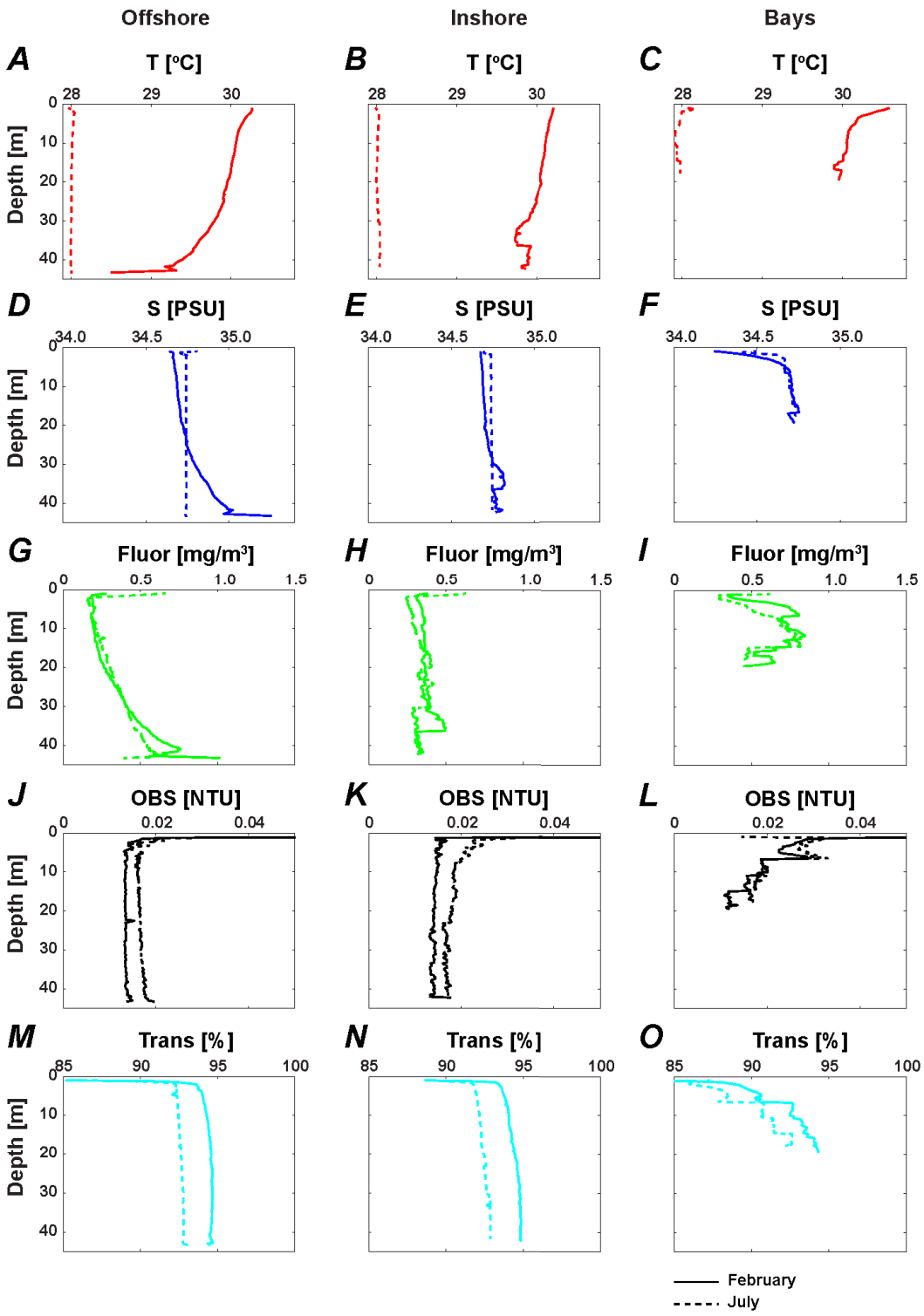

Figure 19. Plots showing vertical and spatial variations in water-column properties from February (solid lines) and July (dashed lines) surveys showing mean profiles from offshore (left column), inshore (middle column), and in embayments (right column). Mean profiles are for measurements of temperature (T; top row, red lines), in degrees Celsius (°C); salinity (S; second row, blue lines), in practical salinity units (PSU); chlorophyll fluorescence (Fluor; third row, green lines), in milligrams per cubic meter (mg/m^3); turbidity (OBS; fourth row, black lines), in Nephelometric Turbidity Units (NTU); and light transmission (Trans; bottom row, light-blue lines), in percent (%).

Salinity—Water column profiler surveys also show how vertical salinity patterns vary across the study area between the two seasons (fig. 19, appendix 11). During the non-trade wind season (February), outer shelf salinity increased near the seabed; this increase was associated with cooler temperatures at depth. In the trade wind season (July), salinity was relatively uniform with depth. The profiles taken within the embayments show evidence of freshwater influence, with decreasing salinities at the surface.

Chlorophyll, Turbidity, and Light Transmission—In general, optical properties measured by the water column profiler show that offshore and inshore water in the NPSA study area was relatively clear, with little phytoplankton or other suspended material (fig. 19, appendix 11). Only the embayment profiles had slightly decreased water clarity, resulting from turbidity and phytoplankton fluorescence. February and July surveys show similar chlorophyll fluorescence patterns, with elevated fluorescence found at depth on the offshore profiles and near the surface in the shallow bays. During the non-trade wind season (February), the deep chlorophyll maximum was associated with cooler, more saline waters found below 30 m depth. Overall, turbidity was low in all areas, except at the surface, which may result from sunlight and (or) bubbles present at the surface. Similarly, for offshore and inshore profiles, the percentage of light transmission shows clear waters for the majority of the water column, except at the surface. The embayment profiles, however, show a decrease in water clarity that extends down to 10–15 m depth. The repeat surveys performed in February indicate that optical properties in the sampled bays could vary on a daily basis, indicating high short-term temporal variability in bay water clarity.

Discussion

Spatial and Temporal Variability in Circulation Patterns and Water-Column Properties

Fluctuations in tides, winds, and waves all occurred on different time scales during the experiment and contributed to the overall circulation in NPSA. The resulting circulation patterns and water-column properties are described below for each of these oceanographic forcing processes. In addition, the overall circulation and transport patterns are summarized.

Tides

Most daily variability in current speed and direction at the nearshore study sites resulted from tides. The internal tidal signal (for example, the fluctuations of water column structure and current velocity occurring at tidal periods) was highly correlated ($r = -0.9$, $p < 0.05$, $n = 10{,}867$, for West-Central site) to surface tide, but with a delay of about 3 hr. Because of this correlation, the magnitude of the internal tidal currents is driven by the lunar tidal cycle, with the highest tidal current speeds occurring during the spring tides (new and full moons) and the weakest during the neap tides (quarter moons). Flood (rising tides) drove southwestward currents, whereas ebb (falling) tides resulted in northeastward currents (fig. 5–6). Near-bed temperature also fluctuated at a semidiurnal periodicity (figs. 9, 13), with temperatures cooling in response to southwestward flows (flood), and warming during northeastward flows (ebb). However, the magnitude of temperature fluctuations was not correlated with tide strength; instead, the larger wind patterns (trade wind versus non-trade wind seasons) set a low-frequency control on the overall magnitude of water column temperature.

Winds

Regional wind patterns are characterized by two distinct seasons: the southeasterly trade wind season during austral winter months (about April through September), and the wet, rainy (non-trade

wind) season during austral summer months (about October through March). Instrument deployment in the NPSA study area captured the transition between these two seasons. The first 45 days of the study were characterized by weak to moderate, variable-direction winds (fig. 2). The southeasterly trade wind pattern began in April (about YD 90), about a month and a half after the start of the experiment (fig. 2). Throughout the remainder of the study, the resulting wind direction was primarily from the southeast, with an average speed of about 7 m/s. Mean current velocities during the period of southeasterly trade winds are shown in fig. 7. There was no large change in mean nearshore current patterns from one season to the next (fig. 7–8), probably owing to strong tidal control on nearshore current patterns.

Water-column properties, however, show a marked shift coinciding with different wind seasons, with warmer, more saline water during the non-trade wind season, transitioning to cooler, less-saline water during the trade wind season (figs. 9–12). Thermal stratification and nearshore wave heights also decreased during the trade wind season (figs. 10, 12). During the wet, non-trade wind season, the water column was characterized by strong thermal heating near the surface coupled with influx of cooler waters at depth, creating a strong thermocline characterized by a high temperature variability for nearshore waters. In addition, subtidal temperature fluctuations were strongly tied to regional wind patterns. In contrast, during the trade wind season, vertical stratification decreased markedly, and overall temperatures decreased gradually throughout the remainder of the study period.

Waves

Regional, offshore wave patterns are primarily out of the southeast to southwest, making the north coast of Tutuila, American Samoa, relatively protected from these larger scale wave patterns (figs. 3–4). The largest nearshore wave heights in NPSA were observed during the non-trade wind season at the beginning of the study, with significant wave heights exceeding 2.5 m at the East site. This wave forcing did not alter the overall nearshore circulation patterns except at the Central site, where mean currents were directed to the southwest away from Pola Island instead of the northeast (fig. 8). During the trade wind season, although wave heights were smaller, wave periods were much longer at the West and West-Central sites. These longer period waves were directed out of the east to northeast.

Circulation and Transport Patterns

Nearshore current patterns showed high spatial variability between the study sites. These disparate hydrographic patterns likely reflect the strong steering by the coastline curvature and bathymetric steepness.

In general, the strongest nearshore currents occurred at the outer boundaries of NPSA's waters at the West, West-Central, and East sites. The slowest current speeds occurred at the sites closest to Pola Island. In contrast, the VM-ADCP surveys revealed a different flow pattern in the mid- to outer-shelf region with the most vigorous currents found close to Pola Island. The time-averaged currents reveal that near-surface waters had a mean flow directed towards Pola Island, whereas near-bed currents had a mean flow directed away. This, taken together with the offshore current patterns found by the VM-ADCP surveys, suggests a flow convergence centered around Pola Island as well as complex recirculating flow patterns, including the possible presence of submesoscale (diameter of about 1 km) eddies. These submesoscale eddies are likely transient features formed in response to tidally driven flows around the Pola Island headland. The presence of these recirculation eddylike features may be important to coral reef communities in the nearshore and deeper regions of the shelf by increasing the connectivity between these environments and also providing a recruitment pathway and (or) a mechanism for decreased larval dispersal. In addition, because these eddies exhibit clockwise flows,

they may act to upwell cold, higher nutrient water from depth. This, coupled with near-bottom influxes of cooler water during the wet non-trade wind season, may help alleviate thermal stress in the nearshore.

Spatially limited but temporally extensive residence times calculated for each mooring site also suggest decreased transport near Pola Island (figs. 20–22). Overall current patterns show longer residence times to the west of Pola Island (Central site), as well as the East site. These residence times decrease further with proximity to the seabed. Under strong southeasterly trade wind forcing, however, mean residence time at the Central site decreases substantially (by about 44 percent). In general, under strong southeasterly trade wind forcing, residence times decreased for all sites except East, which actually increased by nearly 2.5-fold, likely because of vertical velocity shear. During variable winds, but larger waves, residence times were short across the entire NPSA region and showed little change with depth. Thus, large wave events affecting the NPSA coastline during the wet season may significantly shorten residence times for planktonic organisms and suspended material found near the seabed, particularly at the Central and East sites.

Spatially extensive but temporally limited residence times calculated for the VM-ADCP surveys demonstrated that, in general, residence times were longer in the western half of the survey area as compared with the eastern half, longer closer to shore than offshore, and longer near the bottom than at the surface, with some exceptions (fig. 23). Transect 9 on the far eastern edge of the survey area had greater residence times (1.5–3.8 hr), particularly near the bottom, than several of the other transects. Residence times were slightly longer at the offshore end of transect 8, in the vicinity of a small plateau in the bathymetry. In some cases, at the most inshore parts of transects, residence times were shorter than those just offshore in slightly deeper water, such as was observed along transects 2, 4, and 9. Longer residence times that were uniform with depth were noted at the shoreward end of transects 1, 4, and 5. Given slow mean near-surface current velocities measured at transect 1, long residence times (averaging 3.7 hr for a 250-m square area) are expected. Similarly, given strong mean currents at transect 7 off the tip of Pola Island, the shortest residence times were found here, averaging 0.5 hr. Similar patterns of long residence times (more than 2 hr) in the embayments and close to shore with shorter residence times (less than 1 hr) farther offshore were calculated from the spatially extensive but temporally limited LSCD deployments' residence times (fig. 24). Together with data from the water column profiler (fig. 19), it is apparent that warmer, lower salinity, higher chlorophyll, and more turbid waters in embayments tend to reside in those locations for much greater durations, resulting in greater exposure of embayment ecosystems to those waters. This is in contrast with farther offshore, where cooler, higher salinity, lower chlorophyll, and less turbid waters are quickly transported alongshore.

In addition to transient generation of clockwise recirculation patterns, the amount of current shear at nearshore sites may also add to the complexity of circulation and transport patterns within the NPSA area. At the West-Central site, time-averaged near-surface current velocity corresponds to a transport of nearly 500 m over an hour (about 0.1 m/s) to the north-northeast (13° true North), whereas the time-averaged near-bed current velocity for this same site corresponds to a transport of about 200 m downcoast, to the west (−75° true North). This highlights the strong current shear present at these nearshore sites, and also suggests that the depth of planktonic organisms and suspended material in the water column may be a strong determinant of resultant transport patterns. For example, planktonic larvae that can employ depth-keeping behavior may be able to control and (or) vary the direction of their transport by changing their vertical placement in the water column, particularly in the nearshore regions.

In addition, strong vertical velocities at nearshore sites may also act to efficiently transport water and suspended matter toward and away from the shoreline. Vigorous (more than 0.05 m/s) upward and downward velocities were observed at the West, West-Central, and East sites, and were coincident with

strong horizontal current velocities (fig. 25). This suggests that elevated vertical velocities arise from interaction of these horizontal flows and the steep nearshore bathymetry, which, through mass conservation, effectively redirects these horizontal currents both upward and downward. At the West-Central and East sites, depth-averaged vertical velocities regularly reach 0.05 m/s. A planktonic organism in near-surface waters that experienced a downward flow of 0.05 m/s would reach the bottom in less than 7 min.

In addition to regional winds and tides, other low-frequency, large-scale processes may play a role in driving the current field along the north Tutuila coastline. These processes include regional and mesoscale eddies, island-trapped shelf waves, and modulations in basin-scale currents (such as the South Equatorial Counter Current). However, surveys with more extensive spatial and temporal coverage are requisite for resolving and evaluating these processes.

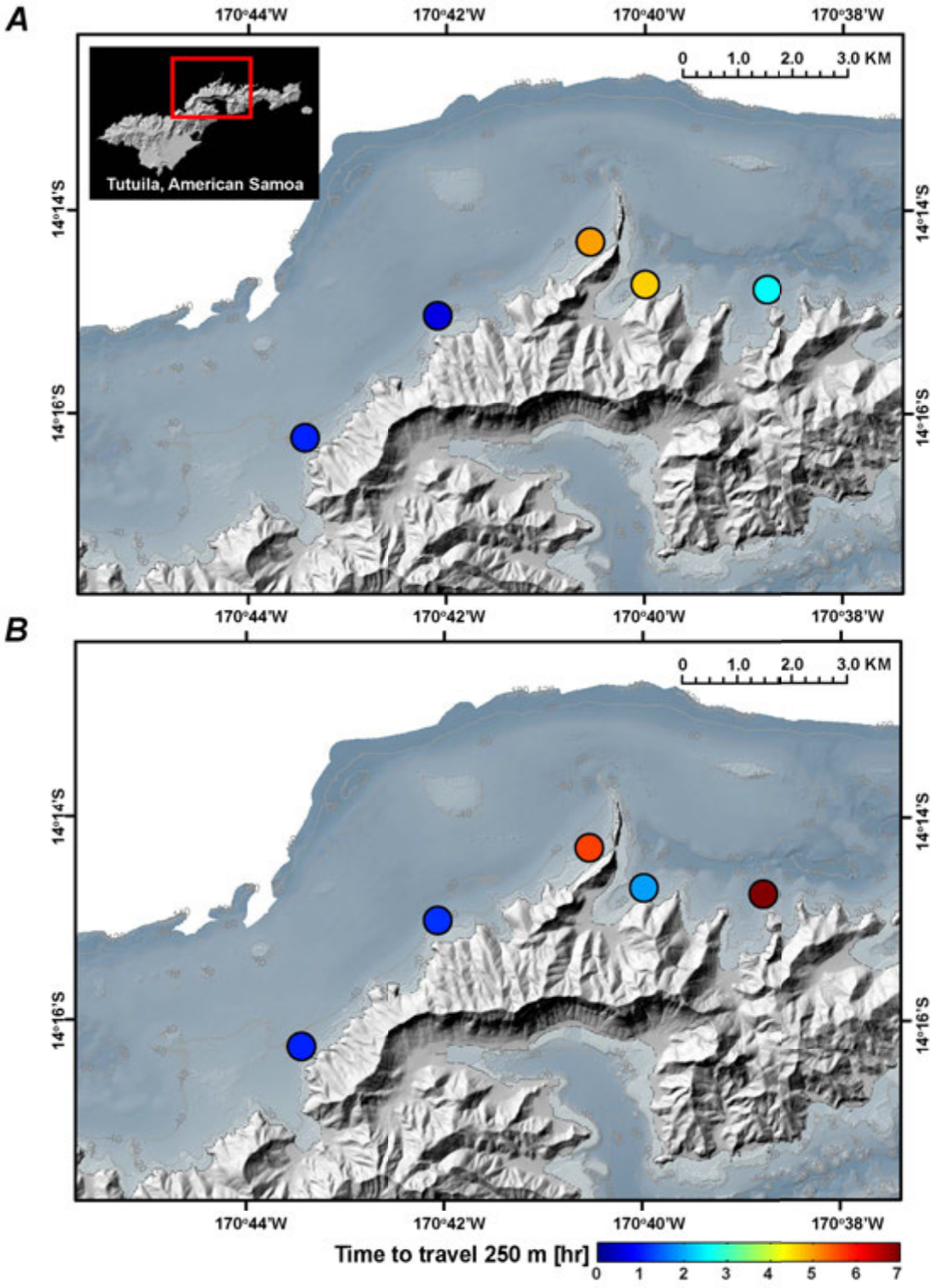

Figure 20. Maps showing computed residence times, with colors indicating time, in hours (hr), to travel 250 meters (m), for each nearshore study site by using measurements from a period of weak winds and waves (2015 Year Day 110–116). *A*, Residence times using near-surface current velocities. *B*, Residence times using near-bed current velocities.

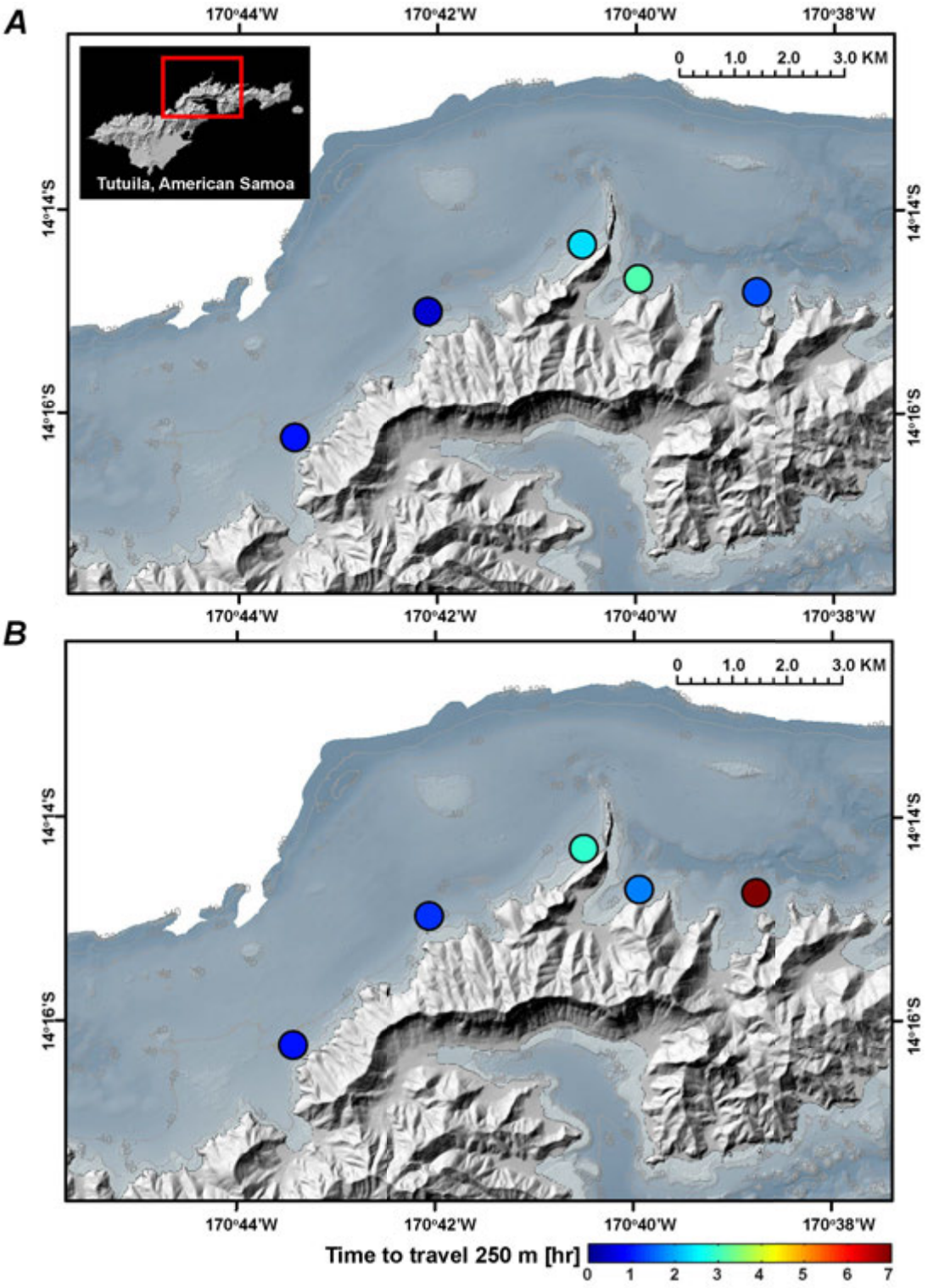

Figure 21. Maps showing computed residence times, with colors indicating time, in hours (hr), to travel 250 meters (m) for each nearshore study site by using measurements from a period of strong trade wind forcing (2015 Year Day 160–166). *A*, Residence times using near-surface current velocities. *B*, Residence times using near-bed current velocities.

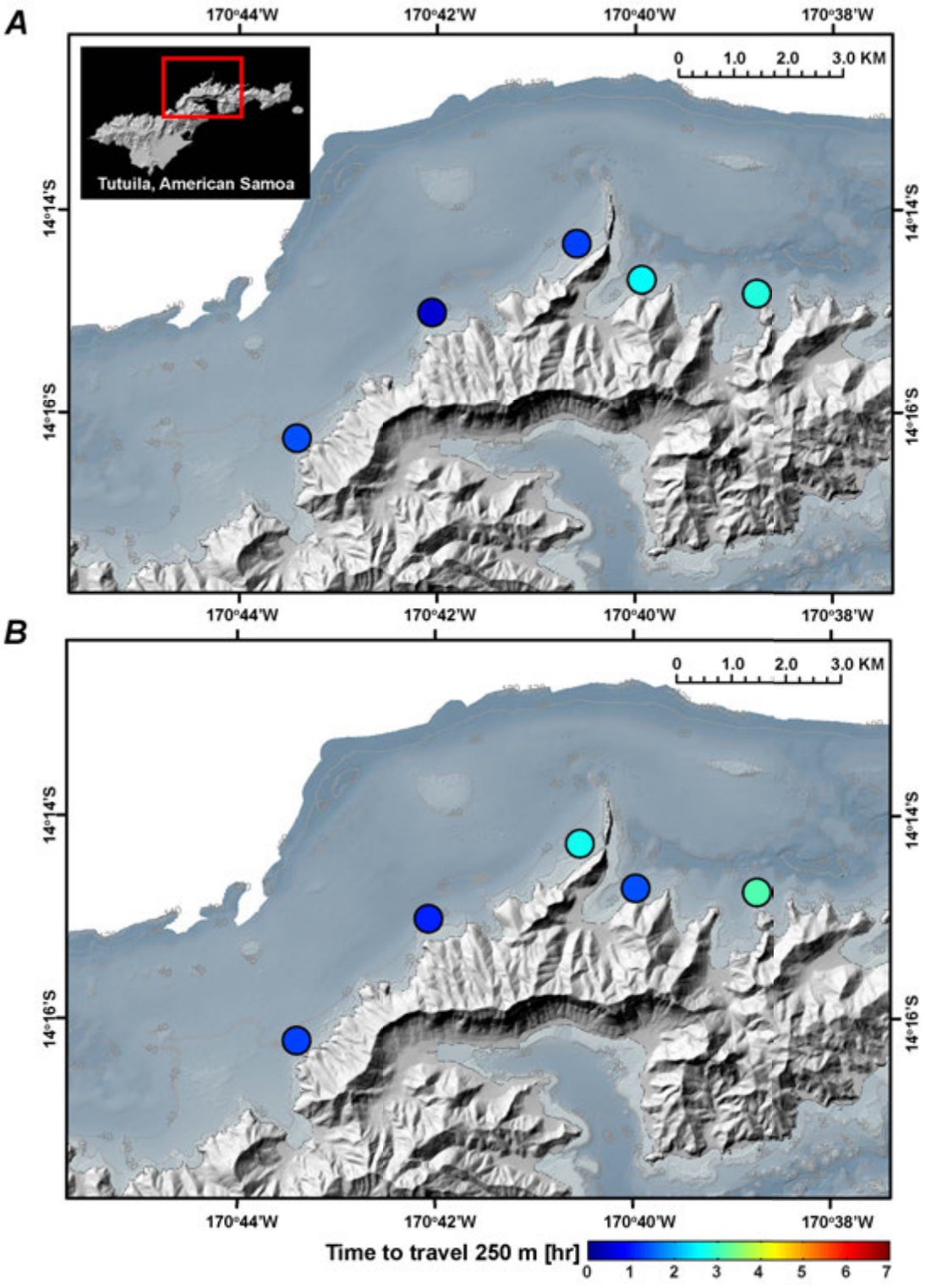

Figure 22. Maps showing computed residence times, with colors indicating time, in hours (hr), to travel 250 meters (m) for each nearshore study site by using measurements from a period of larger waves (2015 Year Day 50–56). *A*, Residence times using near-surface current velocities. *B*, Residence times using near-bed current velocities.

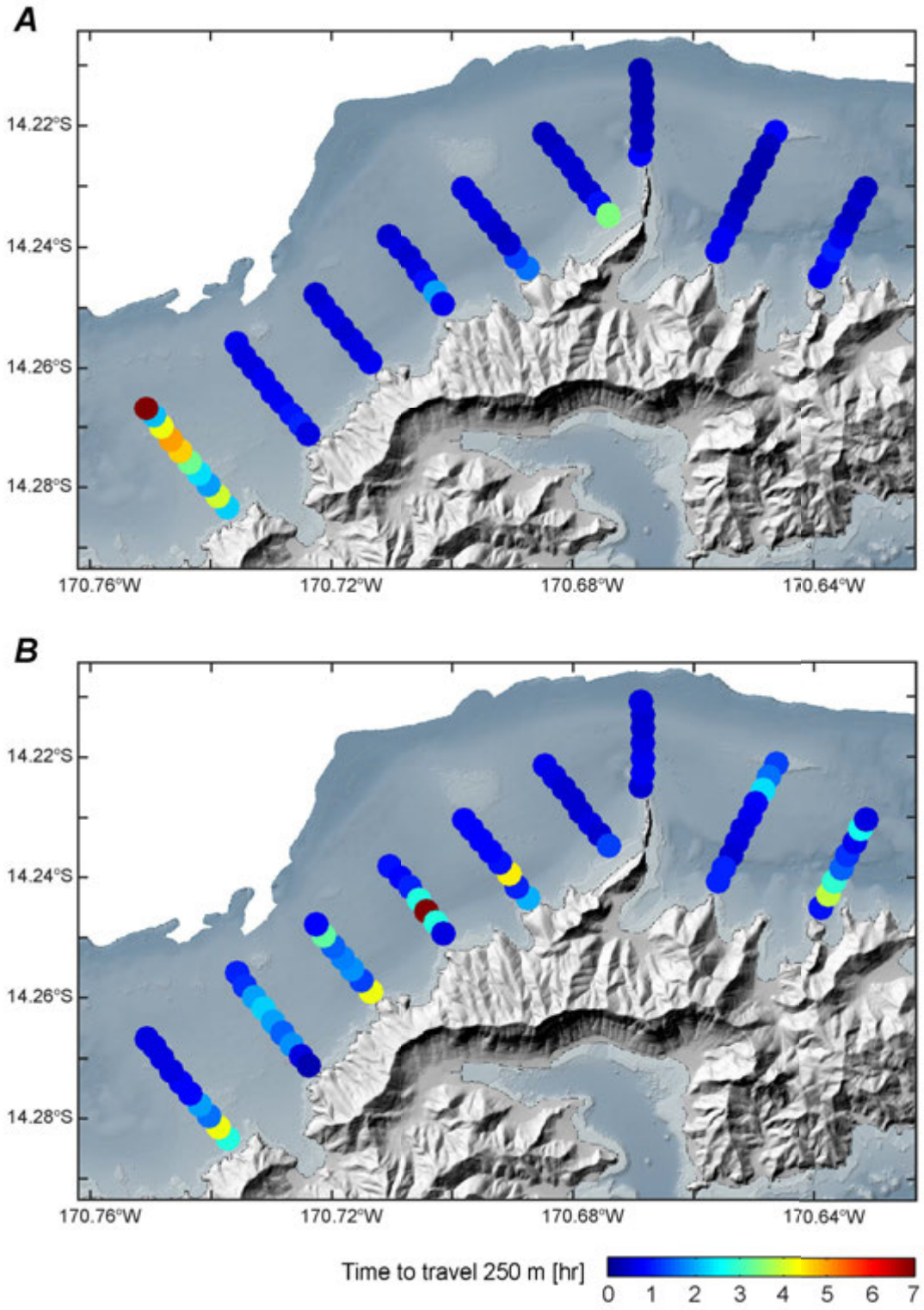

Figure 23. Maps showing computed residence times, with colors indicating time, in hours (hr), to travel 250 meters (m) along vessel-mounted acoustic Doppler current profiler (VM-ADCP) transects. A, Residence times using near-surface current velocities. *B*, Residence times using near-bed current velocities.

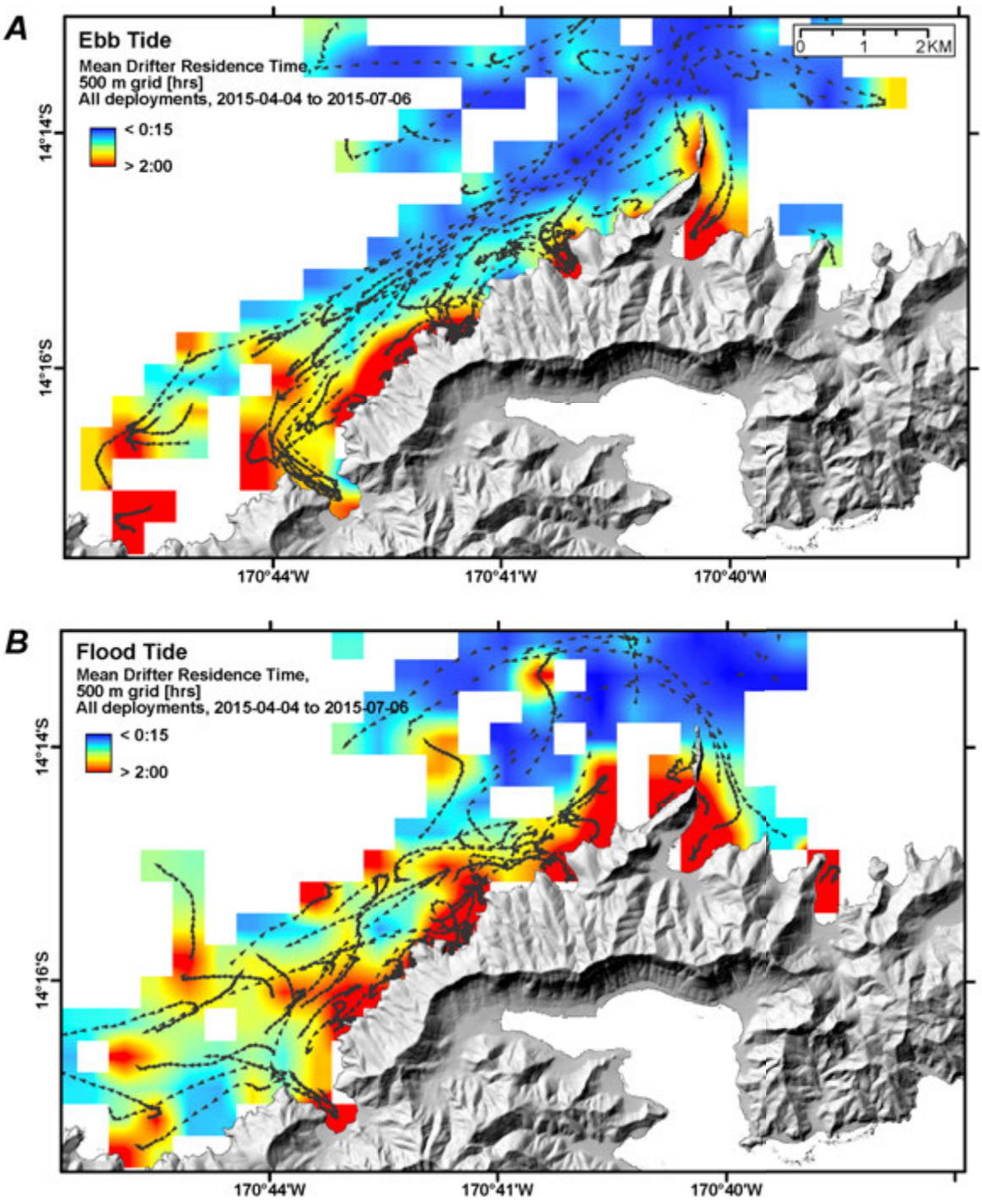

Figure 24. Maps showing Lagrangian Surface Current Drifters (LSCD) positions about every 15 minutes, mean current directions as heading ("going to"), in degrees from true north, and computed residence times, with colors indicating time, in hours (hrs), to travel 250 meters (m) from the LSCD data. *A*, Residence times during rising (flood) tides. *B*, Residence times during falling (ebb) tides.

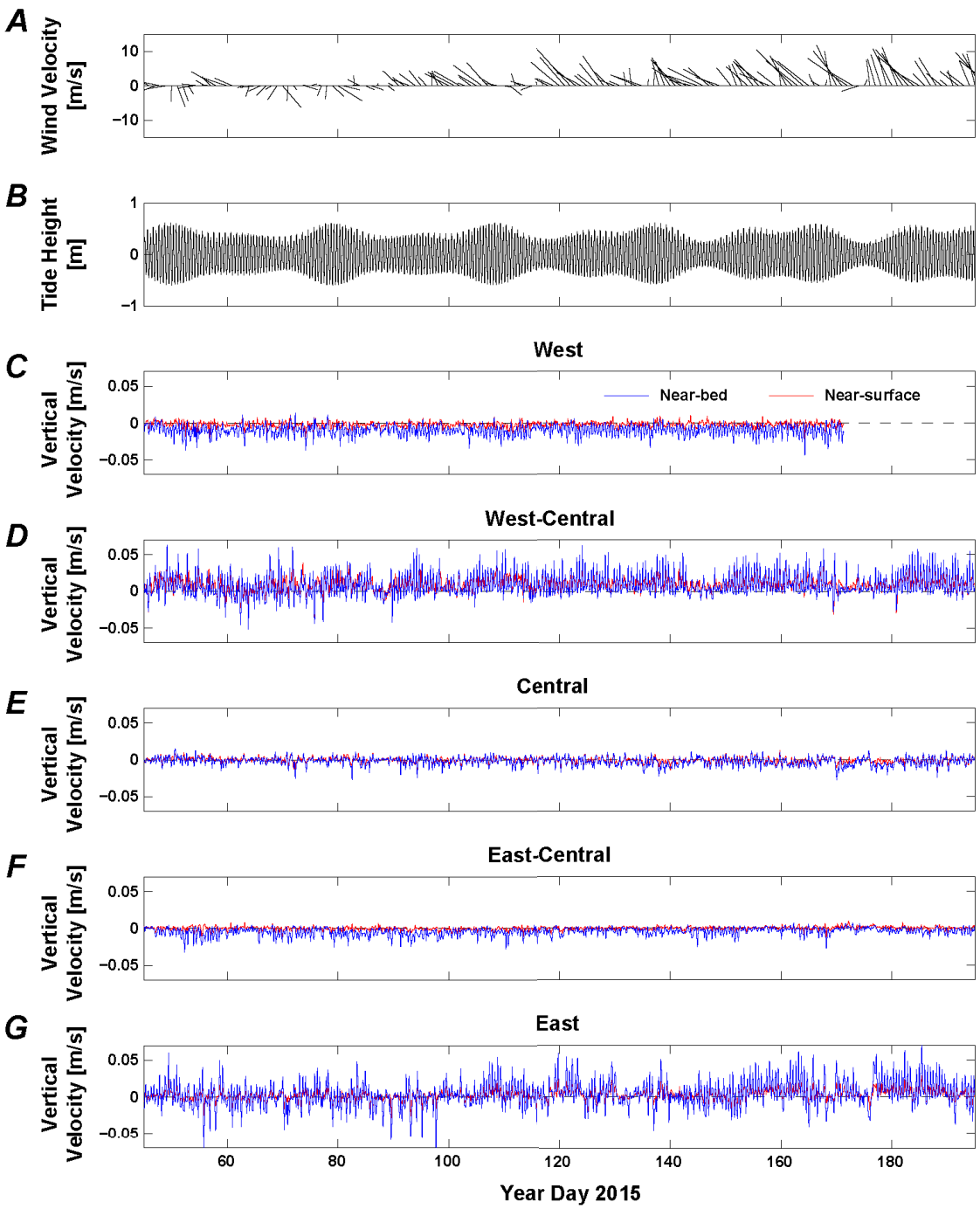

Figure 25. Time-series plots of vertical velocities measured by the MiniPROBE acoustic Doppler current profilers (ADCPs). *A*, Daily-averaged wind velocity from the Cape Matatula American Samoa Observatory, with direction shown as heading in degrees clockwise from true north and speed in meters per second (m/s) during the experiment. *B*, Tidal height, in meters (m), from the Central site. *C*, Near-bed and near-surface 3-hour-averaged vertical velocity, in meters per second (m/s), for the West site. *D*, Near-bed and near-surface 3-hour-averaged vertical velocity, in meters per second (m/s), for the West-Central site. *E*, Near-bed and near-surface 3-hour-averaged vertical velocity, in meters per second (m/s), for the Central site. *F*, Near-bed and near-surface 3-hour-averaged vertical velocity (m/s), in meters per second, for the East-Central site. *G*, Near-bed and near-surface 3-hour-averaged vertical velocity, in meters per second (m/s), for the East site.

Conclusions

During the 150 days from 14 February through 14 July 2015 (YD 45–195), more than 2 million measurements of meteorological and oceanographic parameters were made along north-central Tutuila in the National Park of American Samoa (NPSA) to characterize the important physical processes and resulting water column conditions in this region. Key findings from these measurements and analyses include the following:

1. Circulation was strongly driven by regional winds at longer (greater than day) timescales and by tides at shorter (less than day) timescales. Flows were primarily directed alongshore, with current speeds faster offshore to the north and slower closer to shore, especially in embayments. Flow generally converged around Pola Island, which appears to have been flanked by submesoscale (diameter of about 1 km) transient eddies likely formed in response to tidally driven flows around Pola Island.
2. Water-column properties exhibit strong seasonality coupled to the shift from the non-trade wind season to the trade wind season. During the non-trade wind season that was characterized by variable winds and larger waves in NPSA, waters in the Park were warmer, slightly more saline, relatively less optically clear (but still relatively clear compared with most waters close to land), and more stratified. When the winds shifted to a more consistent trade wind pattern in the austral fall, the waters cooled and became less stratified because of decreased insolation. Spatially, waters were warmer and less saline closer to the surface and closer to shore, especially in embayments, which tended to be more turbid, less clear, and were characterized by higher chlorophyll than waters offshore.
3. In general, water residence times were shorter farther offshore and longer closer to shore and in embayments, but varied spatially and temporally because of different forcing (tides, waves, winds), especially around Pola Island.
4. Warmer, lower salinity, higher chlorophyll, and more turbid waters in the embayments tend to reside in those locations for much longer durations, resulting in greater exposure of embayment ecosystems to those waters. This is in contrast with farther offshore, where the combination of shorter residence times and the prevalence of cooler, higher salinity water results in less exposure to land runoff.

Taken together, these field observations provide information on the predominant patterns of and controls on flow and water-column properties along north-central Tutuila. Understanding coastal circulation patterns and water-column properties in NPSA's waters along north-central Tutuila may help to better understand how meteorological and oceanographic processes, at both the regional and local scale, affect coral reef health and sustainability in this region.

Acknowledgments

This work was carried out as part of the USGS Pacific Coral Reef Project as part of an effort in the United States and its trust territories to better understand the effect of geologic and oceanographic processes on coral reef systems. This project was funded by the USGS Coastal and Marine Geology Program, the NPS's Pacific West Region Coral Reef Research Program, and NPS-NPSA base funding under Interagency Agreement P13PG00284. Bert Fuiava, Ari Halpern, Caitlyn Webster, Ian Moffitt, Kersten Schnurle, and Paolo Marra-Biggs of the NPS-NPSA Natural Resource Division contributed substantially to this project in innumerous ways, and without their efforts none of this would have been possible. The NPS maintenance and office staff graciously donated their time, effort, and space during

our numerous field operations. The NPS-Pacific Islands Inventory and Monitoring Program provided some of the instruments used in this field experiment. Liv Herdman (USGS) and Jessica Lovering (USGS) contributed numerous excellent suggestions and a timely review of our work.

References Cited

Coastal and Hydraulics Laboratory, U.S. Army Corps of Engineers, 2015, Wave Information Studies (WIS) hindcast wave climate information for U.S. coastal waters; Station #81159, accessed August 2015, at http://wis.usace.army.mil/products.html?staid=81159&lat=-14.50&lon=-170.00&dep=2826.

Center for Operational Oceanographic Products and Services, National Oceanographic and Atmospheric Administration, 2015, Tide data for Pago Pago, American Samoa, CO-OPS ID: 1770000, accessed August 2015, at http://tidesandcurrents.noaa.gov/stationhome.html?id=1770000.

Central Intelligence Agency, 2015, The World Fact Book, American Samoa, accessed August 2015, at https://www.cia.gov/library/publications/the-world-factbook/geos/aq.html.

National Centers for Coastal Ocean Science, National Oceanographic and Atmospheric Administration, 2005, Benthic Habitat Mapping of American Samoa, Guam, and the Commonwealth of the Northern Mariana Islands: NOAA Technical Memorandum NOS NCCOS 8, Biogeography Branch, accessed July 2015 at http://ccma.nos.noaa.gov/ecosystems/coralreef/us_pac_mapping.aspx.

National Park Service, 2015, National Park of American Samoa, accessed July 2015 at http://www.nps.gov/npsa/.

Storlazzi, C.D., McManus, M.A., and Figurski, J.D., 2003, Long-term high-frequency ADCP and temperature measurements along central California—Insights into upwelling and internal waves on the inner shelf: Continental Shelf Research, v. 23, p. 901–918.

Storlazzi, C.D., Field, M.E., Cheriton, O.M., Presto, M.K., and Logan, J.B., 2013, Rapid fluctuations in flow and water-column properties in Asan Bay, Guam—Implications for selective resilience of coral reefs in warming seas: Coral Reefs, v. 32, p. 949–961.

Additional Digital Information

The data used to produce this report can be found here:
https://doi.org/10.5066/F7RN362H

For additional information on the instrument deployments, please see the following:
http://compass.er.usgs.gov/fan_info.php?fan=2015-601-FA
http://compass.er.usgs.gov/fan_info.php?fan=2015-626-FA

For an online portable document format (PDF) version of this report, visit
https://doi.org/10.3133/ofr20171060.

For more information on the U.S. Geological Survey Pacific Coastal and Marine Science Center, visit
https://walrus.wr.usgs.gov/.

For more information on the U.S. Geological Survey's Coral Reef Project, visit
https://coralreefs.wr.usgs.gov/.

Direct Contact Information

Regarding this Report
Curt D. Storlazzi (USGS Coral Reef Project Chief): cstorlazzi@usgs.gov

Appendix 1. Acoustic Doppler Current Profiler (ADCP) Information

RD Instruments 600 kilohertz (kHz) Workhorse Monitor upward-looking acoustic Doppler current profiler

s/n: 2074, 3648, 7447, 7449

Transmitting Frequency:	614 kHz
Depth of Transducer:	20 meters (m)
Blanking Distance:	1.2 m
Height of First Bin above Bed:	2.1 m
Bin Size:	1.0 m
Number of Bins:	25
Operating Mode:	High-resolution, broad bandwidth
Sampling Frequency:	2 hertz (Hz)
Time per Ping:	0:00:0.5 second (s)
Pings per Ensemble:	240
Profile Ensemble Interval:	0:20:00.00
Wave Ensemble Interval:	2:00:00.00
Sound Speed Calculation:	Set salinity, updating temperature via sensor

RD Instruments 600 kHz Workhorse Monitor downward-looking vessel-mounted acoustic Doppler current profiler

s/n: 7419

Transmitting Frequency:	614 kHz
Depth of Transducer: 20 m	
Blanking Distance:	1.2 m
Height of First Bin above Bed:	2.1 m
Bin Size:	1.0 m
Number of Bins:	25
Operating Mode:	High-resolution, broad bandwidth
Sampling Frequency:	2 Hz
Time per Ping:	0:00:0.5 s
Pings per Ensemble:	240
Profile Ensemble Interval:	0:20:00.00
NO WAVE SAMPLING	
Sound Speed Calculation:	Set salinity, updating temperature via sensor

Data Processing:

The RDI current data were processed by using the WinADCP program and the wave data by using the WavesMon program.

All spurious data above the water surface were removed and all data in bins where beam correlation dropped below 90 percent were removed for visualization and analysis.

Appendix 2. Temperature Logger (TL) and Conductivity and Temperature (CT) Sensor Information

Onset HOBO U22-001 temperature logger (TL)
s/n: 2233014, 2233014, 2233015, 2240561, 2240564, 2386840, 10019064, 10019065, 10019067, 10019069, 10019070, 10019073, 10019074, 10019075, 10019076, 10019077, 10019078, 10019079, 10019080, 10019081, 10466198, 10466199, 10466200, 10466201
Sampling Interval: 2 minutes

Seabird Microcat SBE-37SM temperature-conductivity (CT) sensors
s/n: 3825, 3830, 3833, 4087, 4088
Sampling Interval: 3 minutes
Number of samples averaged: 4

Seabird Microcat SBE-37SMP pumped temperature-conductivity (CT) sensors
s/n: 4221, 4361, 4362
Sampling Interval: 3 minutes
Number of samples averaged: 4

Data Processing:
The TL temperature data were processed using HOBOware. The CT data were processed by using the SeaTerm. Further quality control and data analysis was performed on the data by using MatLab.

Appendix 3. Water Column Profiler (WCP) Information

Instruments:

Seabird 19plus CTD sensor; s/n:	5250
D&A Instruments OBS-3 sensor; s/n:	1134
Wet Labs CSTAR transmissometer; s/n:	712
Wet Labs WetStar fluorometer; s/n:	21
Sampling Frequency:	4 hertz (Hz)

Position Information:

Garmin GPS-76 global positioning system (GPS); s/n: 80207465; USGS/CRP unit#1

Data Processing:

Profiler data were processed by using the SBEDataProcessing program.

Data were averaged into 0.25 m vertical bins and all spurious data marked by a flag in the raw data were removed for visualization and analysis.

Appendix 4. Water Column Profiler Log

Table 4-1. Water column profiler log for Year Day 48 (17 February 2015).
[m, meters; SST, Samoa Standard Time]

Cast #	Time (SST)	Latitude (decimal degrees)	Longitude (decimal degrees)	Depth (m)
1	10:42	−14.2564	−170.6523	10.8
2	10:56	−14.2485	−170.6444	10.0
3	11:19	−14.2336	−170.6368	43.3
4	11:32	−14.2259	−170.6514	37.3
5	12:13	−14.2447	−170.6608	31.0
6	12:23	−14.2492	−170.6736	5.5
7	12:33	−14.2289	−170.6721	36.3
8	13:01	−14.2148	−170.6716	41.3
9	13:14	−14.2249	−170.6880	41.5
10	13:38	−14.2394	−170.6757	11.3
11	13:48	−14.2527	−170.6900	19.5
12	13:54	−14.2471	−170.6886	20.0
13	14:27	−14.2337	−170.7000	41.0
14	14:34	−14.2401	−170.7107	41.3
15	14:59	−14.2518	−170.7018	24.5
16	15:08	−14.2611	−170.7124	17.5
17	15:25	−14.2489	−170.7233	41.5
18	15:33	−14.2556	−170.7351	40.8
19	15:58	−14.2720	−170.7226	16.8
20	16:08	−14.2831	−170.7344	6.5
21	16:28	−14.2664	−170.7490	41.3
22	16:40	−14.2854	−170.7228	15.5

Table 4-2. Water column profiler log for Year Day 49 (18 February 2015).
[m, meters; SST, Samoa Standard Time]

Cast #	Time (SST)	Latitude (decimal degrees)	Longitude (decimal degrees)	Depth (m)
1	09:50	−14.2855	−170.7231	14.8
2	10:19	−14.2831	−170.7350	11.3
3	10:41	−14.2663	−170.7492	41.3
4	10:51	−14.2571	−170.7354	41.8
5	11:18	−14.2713	−170.7230	30.5
6	11:29	−14.2604	−170.7124	21.5
7	11:18	−14.2487	−170.7232	38.8
8	12:00	−14.2387	−170.7121	38.5
9	12:23	−14.2511	−170.7014	14.3
10	12:30	−14.2530	−170.6902	9.0
11	12:45	−14.2430	−170.6976	40.0
12	12:57	−14.2466	−170.6884	27.5

Cast #	Time (SST)	Latitude (decimal degrees)	Longitude (decimal degrees)	Depth (m)
13	13:14	−14.2331	−170.7000	40.3
14	13:27	−14.2241	−170.6872	39.8
15	13:50	−14.2393	−170.6752	7.3
16	14:01	−14.2292	−170.6721	18.8
17	14:19	−14.2143	−170.6722	42.8
18	14:49	−14.2492	−170.6736	6.5
19	15:39	−14.2447	−170.6608	41.0
20	15:20	−14.2263	−170.6511	42.5
21	16:16	−14.2315	−170.6359	17.5
22	16:19	−14.2479	−170.6451	8.5

Table 4-3. Water column profiler log for Year Day 50 (19 February 2015).
[m, meters; SST, Samoa Standard Time]

Cast #	Time (SST)	Latitude (decimal degrees)	Longitude (decimal degrees)	Depth (m)
1	10:23	−14.2568	−170.6524	10.0
2	10:57	−14.2567	−170.6523	17.5
3	11:15	−14.2484	−170.6444	42.0
4	11:25	−14.2338	−170.6369	23.0
5	11:55	−14.2258	−170.6511	19.3
6	12:22	−14.2449	−170.6608	5.3
7	12:34	−14.2493	−170.6739	42.3
8	12:54	−14.2287	−170.6715	42.0
9	13:05	−14.2146	−170.6715	43.0
10	13:29	−14.2238	−170.6862	13.8
11	13:38	−14.2394	−170.6758	14.8
12	14:02	−14.2527	−170.6896	27.3
13	14:22	−14.2466	−170.6886	39.8
14	14:30	−14.2331	−170.6998	40.8
15	14:51	−14.2388	−170.7106	7.0
16	15:01	−14.2530	−170.7005	27.8
17	15:20	−14.2606	−170.7125	41.8
18	15:29	−14.2488	−170.7232	41.8
19	15:52	−14.2566	−170.7351	8.5
20	16:13	−14.2719	−170.7231	14.5
21	16:46	−14.2857	−170.7228	7.3
22	17:12	−14.2833	−170.7344	41.0

Table 4-4. Water column profiler log for Year Day 51 (20 February 2015).
[m, meters; SST, Samoa Standard Time]

Cast #	Time (SST)	Latitude (decimal degrees)	Longitude (decimal degrees)	Depth (m)
1	10:30	−14.2664	−170.7491	12.8
2	10:47	−14.2858	−170.7227	25.5
3	11:13	−14.2833	−170.7354	39.8
4	11:28	−14.2666	−170.7493	41.3
5	11:55	−14.2564	−170.7355	27.5
6	12:08	−14.2714	−170.7234	41.3
7	12:28	−14.2608	−170.7134	42.3
8	12:42	−14.2485	−170.7228	42.8
9	13:04	−14.2382	−170.7132	7.0
10	13:12	−14.2529	−170.7003	16.8
11	13:20	−14.2526	−170.6898	31.8
12	13:44	−14.2464	−170.6885	40.8
13	13:54	−14.2335	−170.6995	42.3
14	14:13	−14.2250	−170.6876	8.3
15	14:23	−14.2394	−170.6757	42.0
16	14:47	−14.2286	−170.6714	41.8
17	14:59	−14.2149	−170.6713	24.3
18	15:27	−14.2259	−170.6511	33.0
19	15:36	−14.2444	−170.6604	6.5
20	15:51	−14.2492	−170.6734	12.5
21	16:00	−14.2563	−170.6523	17.0
22	16:20	−14.2484	−170.6443	41.5

Table 4-5. Water column profiler log for Year Day 199 (18 July 2015).
[m, meters; SST, Samoa Standard Time]

Cast #	Time (SST)	Latitude (decimal degrees)	Longitude (decimal degrees)	Depth (m)
1	10:31	−14.24794	−170.64458	23.2
2	10:43	−14.23316	−170.63645	41.6
3	10:52	−14.22593	−170.65132	36.8
4	11:03	−14.25668	−170.65217	10.6
5	11:12	−14.24466	−170.66063	30.6
6	11:19	−14.24923	−170.67358	6.6
7	11:29	−14.22869	−170.67188	41.6
8	11:38	−14.21461	−170.67164	40.6
9	11:48	−14.22440	−170.68715	42.3
10	11:56	−14.23912	−170.67551	16.0
11	12:03	−14.24678	−170.68843	20.5
12	12:12	−14.25273	−170.68990	17.9
13	12:19	−14.24277	−170.69725	44.0
14	12:26	−14.23336	−170.69970	41.4

Cast #	Time (SST)	Latitude (decimal degrees)	Longitude (decimal degrees)	Depth (m)
15	12:33	−14.23922	−170.71134	43.8
16	12:41	−14.25131	−170.70105	19.6
17	12:49	−14.24852	−170.72322	41.9
18	12:58	−14.26088	−170.71266	24.7
19	13:06	−14.25649	−170.73534	42.4
20	13:15	−14.27162	−170.72294	20.2
21	13:23	−14.26623	−170.74912	43.2
22	13:33	−14.28318	−170.73477	7.6
23	13:41	−14.28556	−170.72295	14.6

Appendix 5. Internal Tide Schematic

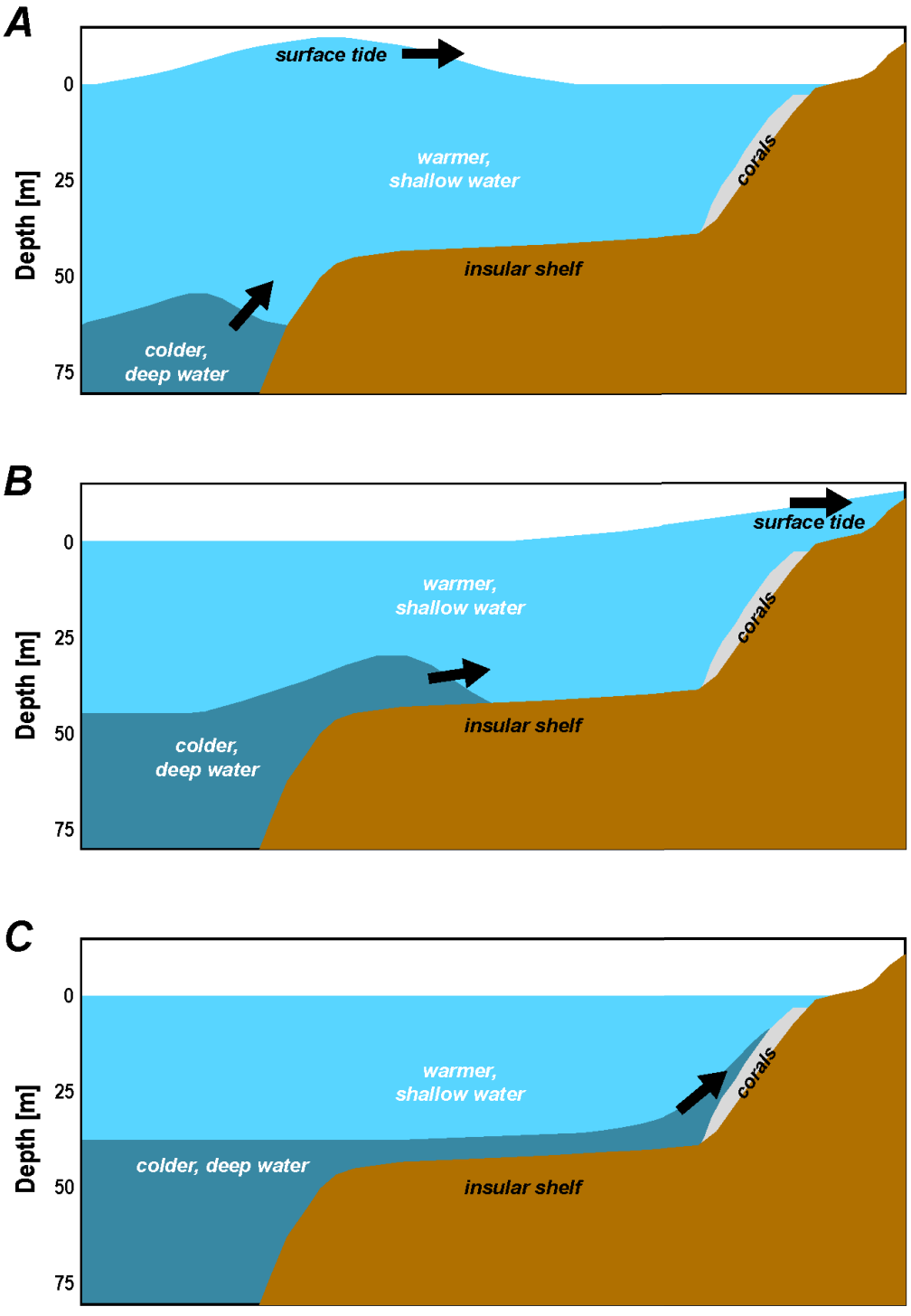

Figure 5–1. Schematic showing phasing between surface tide and internal tide off northern Tutuila and associated advection of colder, deep water up into the shallows and over National Park of American Samoa (NPSA) coral reefs.

Appendix 6. Time-Series Data from Mooring Sites

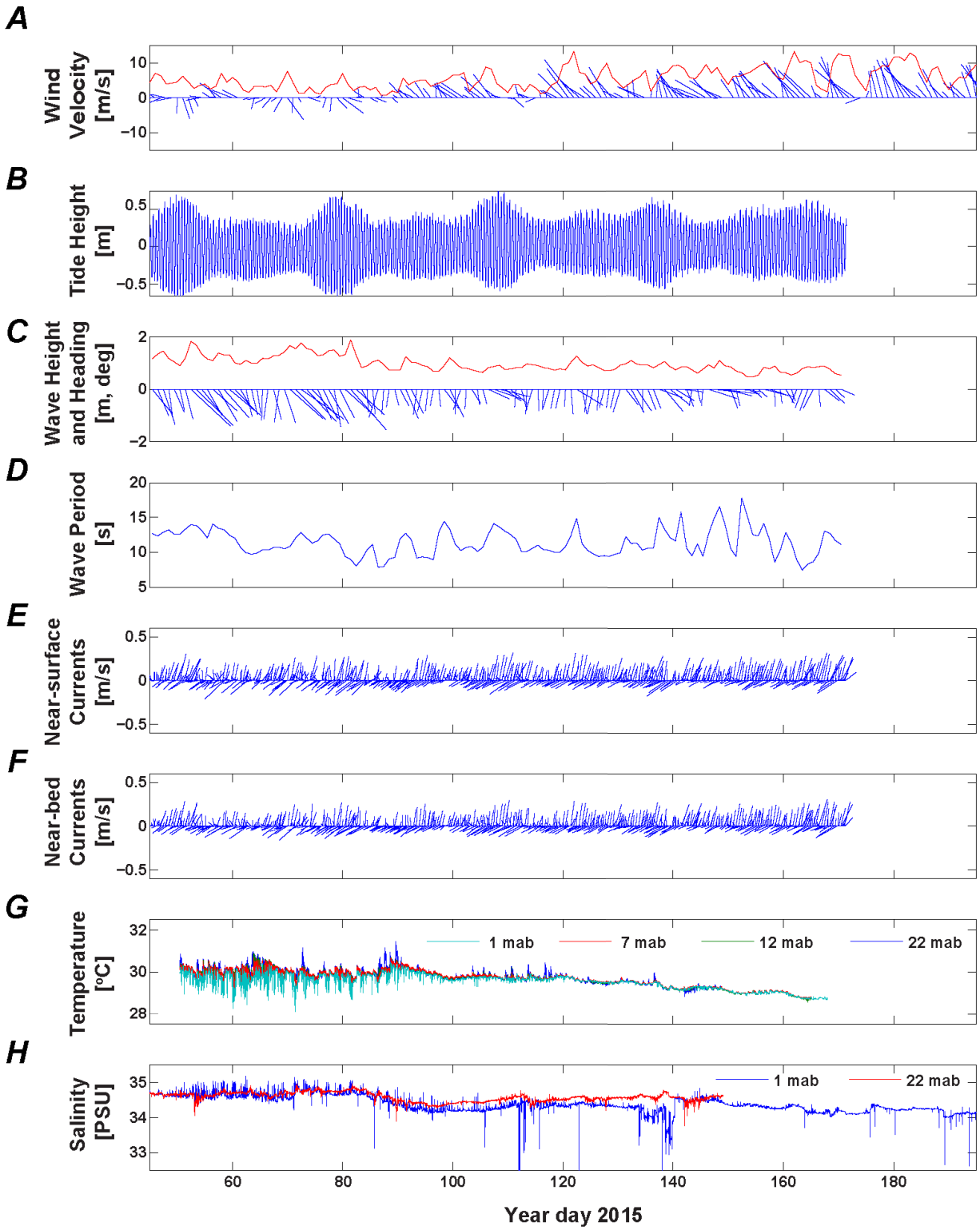

Figure 6–1. (previous page) Time-series plot of meteorological data from the Cape Matatula American Samoa Observatory station (SMO) and oceanographic data from the West site. *A*, Daily-averaged wind velocity (blue lines), with direction indicating heading ("going to"), in degrees clockwise from true north and speed in meters per second (m/s), and daily-averaged wind speed (red line) in meters per second. *B*, Tidal height, in meters (m). *C*, Daily-averaged wave vectors (blue line), where vector length is wave height in meters (m) and direction indicating heading ("going to") measured in degrees (deg) clockwise from true north, with daily-averaged significant wave height (red line) in meters. *D*, Daily-averaged peak wave period in seconds (s). *E*, 4-hour-averaged near-surface current velocity, with direction indicating heading ("going to") measured in degrees clockwise from true north and speed in meters per second (m/s). *F*, 4-hour-averaged near-bed current velocity, with direction indicating heading ("going to") measured in degrees clockwise from true north and speed in meters per second (m/s). *G*, Water temperature, in degrees Celsius (°C), at various heights above the seabed. *H*, Near-bed water salinity in Practical Salinity Units (PSU). mab, meters above bottom.

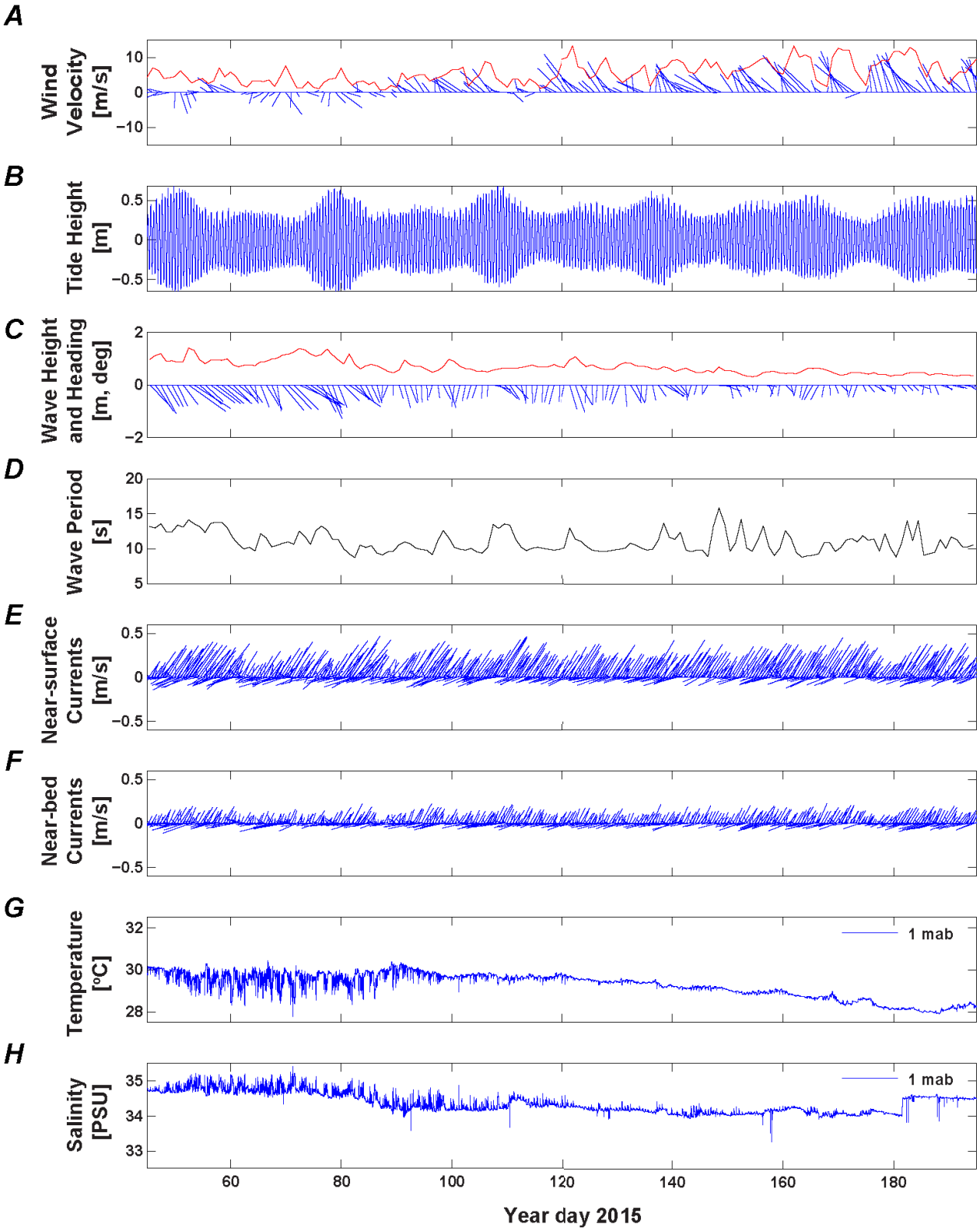
A
Wind Velocity [m/s]
10
0
−10
B
Tide Height [m]
0.5
0
−0.5
C
Wave Height and Heading [m, deg]
2
0
−2
D
Wave Period [s]
20
15
10
5
E
Near-surface Currents [m/s]
0.5
0
−0.5
F
Near-bed Currents [m/s]
0.5
0
−0.5
G
Temperature [°C]
32
30
28
1 mab
H
Salinity [PSU]
35
34
33
1 mab
60
80
100
120
140
160
180
Year day 2015

Figure 6–2. (previous page) Time-series plot of meteorological data from the Cape Matatula American Samoa Observatory station (SMO) and oceanographic data from the West-Central site. *A*, Daily-averaged wind velocity (blue lines), with direction indicating heading ("going to"), in degrees clockwise from true north and speed in meters per second (m/s), and daily-averaged wind speed (red line) in meters per second. *B*, Tidal height, in meters (m). *C*, Daily-averaged wave vectors (blue lines), where vector length is wave height in meters and direction indicating heading ("going to") measured in degrees (deg) clockwise from true north, with daily-averaged significant wave height (red line) in meters (m). *D*, Daily-averaged peak wave period in seconds (s). *E*, 4-hour-averaged near-surface current velocity, with direction indicating heading ("going to") measured in degrees clockwise from true north and speed in meters per second (m/s). *F*, 4-hour-averaged near-bed current velocity, with direction indicating heading ("going to") measured in degrees clockwise from true north and speed in meters per second (m/s). *G*, Near-bed water temperature, in degrees Celsius (°C). *H*, Near-bed water salinity in Practical Salinity Units (PSU). mab, meters above bottom.

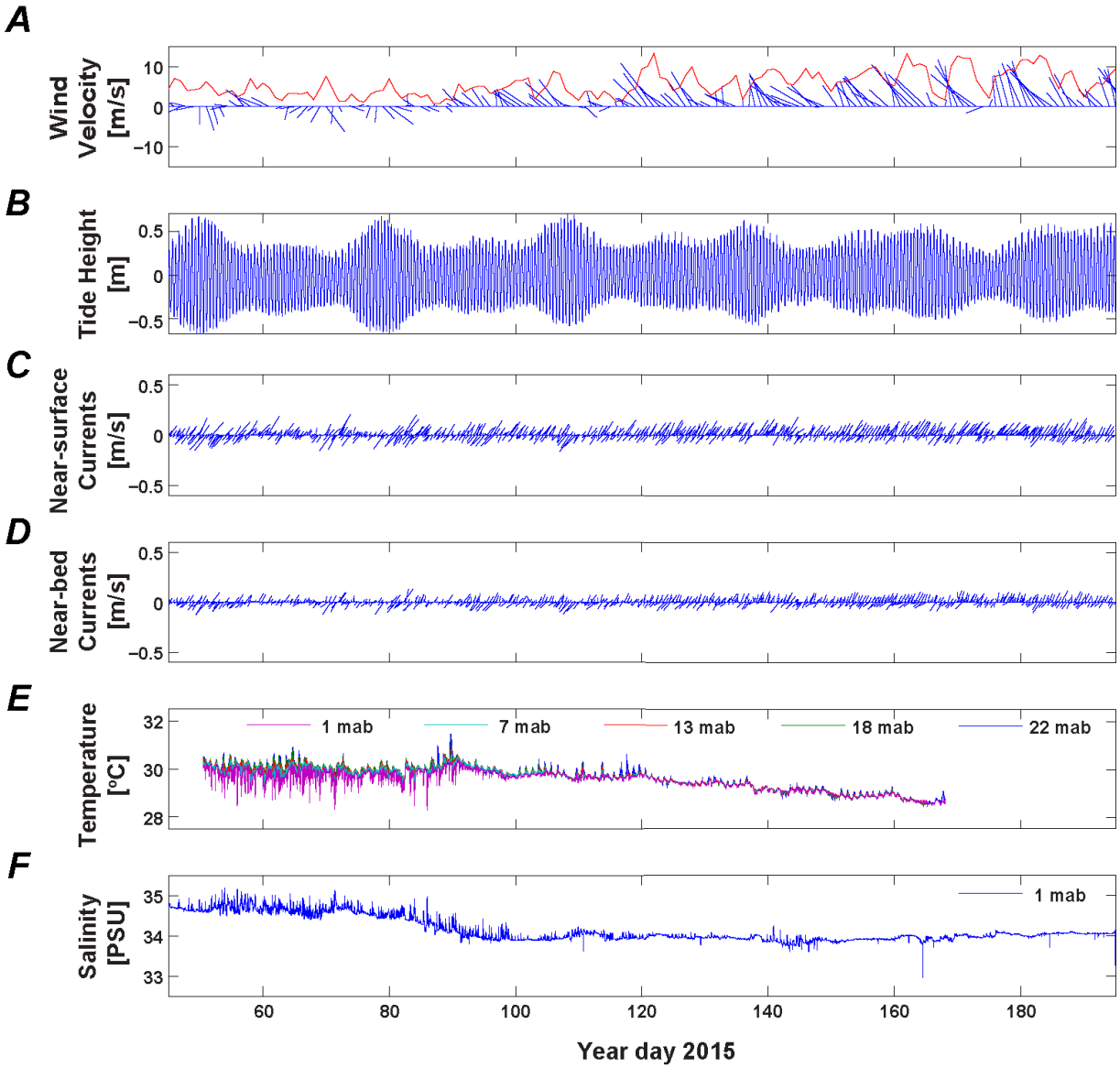

Figure 6–3. Time-series plot of meteorological data from the Cape Matatula American Samoa Observatory station (SMO) and oceanographic data from the Central site. *A*, Daily-averaged wind velocity (blue lines), with direction indicating heading ("going to"), in degrees clockwise from true north and speed in meters per second (m/s), and daily-averaged wind speed (red line) in meters per second. *B*, Tidal height, in meters (m). *C*, 4-hour-averaged near-surface current velocity, with direction indicating heading ("going to") measured in degrees clockwise from true north and speed in meters per second (m/s). *D*, 4-hour-averaged near-bed current velocity, with direction indicating heading ("going to") measured in degrees clockwise from true north and speed in meters per second (m/s). *E*, Water temperature, in degrees Celsius (°C), at various heights above the seabed. *F*, Near-bed water salinity in Practical Salinity Units (PSU). mab, meters above bottom.

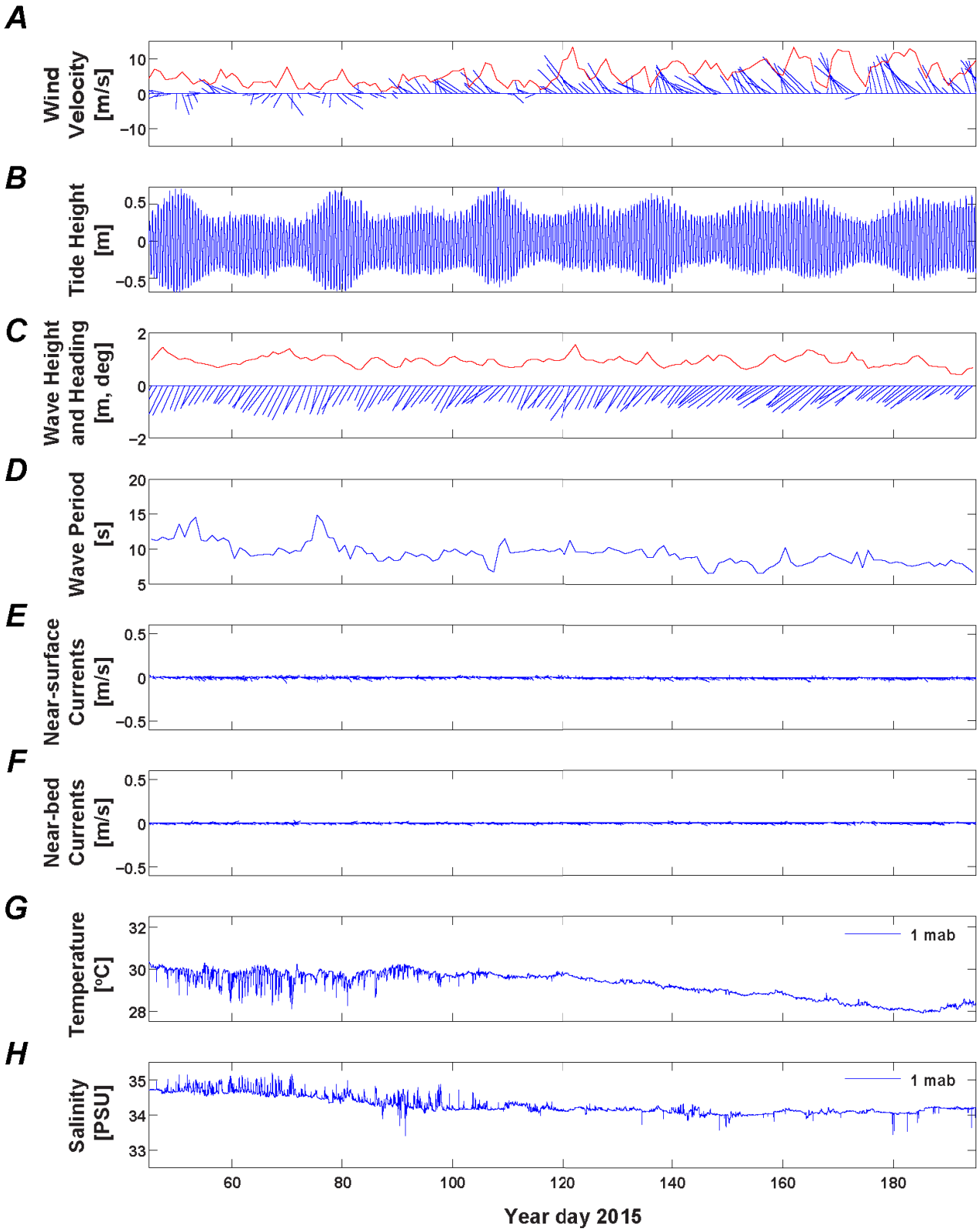
A
Wind Velocity [m/s]
10
0
−10
B
Tide Height [m]
0.5
0
−0.5
C
Wave Height and Heading [m, deg]
2
0
−2
D
Wave Period [s]
20
15
10
5
E
Near-surface Currents [m/s]
0.5
0
−0.5
F
Near-bed Currents [m/s]
0.5
0
−0.5
G
Temperature [°C]
32
30
28
1 mab
H
Salinity [PSU]
35
34
33
1 mab
60
80
100
120
140
160
180
Year day 2015

Figure 6–4. (previous page) Time-series plot of meteorological data from the Cape Matatula American Samoa Observatory station (SMO) and oceanographic data from the East-Central site. *A*, Daily-averaged wind velocity (blue lines), with direction indicating heading ("going to"), in degrees clockwise from true north and speed in meters per second (m/s), and daily-averaged wind speed (red line) in meters per second. *B*, Tidal height, in meters (m). *C*, Daily-averaged wave vectors (blue lines), where vector length is wave height in meters (m) and direction indicating heading ("going to") measured in degrees (deg) clockwise from true north, with daily-averaged significant wave height (red line) in meters. *D*, Daily-averaged peak wave period in seconds (s). *E*, 4-hour-averaged near-surface current velocity, with direction indicating heading ("going to") measured in degrees clockwise from true north and speed in meters per second (m/s). *F*, 4-hour-averaged near-bed current velocity, with direction indicating heading ("going to") measured in degrees clockwise from true north and speed in meters per second (m/s). *G*, Near-bed water temperature, in degrees Celsius (°C). *H*, Near-bed water salinity in Practical Salinity Units (PSU). mab, meters above bottom.

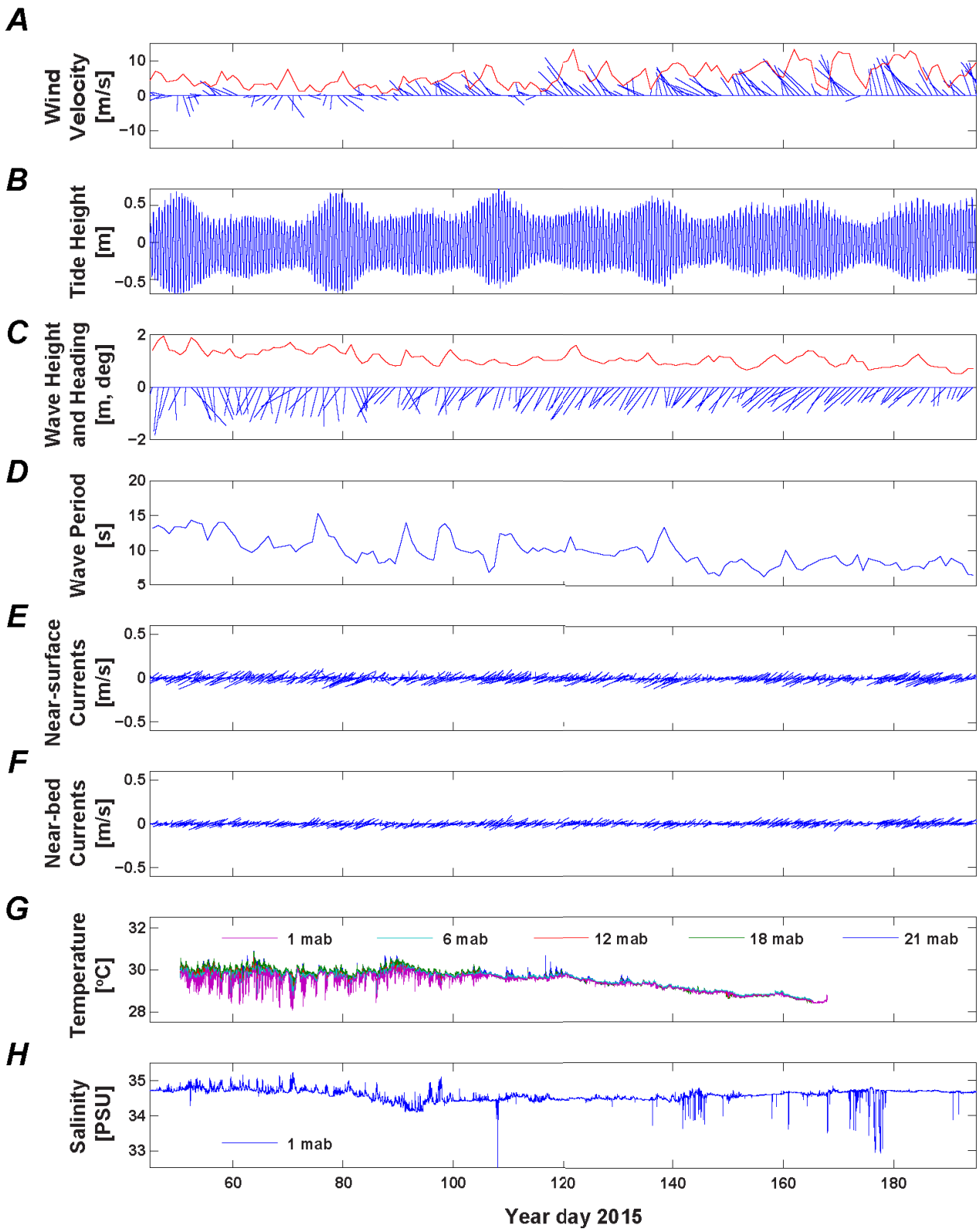
A
Wind Velocity [m/s]
10
0
−10
B
Tide Height [m]
0.5
0
−0.5
C
Wave Height and Heading [m, deg]
2
0
−2
D
Wave Period [s]
20
15
10
5
E
Near-surface Currents [m/s]
0.5
0
−0.5
F
Near-bed Currents [m/s]
0.5
0
−0.5
G
Temperature [°C]
32
30
28
1 mab
6 mab
12 mab
18 mab
21 mab
H
Salinity [PSU]
35
34
33
1 mab
60
80
100
120
140
160
180
Year day 2015

Figure 6–5. (previous page) Time-series plot of meteorological data from the Cape Matatula American Samoa Observatory station (SMO) and oceanographic data from the East site. *A*, Daily-averaged wind velocity (blue lines), with direction indicating heading ("going to"), in degrees clockwise from true north and speed in meters per second, and daily-averaged wind speed (red line) in meters per second (m/s). *B*, Tidal height, in meters (m). *C*, Daily-averaged wave vectors (blue lines), where vector length is wave height in meters (m) and direction indicating heading ("going to") measured in degrees (deg) clockwise from true north, with daily-averaged significant wave height (red line) in meters. *D*, Daily-averaged peak wave period in seconds (s). *E*, 4-hour-averaged near-surface current velocity, with direction indicating heading ("going to") measured in degrees clockwise from true north and speed in meters per second (m/s). *F*, 4-hour-averaged near-bed current velocity, with direction indicating heading ("going to") measured in degrees clockwise from true north and speed in meters per second (m/s). *G*, Water temperature, in degrees Celsius (°C), at various heights above the seabed. *H*, Near-bed water salinity in Practical Salinity Units (PSU). mab, meters above bottom.

Appendix 7. Spatial Wind Data from the Vessel-Mounted ADCP (VM-ADCP) Surveys

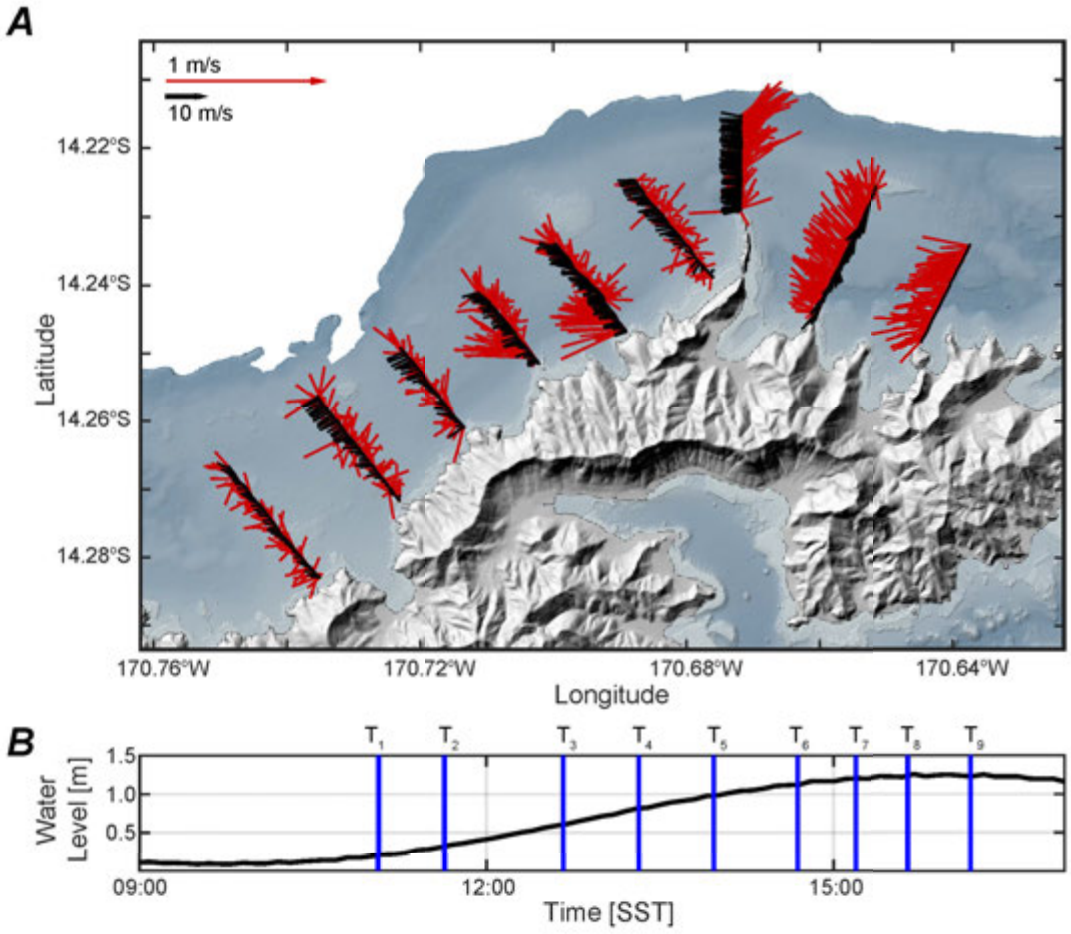

Figure 7–1. Winds and tides during the vessel-mounted acoustic Doppler current profiler (VM-ADCP) survey on Year Day 48 (17 February 2015). *A*, Map of near-surface wind directions (black lines) and resulting currents (red lines) as heading ("going to"), in degrees from true north, and speeds, in meters per second (m/s). *B*, Water level above mean, in meters (m), with the time the transects were started denoted by the blue vertical lines; SST, Samoa Standard Time.

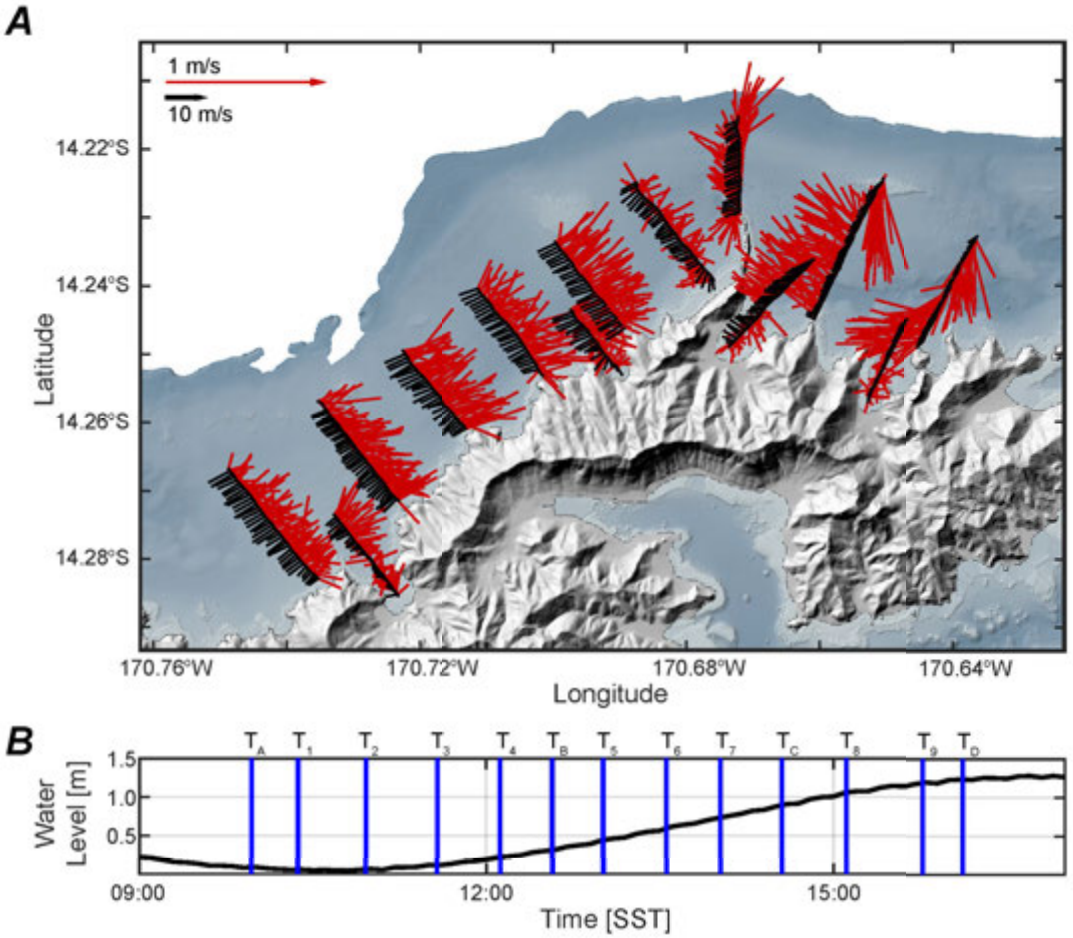

Figure 7–2. Winds and tides during the vessel-mounted acoustic Doppler current profiler (VM-ADCP) survey on Year Day 49 (18 February 2015). *A*, Map of near-surface wind directions (black lines) and resulting currents (red lines) as heading ("going to"), in degrees from true north, and speeds, in meters per second (m/s). *B*, Water level above mean, in meters (m), with the time the transects were started denoted by the blue vertical lines; SST, Samoa Standard Time.

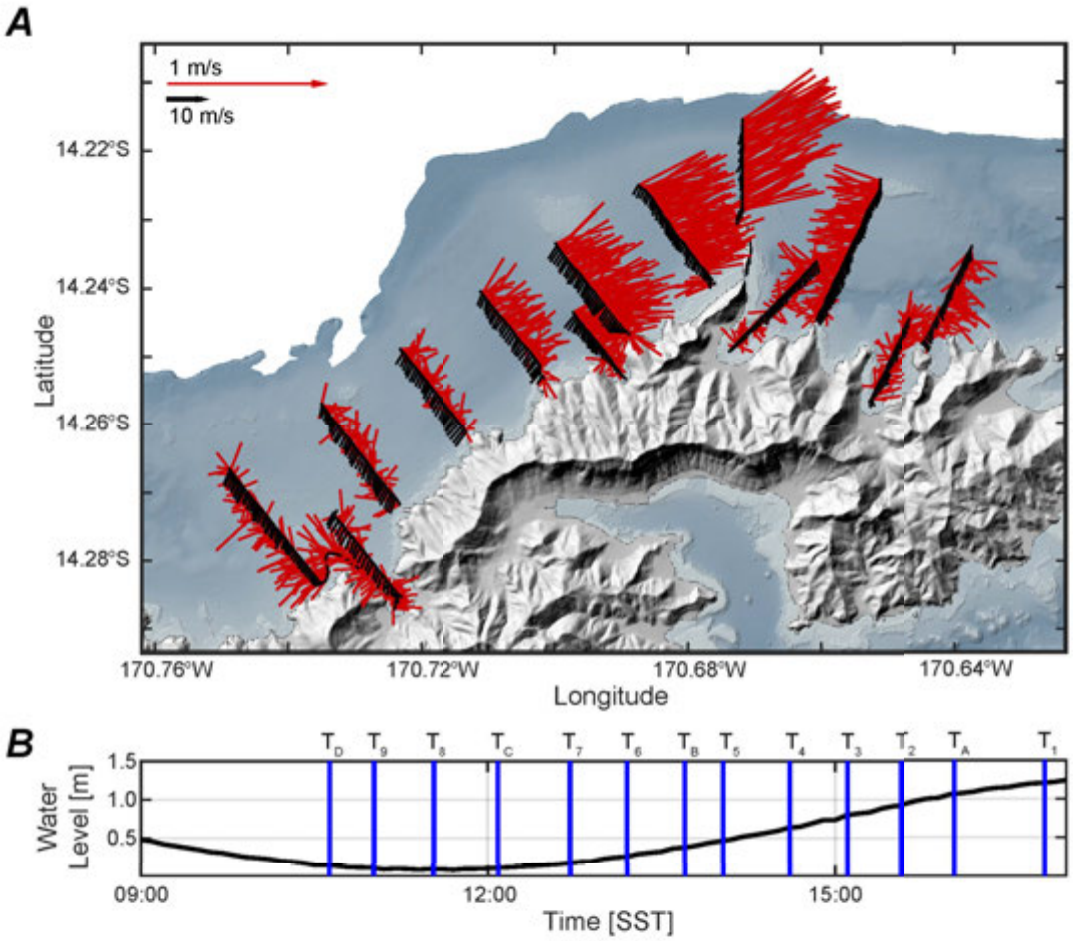

Figure 7–3. Winds and tides during the vessel-mounted acoustic Doppler current profiler (VM-ADCP) survey on Year Day 50 (19 February 2015). *A*, Map of near-surface wind directions (black lines) and resulting currents (red lines) as heading ("going to"), in degrees from true north, and speeds, in meters per second (m/s). *B*, Water level above mean, in meters (m), with the time the transects were started denoted by the blue vertical lines; SST, Samoa Standard Time.

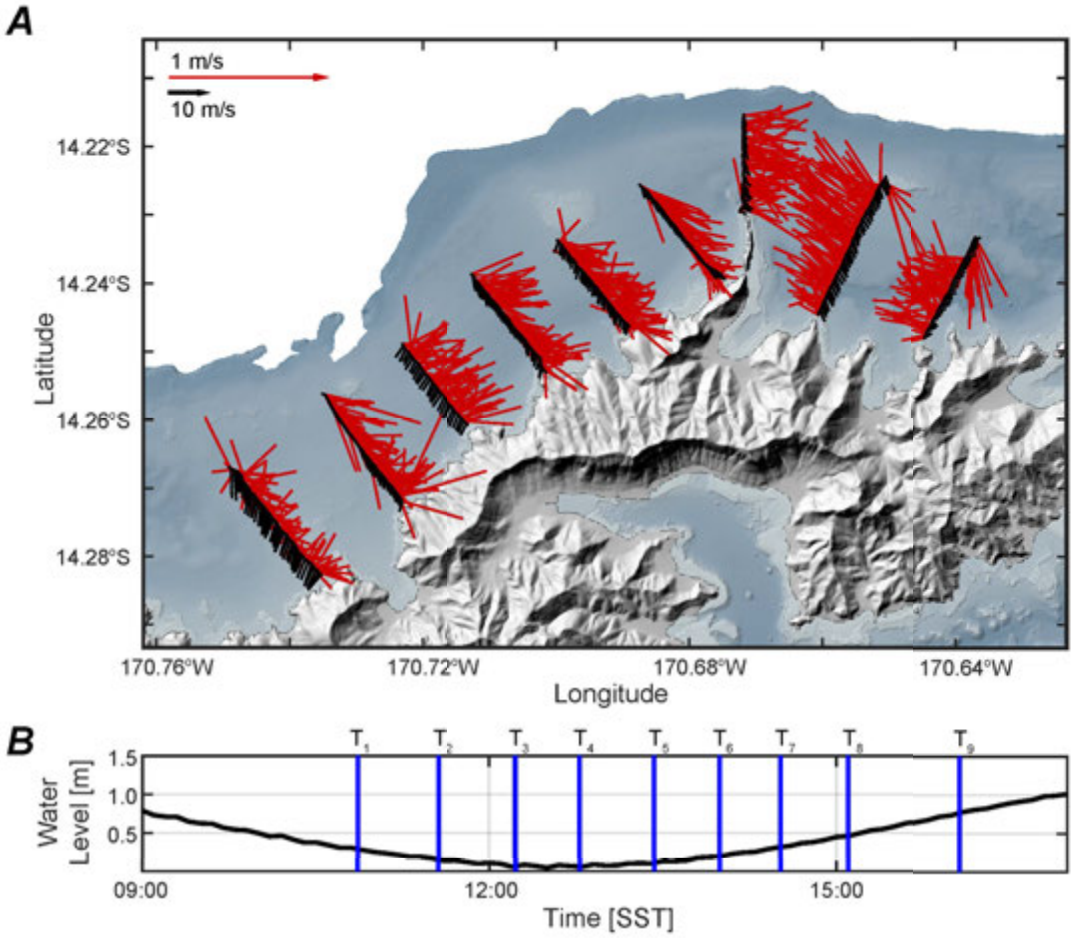

Figure 7–4. Winds and tides during the vessel-mounted acoustic Doppler current profiler (VM-ADCP) survey on Year Day 51 (20 February 2015). *A*, Map of near-surface wind directions (black lines) and resulting currents (red lines) as heading ("going to"), in degrees from true north, and speeds, in meters per second (m/s). *B*, Water level above mean, in meters (m), with the time the transects were started denoted by the blue vertical lines; SST, Samoa Standard Time.

Appendix 8. Time-Series Data from Mooring Sites During the Vessel-Mounted ADCP (VM-ADCP) Surveys

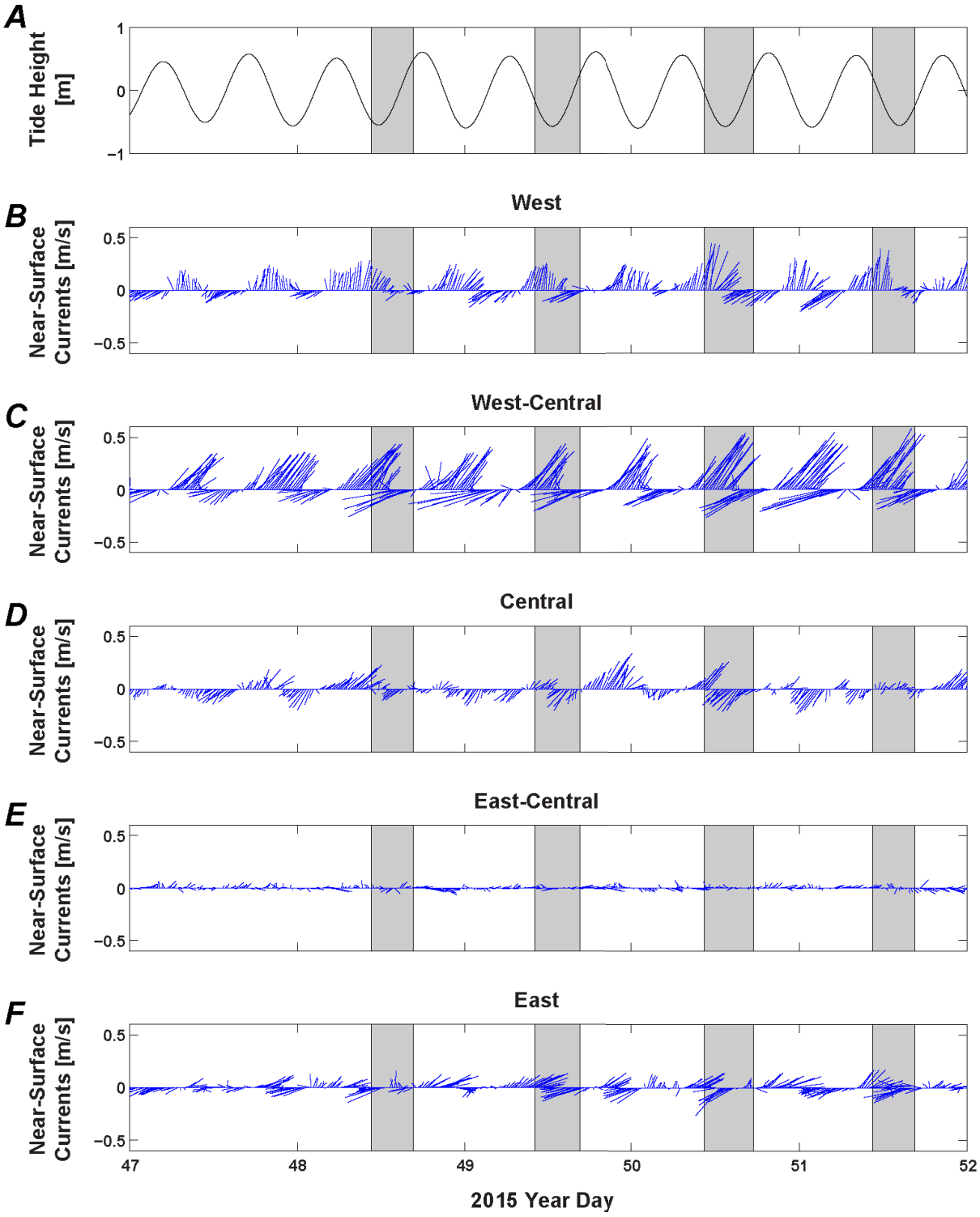

Figure 8–1. (previous page) Time-series plots tidal height and near-surface current velocities from the moorings during the February 2015 vessel-mounted acoustic Doppler current profiler (VM-ADCP) surveys (gray boxes). *A*, Tidal height, in meters (m), from the Central site. *B*, Near-surface current velocity from the West site, with direction indicating heading ("going to") measured in degrees clockwise from true north and speed in meters per second (m/s). *C*, Near-surface current velocity from the West-Central site, with direction indicating heading ("going to") measured in degrees clockwise from true north and speed in meters per second (m/s). *D*, Near-surface current velocity from the Central site, with direction indicating heading ("going to") measured in degrees clockwise from true north and speed in meters per second (m/s). *E*, Near-surface current velocity from the East-Central site, with direction indicating heading ("going to") measured in degrees clockwise from true north and speed in meters per second (m/s). *F*, Near-surface current velocity from the East site, with direction indicating heading ("going to") measured in degrees clockwise from true north and speed in meters per second (m/s).

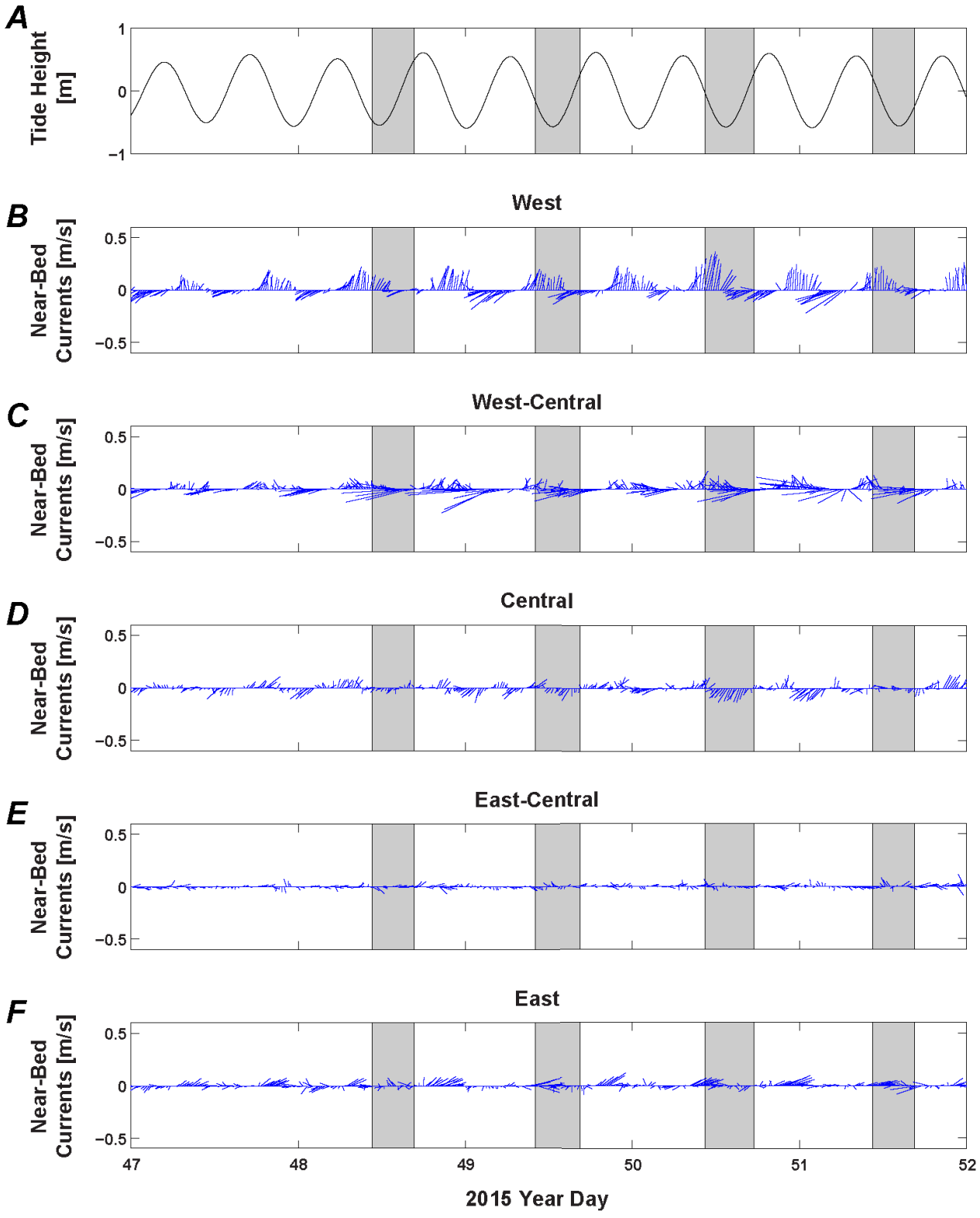
A
Tide Height [m]
1
0
−1
West
B
Near-Bed Currents [m/s]
0.5
0
−0.5
West-Central
C
Near-Bed Currents [m/s]
0.5
0
−0.5
Central
D
Near-Bed Currents [m/s]
0.5
0
−0.5
East-Central
E
Near-Bed Currents [m/s]
0.5
0
−0.5
East
F
Near-Bed Currents [m/s]
0.5
0
−0.5
47
48
49
50
51
52
2015 Year Day

Figure 8–2. (previous page) Time-series plots tidal height and near-bed current velocities from the moorings during the February 2015 vessel-mounted acoustic Doppler current profiler (VM-ADCP) surveys (gray boxes). *A*, Tidal height, in meters (m), from the Central site. *B*, Near-bed current velocity from the West site, with direction indicating heading ("going to") measured in degrees clockwise from true north and speed in meters per second (m/s). *C*, Near-bed current velocity from the West-Central site, with direction indicating heading ("going to") measured in degrees clockwise from true north and speed in meters per second (m/s). *D*, Near-bed current velocity from the Central site, with direction indicating heading ("going to") measured in degrees clockwise from true north and speed in meters per second (m/s). *E*, Near-bed current velocity from the East-Central site, with direction indicating heading ("going to") measured in degrees clockwise from true north and speed in meters per second (m/s). *F*, Near-bed current velocity from the East site, with direction indicating heading ("going to") measured in degrees clockwise from true north and speed in meters per second (m/s).

Appendix 9. Spatial Current Data from the Vessel-Mounted ADCP (VM-ADCP) Surveys

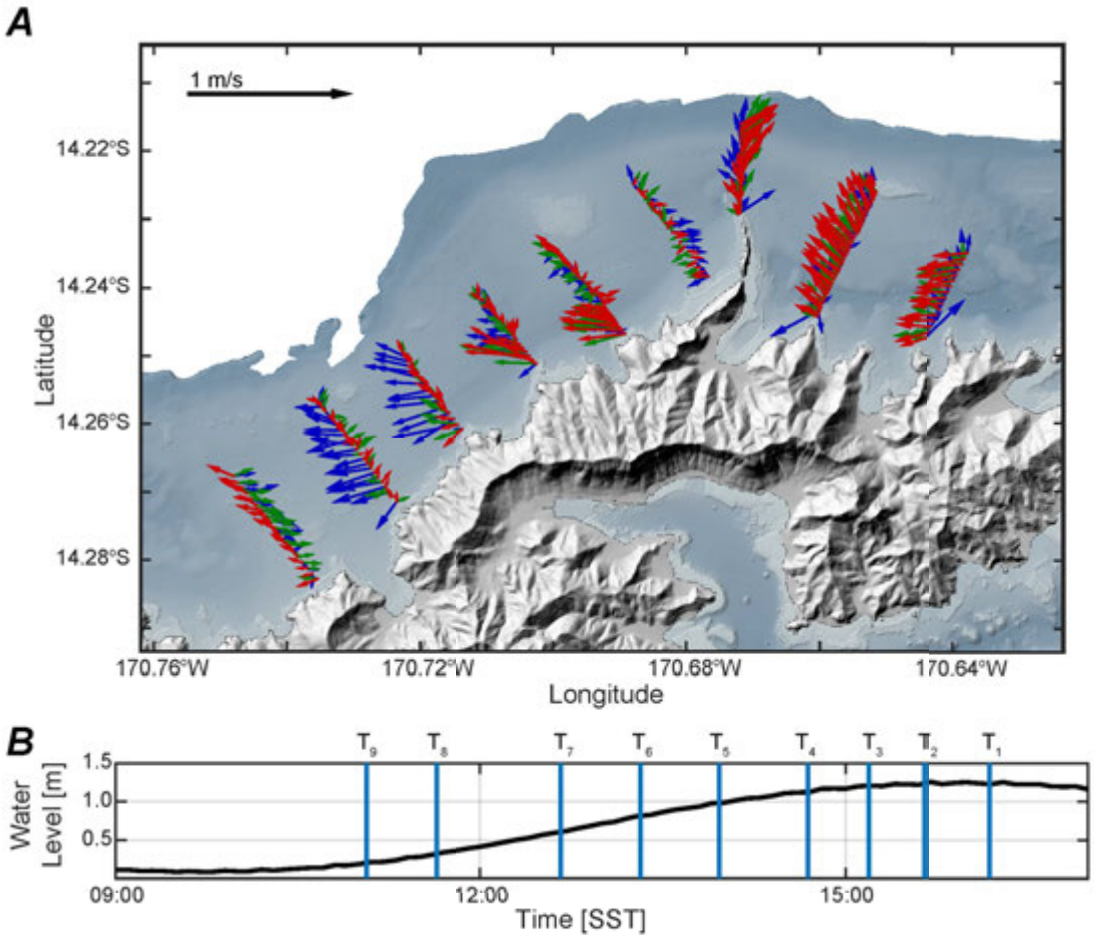

Figure 9–1. Currents and tides during the vessel-mounted acoustic Doppler current profiler (VM-ADCP) survey on Year Day 48 (17 February 2015). *A*, Map of near-surface (red arrows;), mid-water column (green arrows), and near-seabed (blue arrows) current directions as heading ("going to"), in degrees from true north, and speeds, in meters per second (m/s). *B*, Water level above mean, in meters (m), with the time the transects were started denoted by the blue vertical lines; SST, Samoa Standard Time.

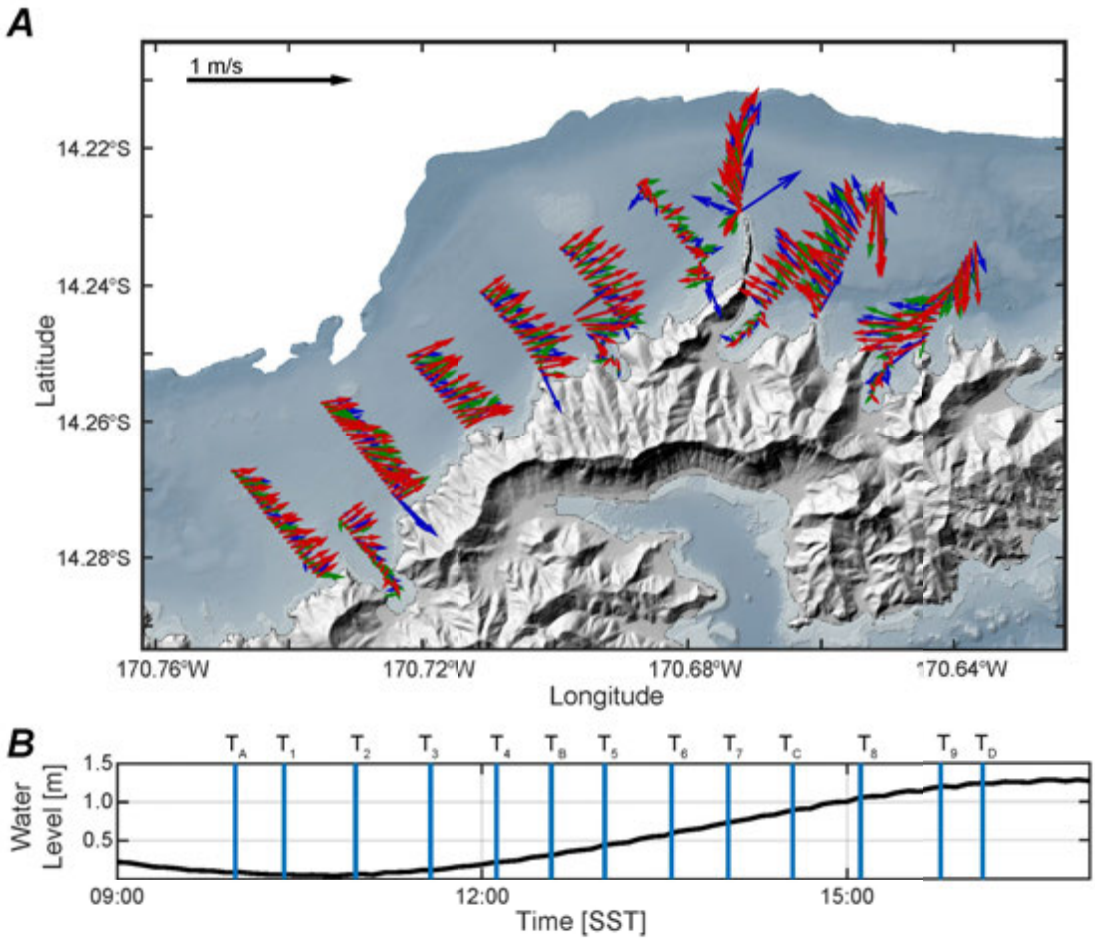

Figure 9–2. Currents and tides during the vessel-mounted acoustic Doppler current profiler (VM-ADCP) survey on Year Day 49 (18 February 2015). *A*, Map of near-surface (red arrows;), mid-water column (green arrows), and near-seabed (blue arrows) current directions as heading ("going to"), in degrees from true north, and speeds, in meters per second (m/s). *B*, Water level above mean, in meters (m), with the time the transects were started denoted by the blue vertical lines; SST, Samoa Standard Time.

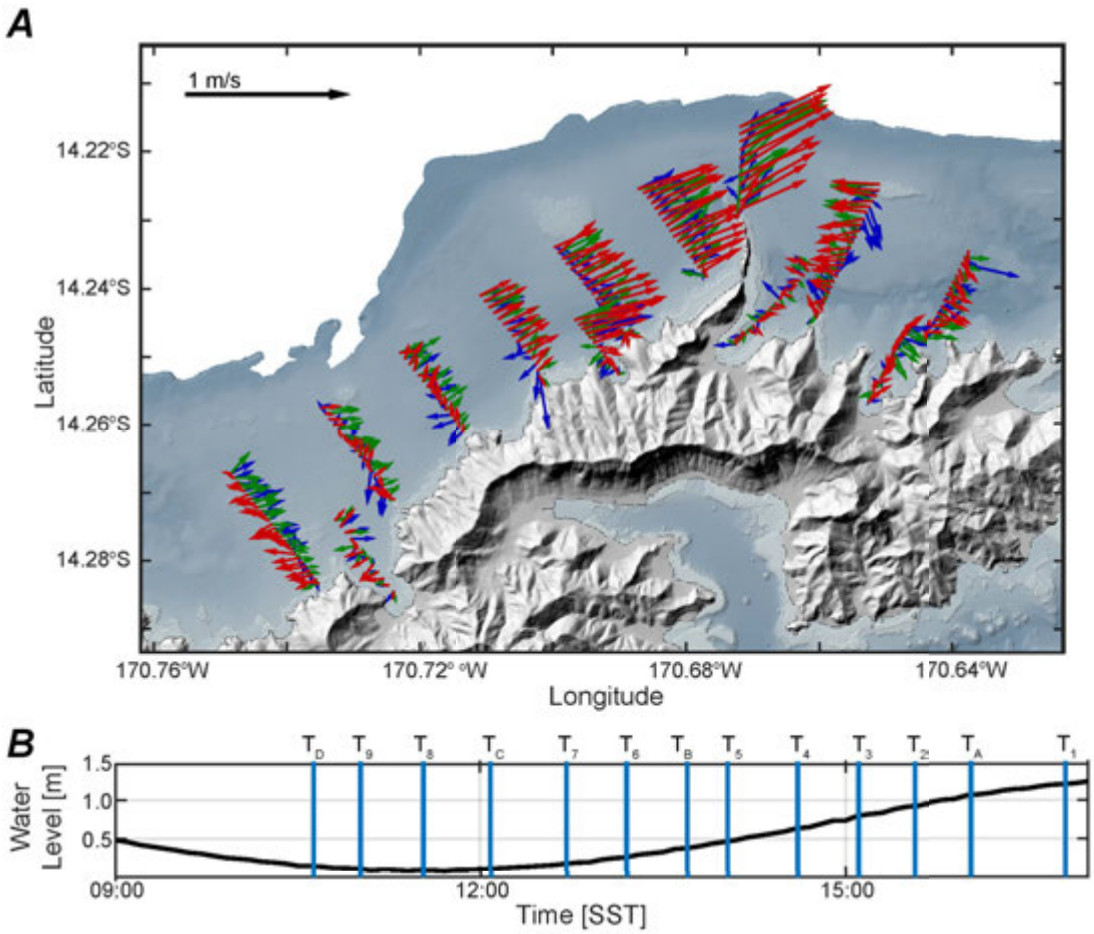

Figure 9–3. Currents and tides during the vessel-mounted acoustic Doppler current profiler (VM-ADCP) survey on Year Day 50 (19 February 2015). *A*, Map of near-surface (red arrows;), mid-water column (green arrows), and near-seabed (blue arrows) current directions as heading ("going to"), in degrees from true north, and speeds, in meters per second (m/s). *B*, Water level above mean, in meters (m), with the time the transects were started denoted by the blue vertical lines; SST, Samoa Standard Time.

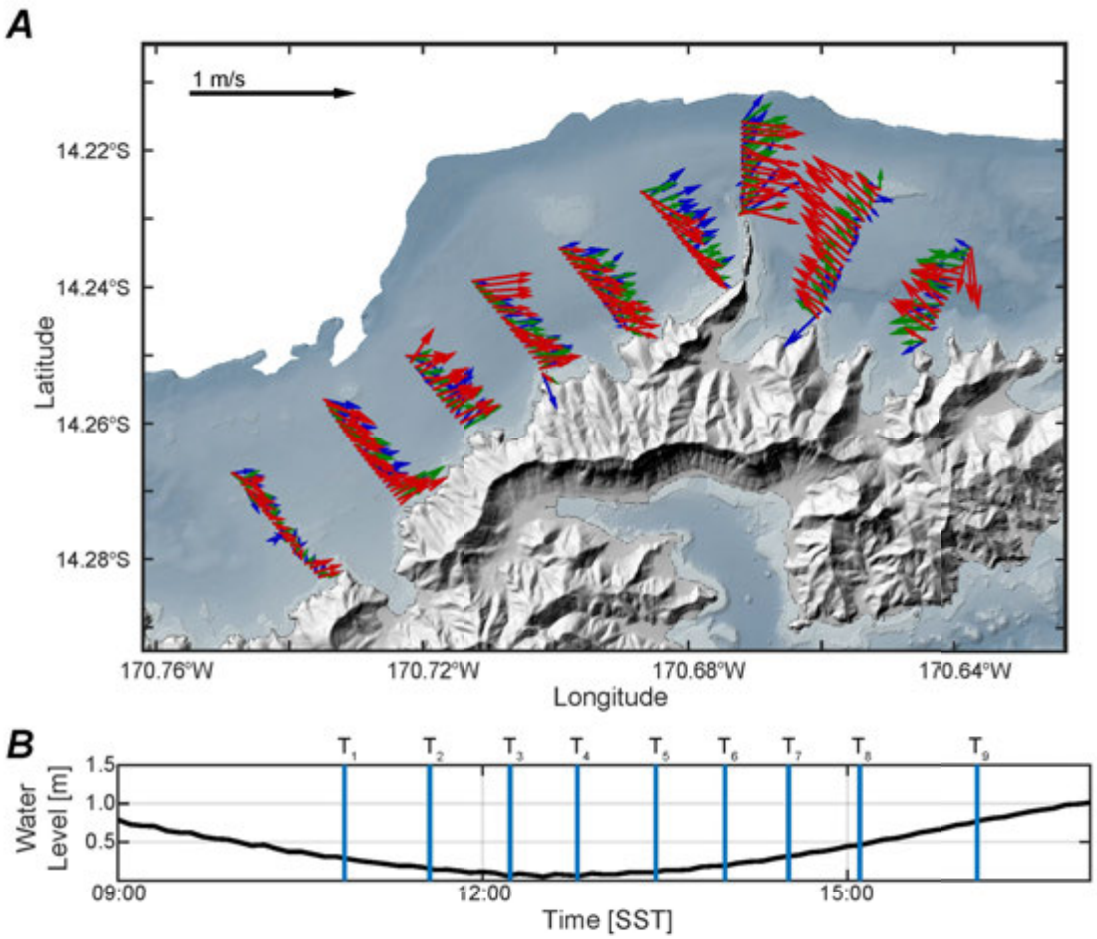

Figure 9–4. Currents and tides during the vessel-mounted acoustic Doppler current profiler (VM-ADCP) survey on Year Day 51 (20 February 2015). *A*, Map of near-surface (red arrows;), mid-water column (green arrows), and near-seabed (blue arrows) current directions as heading ("going to"), in degrees from true north, and speeds, in meters per second (m/s). *B*, Water level above mean, in meters (m), with the time the transects were started denoted by the blue vertical lines; SST, Samoa Standard Time.

Appendix 10. Lagrangian Surface Current Drifter (LSCD) Data

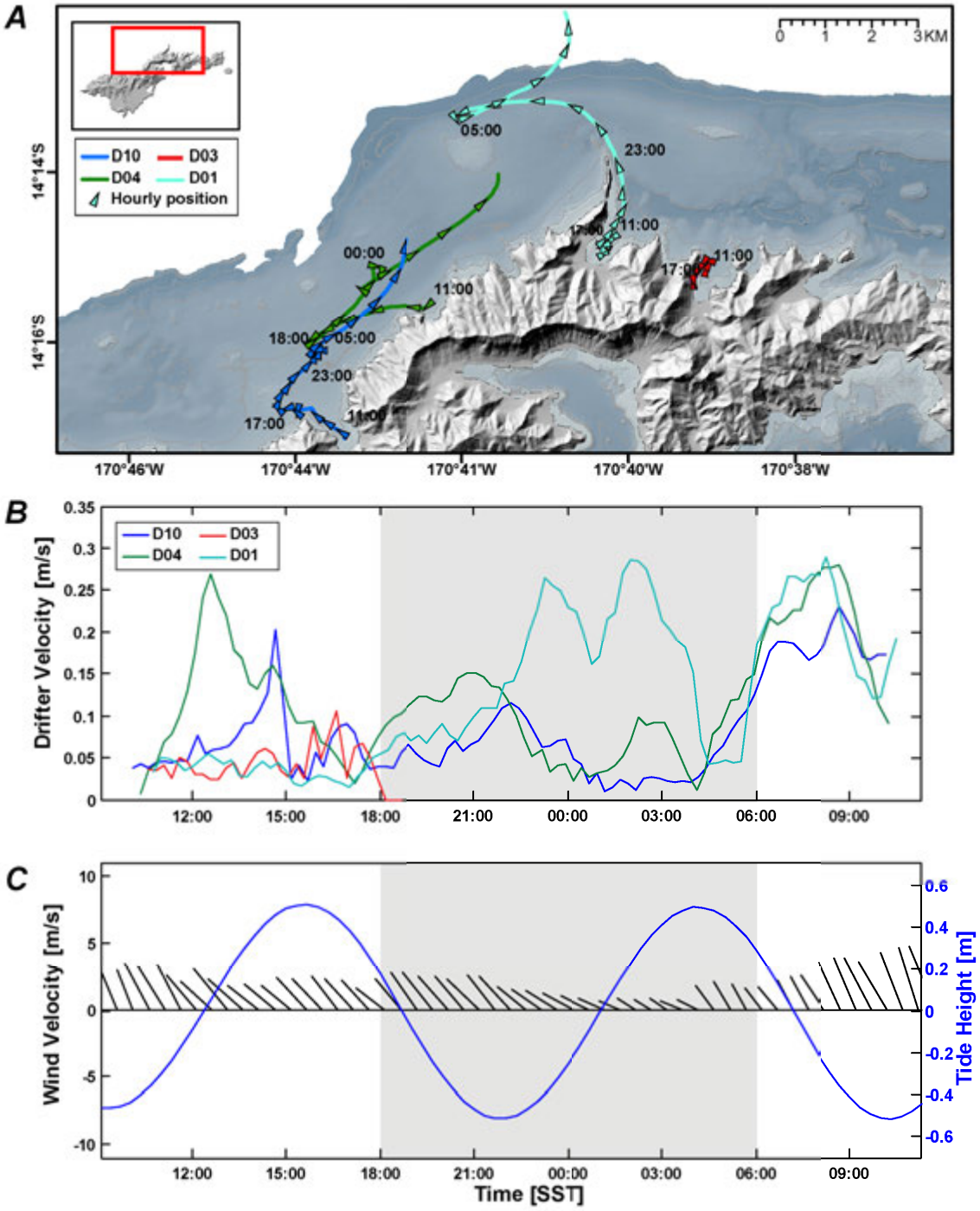

Figure 10–1. Movement of LSCDs D01, D03, D04, and D10 on Year Day 104 (14 April 2015). *A*, Map of LSCD directions as heading ("going to"), in degrees from true north, and speeds, in meters per second; triangles denote approximate hourly positions. *B*, Time series of drifter speed, in meters per second (m/s), during deployment. C, Time series of wind direction indicating heading ("going to") measured in degrees clockwise from true north, and velocity in meters per second (m/s), and tide height, in meters (m), during deployment.

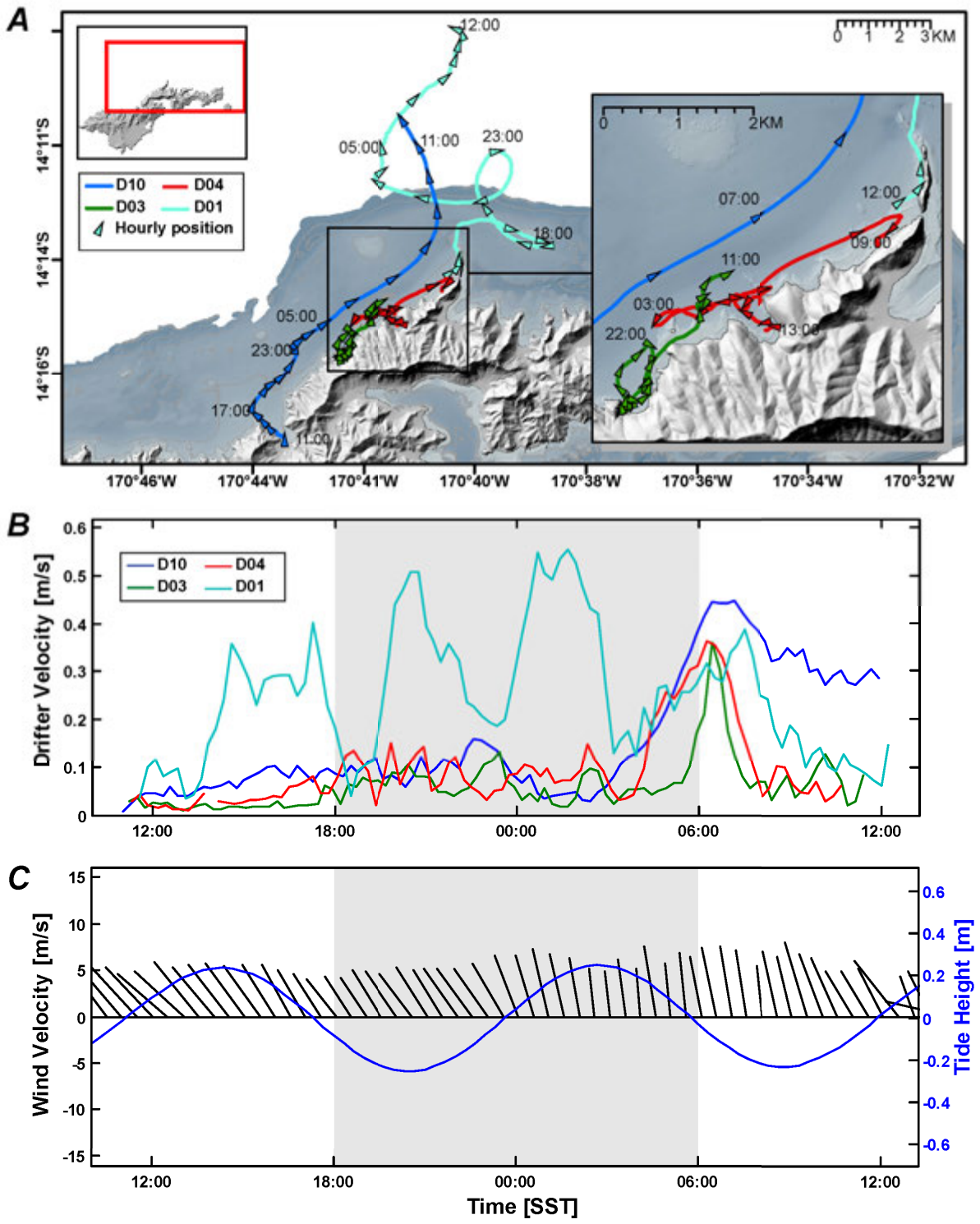

Figure 10–2. Movement of LSCDs D01, D03, D04, and D10 on Year Day 145 (25 May 2015). *A*, Map of LSCD directions as heading ("going to"), in degrees from true north, and speeds, in meters per second; triangles denote approximate hourly positions. *B*, Time series of drifter speed, in meters per second (m/s), during deployment. *C*, Time series of wind direction indicating heading ("going to") measured in degrees clockwise from true north, and velocity in meters per second (m/s), and tide height, in meters (m), during deployment.

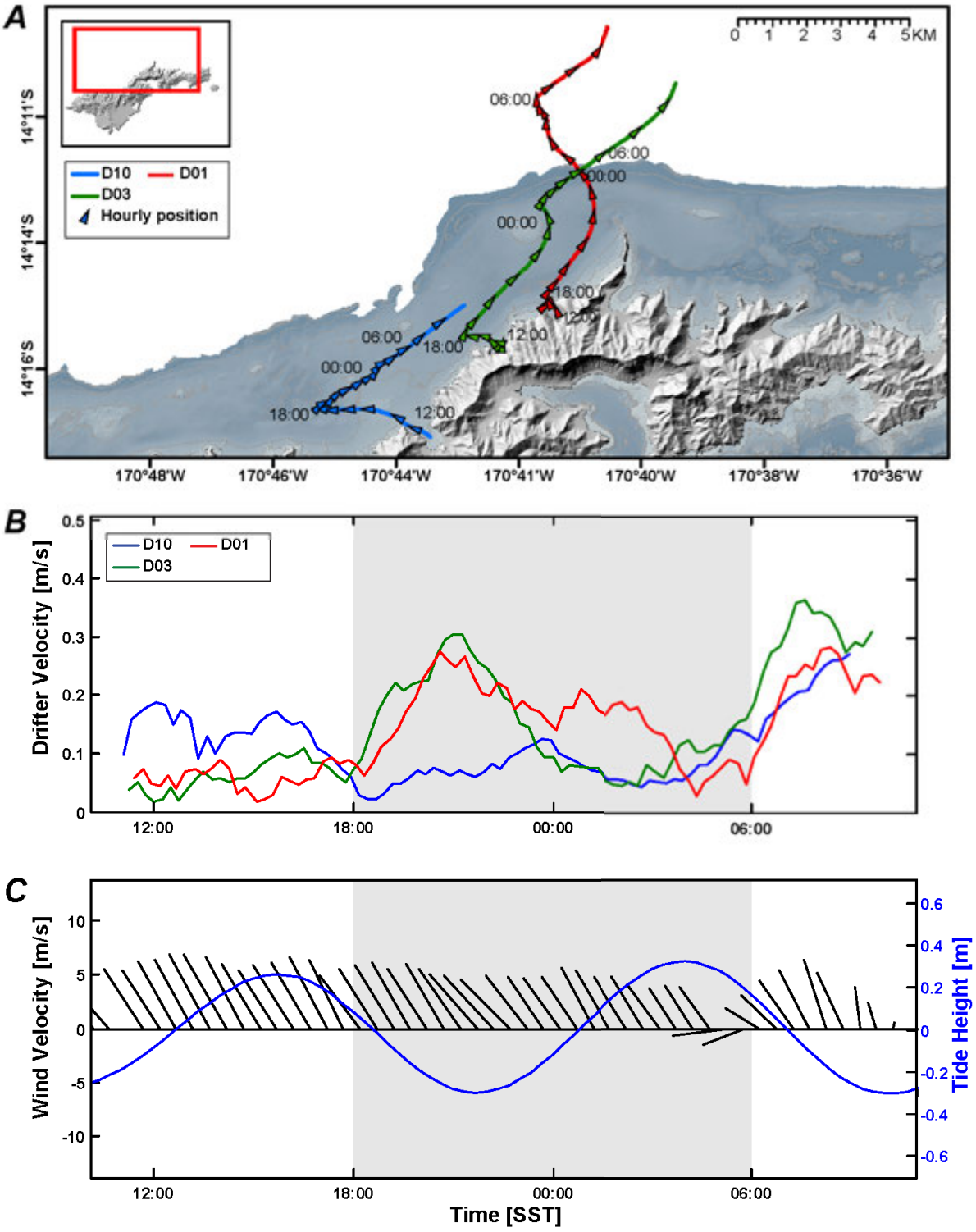

Figure 10–3. Movement of LSCDs D01, D03, and D10 on Year Day 148 (28 May 2015). *A*, Map of LSCD directions as heading ("going to"), in degrees from true north, and speeds, in meters per second; triangles denote approximate hourly positions. *B*, Time series of drifter speed, in meters per second (m/s), during deployment. *C*, Time series of wind direction indicating heading ("going to") measured in degrees clockwise from true north, and velocity in meters per second (m/s), and tide height, in meters (m), during deployment.

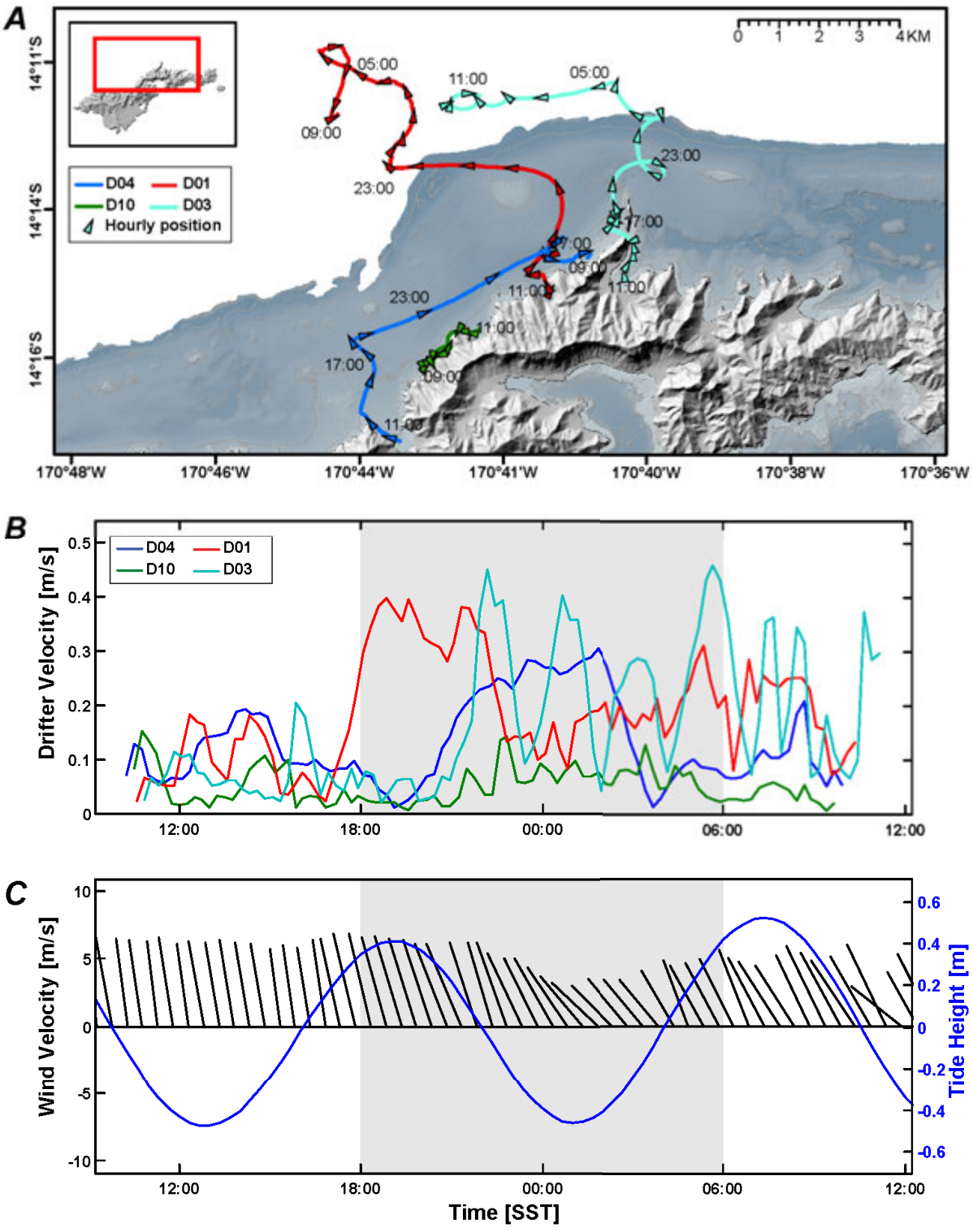

Figure 10–4. Movement of LSCDs D01, D03, D04,and D10 on Year Day 153 (2 June 2015). *A*, Map of LSCD directions as heading ("going to"), in degrees from true north, and speeds, in meters per second; triangles denote approximate hourly positions. *B*, Time series of drifter speed, in meters per second (m/s), during deployment. *C*, Time series of wind direction indicating heading ("going to") measured in degrees clockwise from true north, and velocity in meters per second (m/s), and tide height, in meters (m), during deployment.

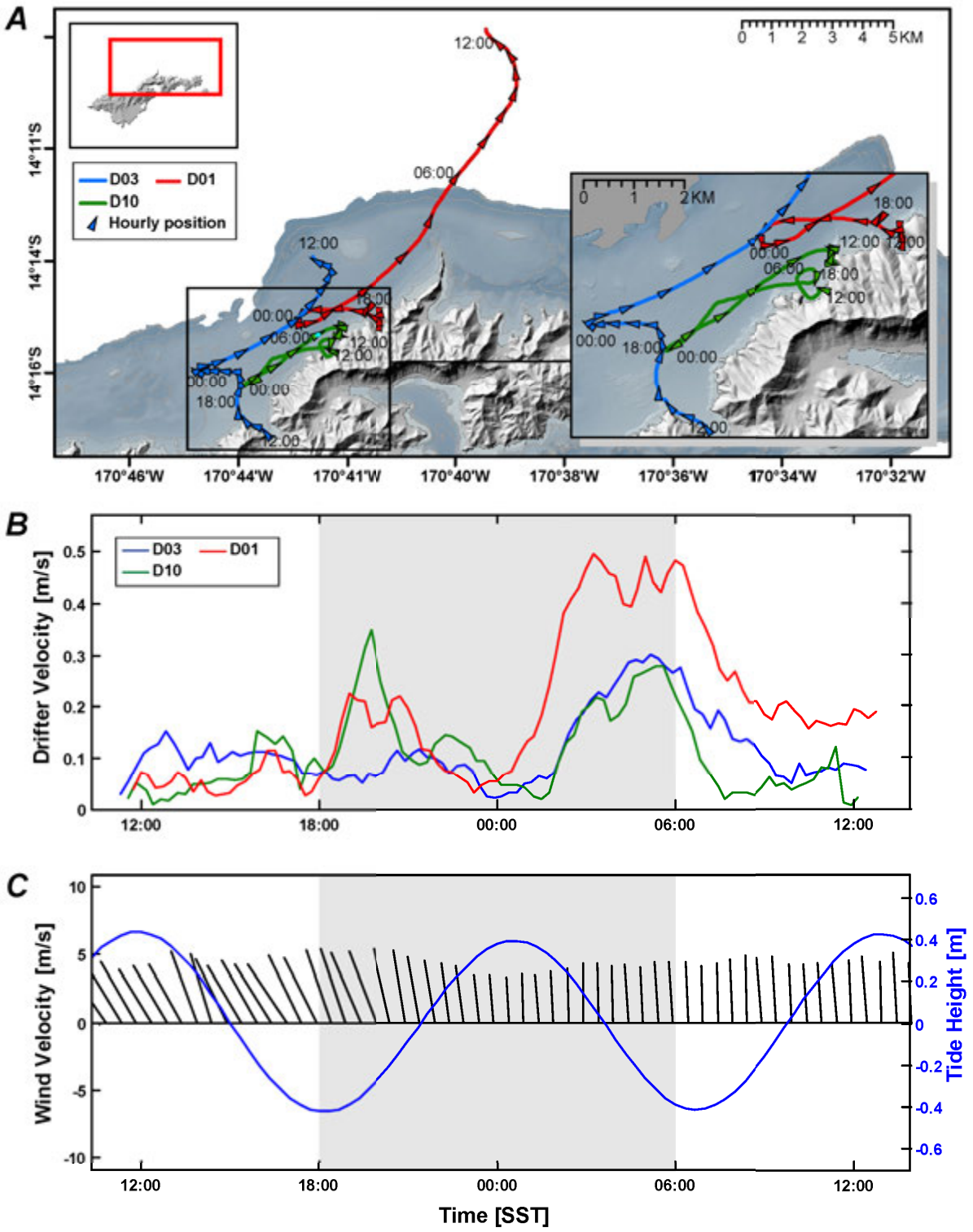

Figure 10–5. Movement of LSCDs D01, D03, and D10 on Year Day 159 (8 June 2015). *A*, Map of LSCD directions as heading ("going to"), in degrees from true north, and speeds, in meters per second; triangles denote approximate hourly positions. *B*, Time series of drifter speed, in meters per second (m/s), during deployment. *C*, Time series of wind direction indicating heading ("going to") measured in degrees clockwise from true north, and velocity in meters per second (m/s), and tide height, in meters (m), during the deployment.

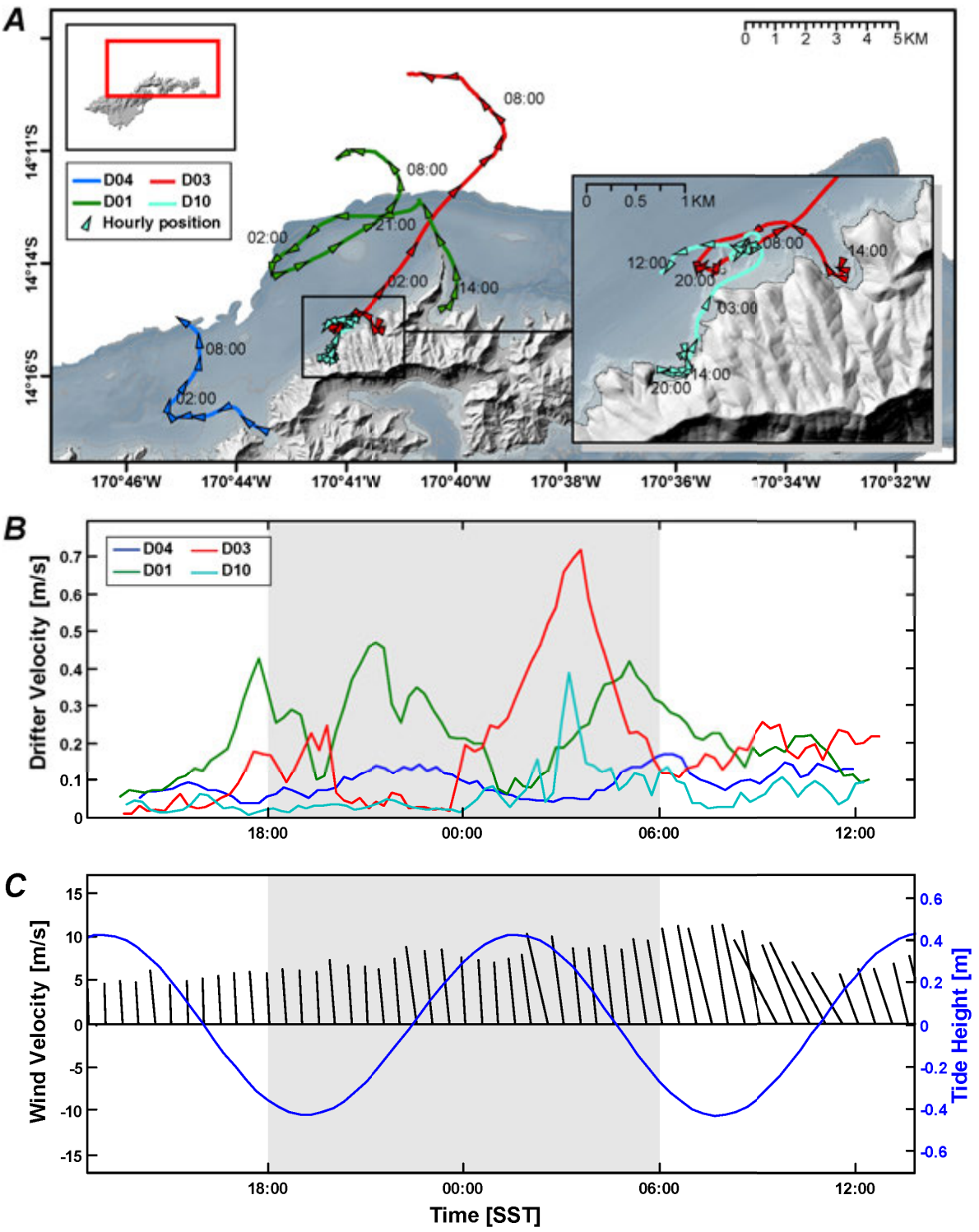

Figure 10–6. Movement of LSCDs D01, D03, D04, and D10 on Year Day 160 (9 June 2015). *A*, Map of LSCD directions as heading ("going to"), in degrees from true north, and speeds, in meters per second; triangles denote approximate hourly positions. *B*, Time series of drifter speed, in meters per second (m/s), during deployment. *C*, Time series of wind direction indicating heading ("going to") measured in degrees clockwise from true north, and velocity in meters per second (m/s), and tide height, in meters (m), during deployment.

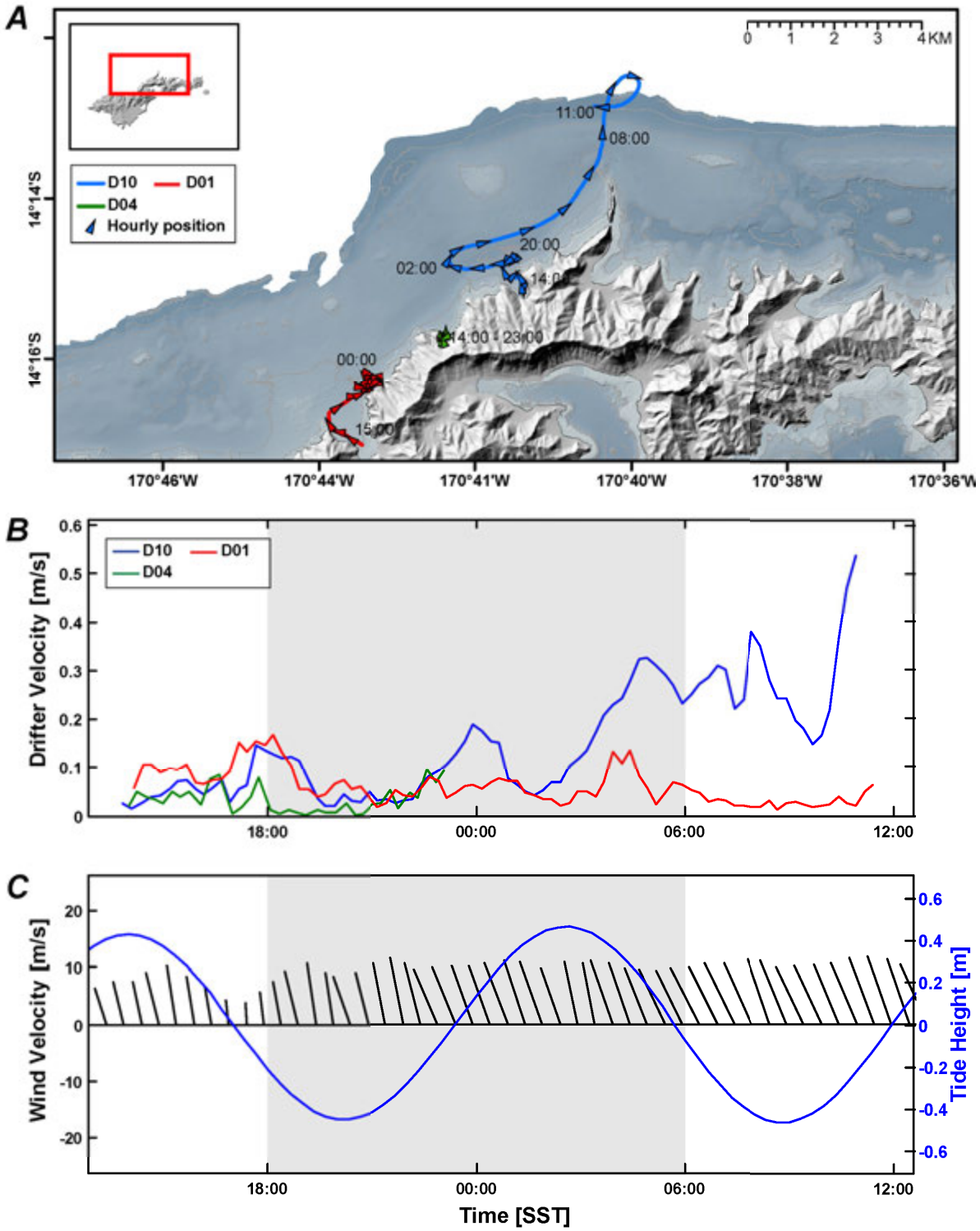

Figure 10–7. Movement of LSCDs D01, D04, and D10 on Year Day 161 (10 June 2015). *A*, Map of LSCD directions as heading ("going to"), in degrees from true north, and speeds, in meters per second; triangles denote approximate hourly positions. *B*, Time series of drifter speed, in meters per second (m/s), during deployment. *C*, Time series of wind direction indicating heading ("going to") measured in degrees clockwise from true north, and velocity in meters per second (m/s), and tide height, in meters (m), during the deployment.

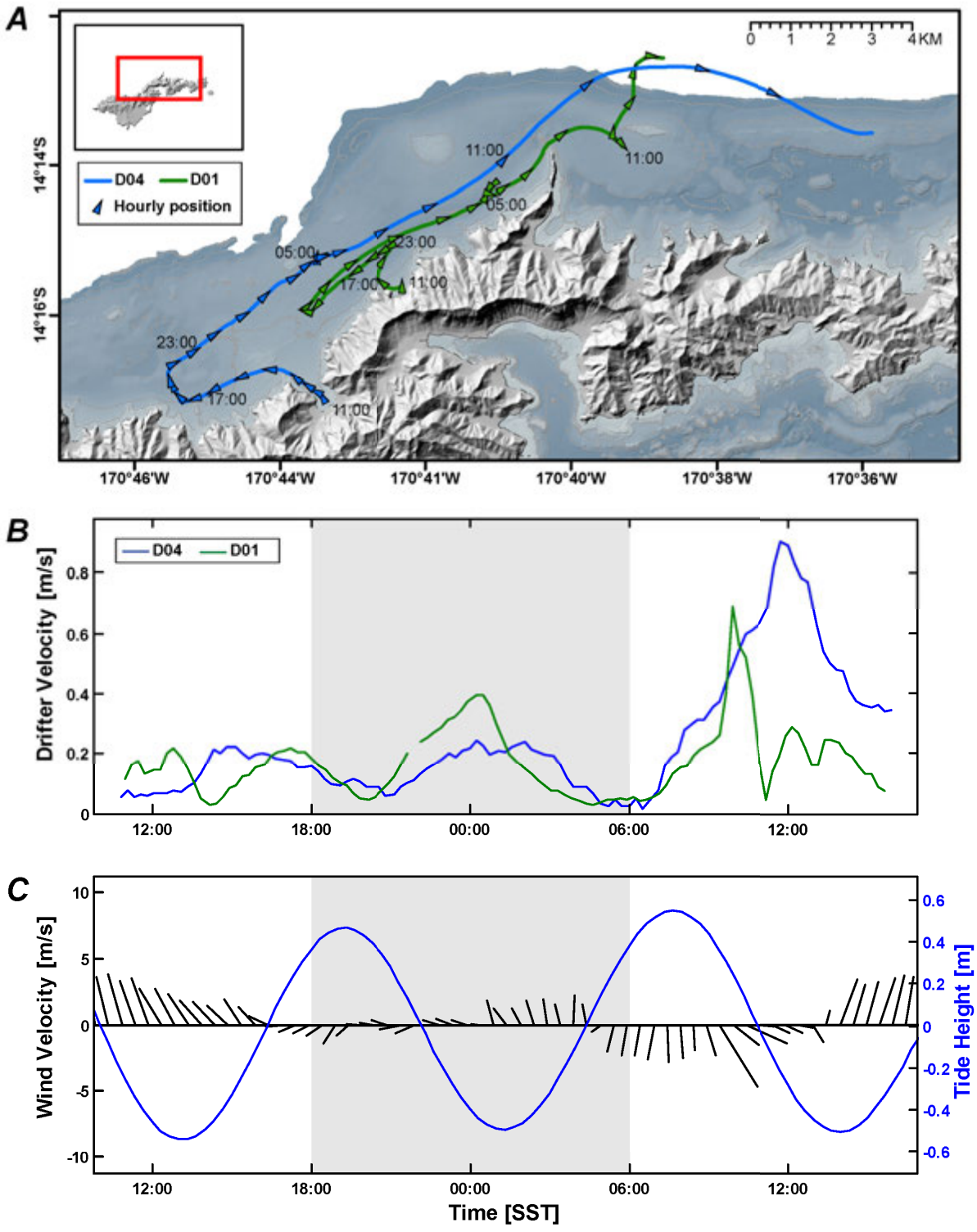

Figure 10–8. Movement of LSCDs D01 and D04 on Year Day 167 (16 June 2015). *A*, Map of LSCD directions as heading ("going to"), in degrees from true north, and speeds, in meters per second; triangles denote approximate hourly positions. *B*, Time series of drifter speed, in meters per second (m/s), during deployment. *C*, Time series of wind direction indicating heading ("going to") measured in degrees clockwise from true north, and velocity in meters per second (m/s), and tide height, in meters (m), during deployment.

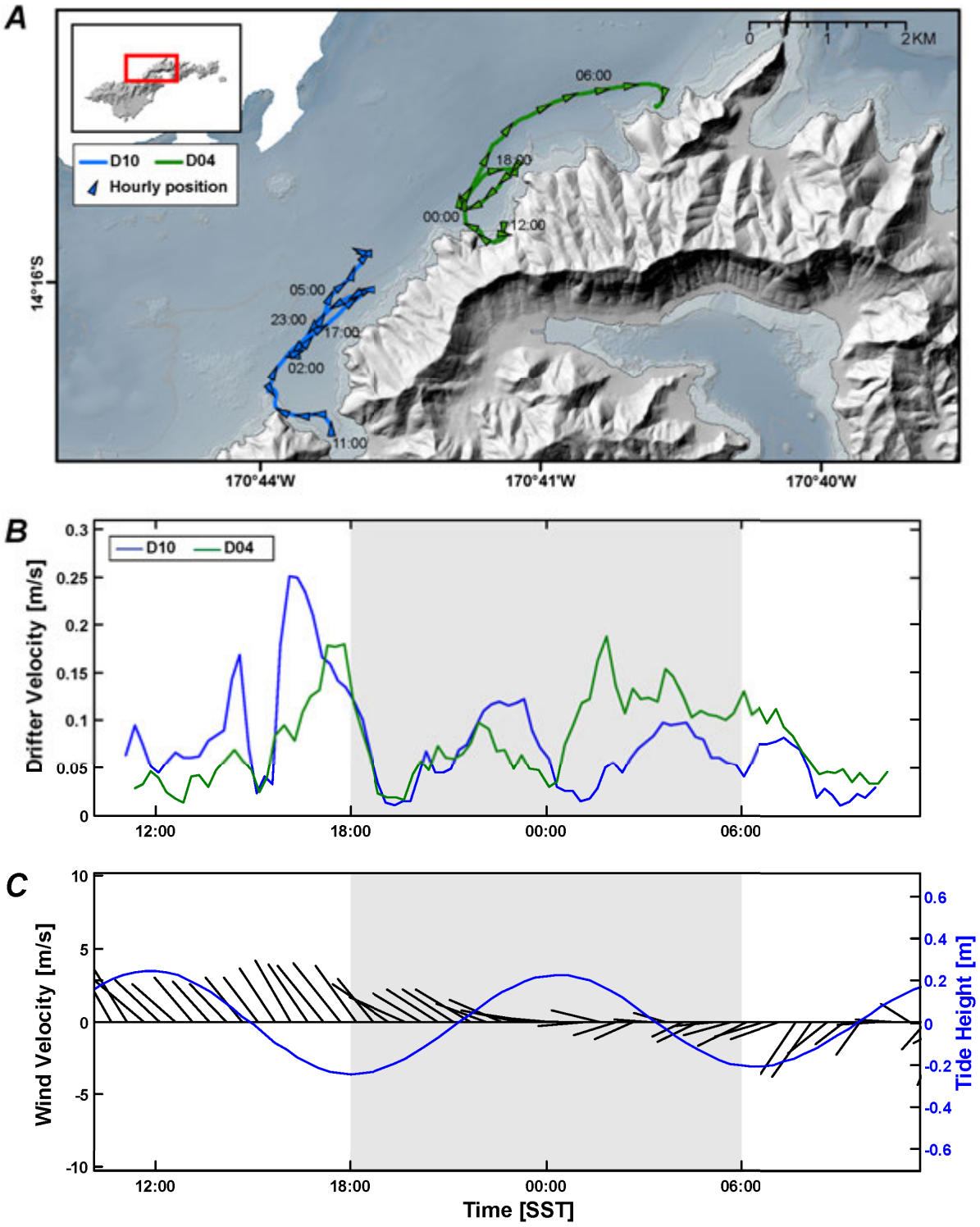

Figure 10–9. Movement of LSCDs D04 and D10 on Year Day 173 (22 June 2015). *A*, Map of LSCD directions as heading ("going to"), in degrees from true north, and speeds, in meters per second; triangles denote approximate hourly positions. *B*, Time series of drifter speed, in meters per second (m/s), during deployment. *C*, Time series of wind direction indicating heading ("going to") measured in degrees clockwise from true north, and velocity in meters per second (m/s), and tide height, in meters (m), during deployment.

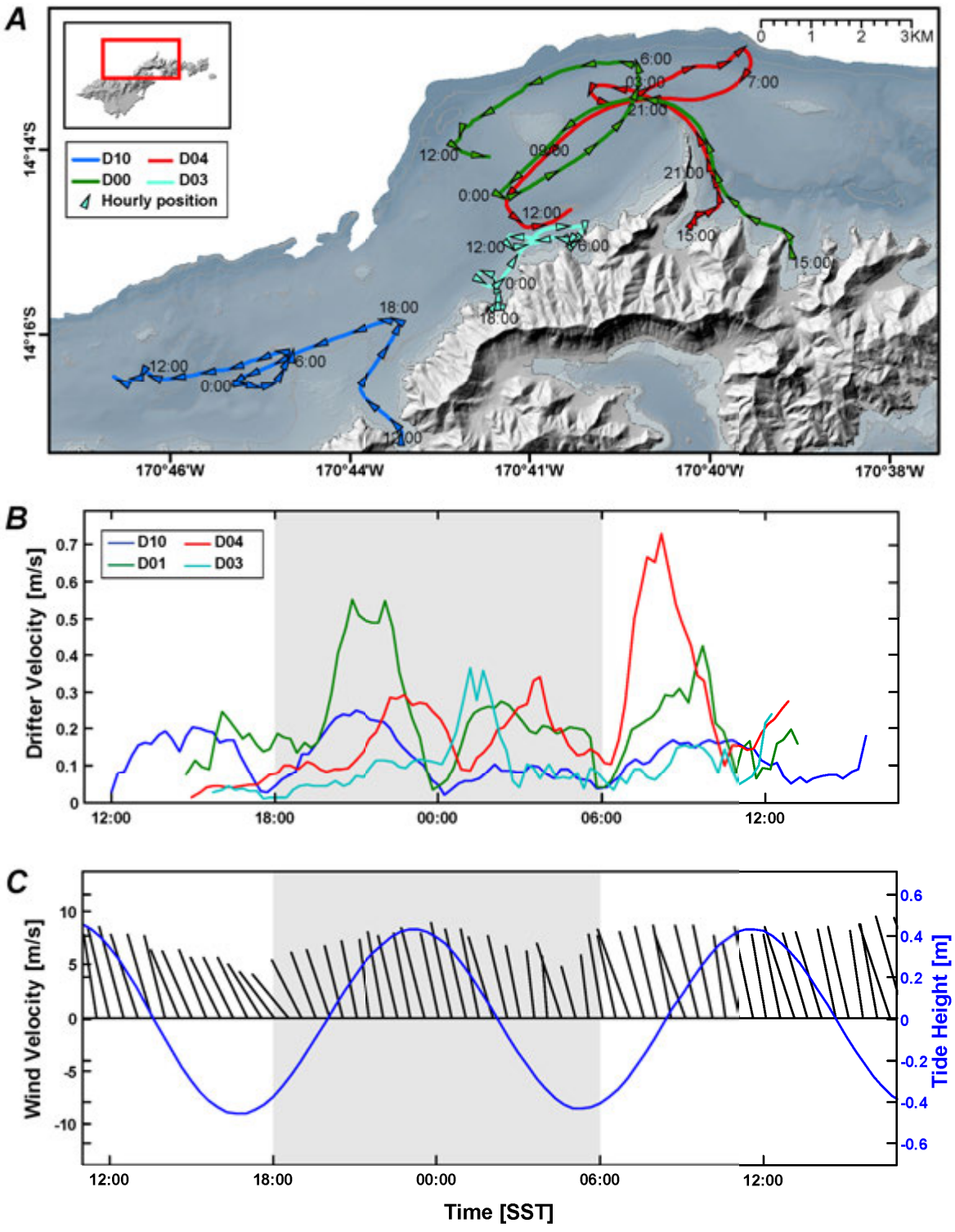

Figure 10–10. Movement of LSCDs D01, D03, D04, and D10 on Year Day 187 (6 July 2015). *A*, Map of LSCD directions as heading ("going to"), in degrees from true north, and speeds, in meters per second; triangles denote approximate hourly positions. *B*, Time series of drifter speed, in meters per second (m/s), during deployment. *C*, Time series of wind direction indicating heading ("going to") measured in degrees clockwise from true north, and velocity in meters per second (m/s), and tide height, in meters (m), during deployment.

Appendix 11. Water Column Profiler Data

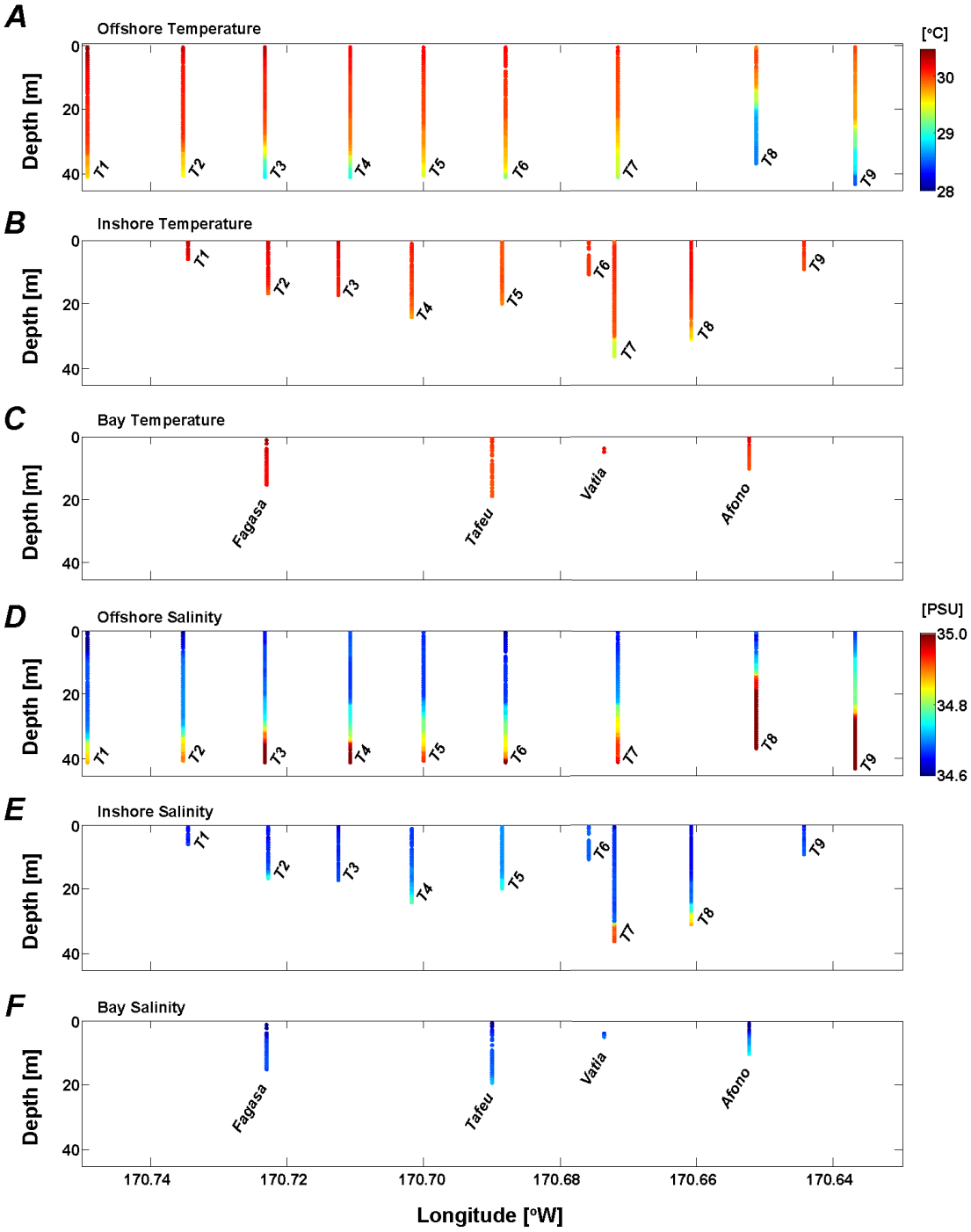

Figure 11–1. Individual vertical profiles by the water column profiler taken on Year Day 48 (17 February 2015), according to longitude in degrees west (left to right is west to east), with depth in meters (m) on y-axis. *A*, Offshore profiles of temperature in degrees Celsius (°C). *B*, Inshore profiles of temperature in degrees Celsius (°C). *C*, Bay profiles of temperature in degrees Celsius (°C). *D*, Offshore profiles of salinity in Practical Salinity Units (PSU). *E*, Inshore profiles of salinity in Practical Salinity Units (PSU). *F*, Bay profiles of salinity in Practical Salinity Units (PSU). Names of bays sampled are shown in panels *C* and *F*.

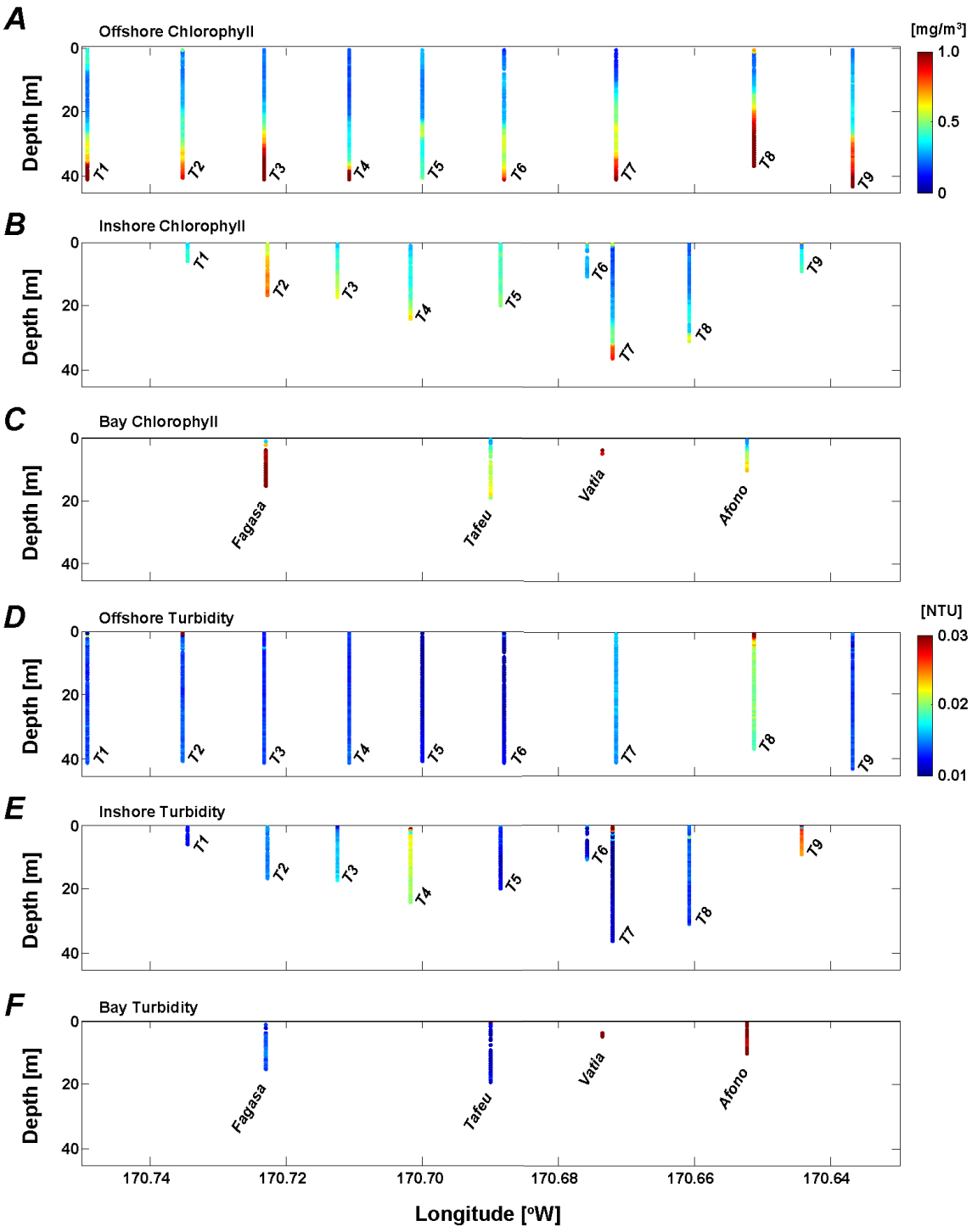

Figure 11–2. Individual vertical profiles by the water column profiler taken on Year Day 48 (17 February 2015), according to longitude in degrees west (left to right is west to east), with depth in meters (m) on y-axis. *A*, Offshore profiles of chlorophyll fluorescence in milligrams per cubic meter (mg/m^3). *B*, Inshore profiles of chlorophyll fluorescence in milligrams per cubic meter (mg/m^3). *C*, Bay profiles of chlorophyll fluorescence in milligrams per cubic meter (mg/m^3). *D*, Offshore profiles of turbidity in Nephelometric Turbidity Units (NTU). *E*, Inshore profiles of turbidity in Nephelometric Turbidity Units (NTU). *F*, Bay profiles of turbidity in Nephelometric Turbidity Units (NTU. Names of bays sampled are shown in panels *C* and *F*.

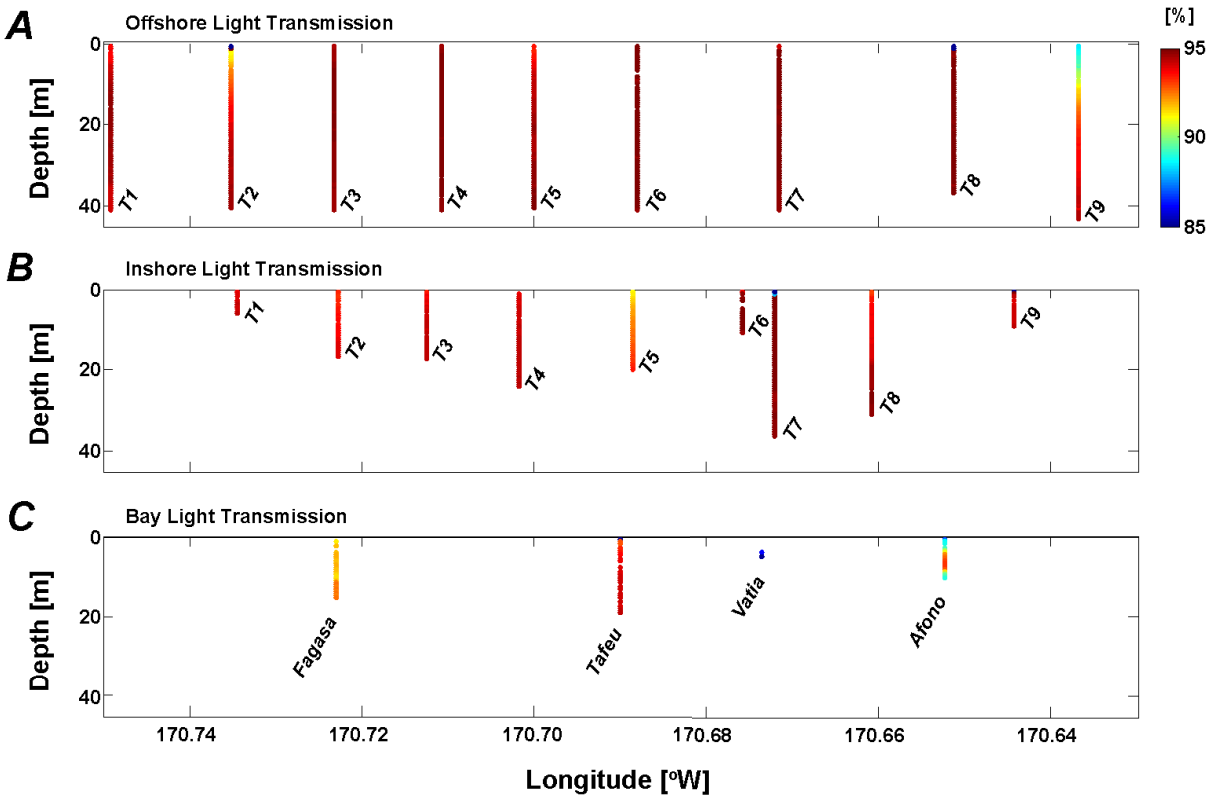

Figure 11–3. Individual vertical profiles by the water column profiler taken on Year Day 48 (17 February 2015), according to longitude in degrees west (left to right is west to east), with depth in meters (m) on y-axis. *A*, Offshore profiles of light transmission in percent (%). *B*, Inshore profiles of light transmission in percent (%). *C*, Bay profiles of light transmission in percent (%). Names of bays sampled are shown in panel *C*.

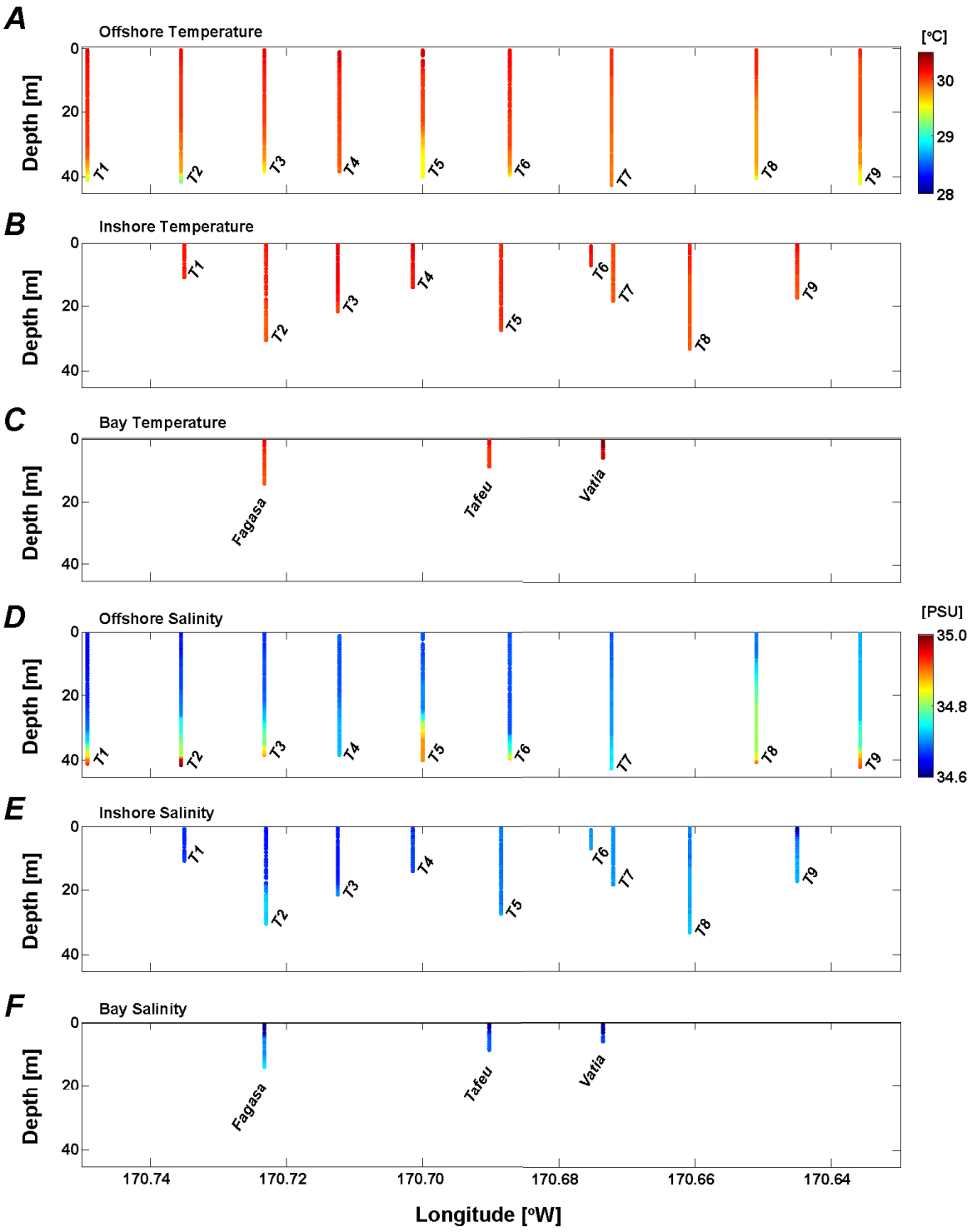

Figure 11–4. Individual vertical profiles by the water column profiler taken on Year Day 49 (18 February 2015), according to longitude in degrees west (left to right is west to east), with depth in meters (m) on y-axis. *A*, Offshore profiles of temperature in degrees Celsius (°C). *B*, Inshore profiles of temperature in degrees Celsius (°C). *C*, Bay profiles of temperature in degrees Celsius (°C). *D*, Offshore profiles of salinity in Practical Salinity Units (PSU). *E*, Inshore profiles of salinity in Practical Salinity Units (PSU). *F*, Bay profiles of salinity in Practical Salinity Units (PSU). Names of bays sampled are shown in panels *C* and *F*.

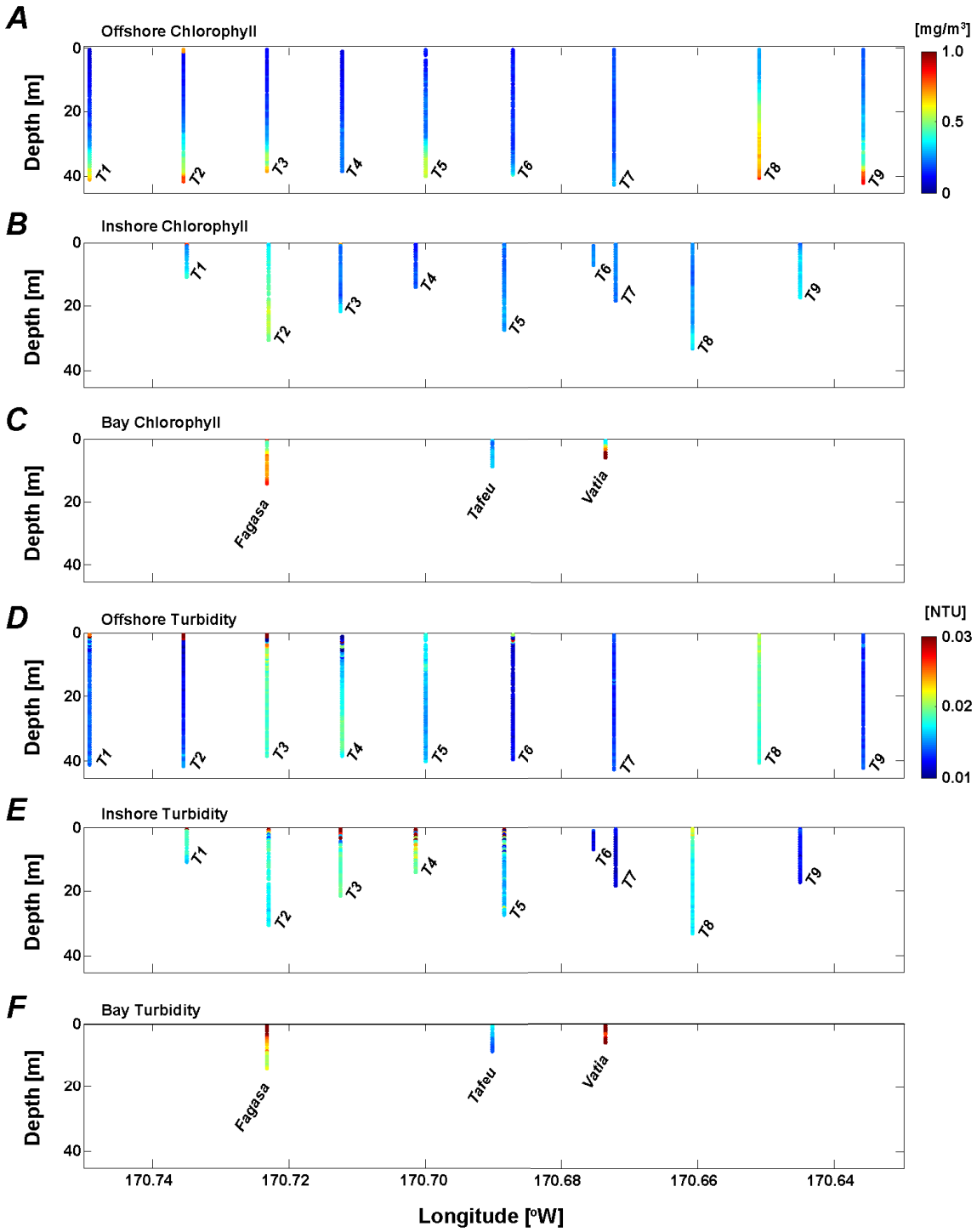

Figure 11–5. Individual vertical profiles by the water column profiler taken on Year Day 49 (18 February 2015), according to longitude in degrees west (left to right is west to east), with depth in meters (m) on y-axis. *A*, Offshore profiles of chlorophyll fluorescence in milligrams per cubic meter (mg/m^3). *B*, Inshore profiles of chlorophyll fluorescence in milligrams per cubic meter (mg/m^3). *C*, Bay profiles of chlorophyll fluorescence in milligrams per cubic meter (mg/m^3). *D*, Offshore profiles of turbidity in Nephelometric Turbidity Units (NTU). *E*, Inshore profiles of turbidity in Nephelometric Turbidity Units (NTU). *F*, Bay profiles of turbidity in Nephelometric Turbidity Units (NTU). Names of bays sampled are shown in panels *C* and *F*.

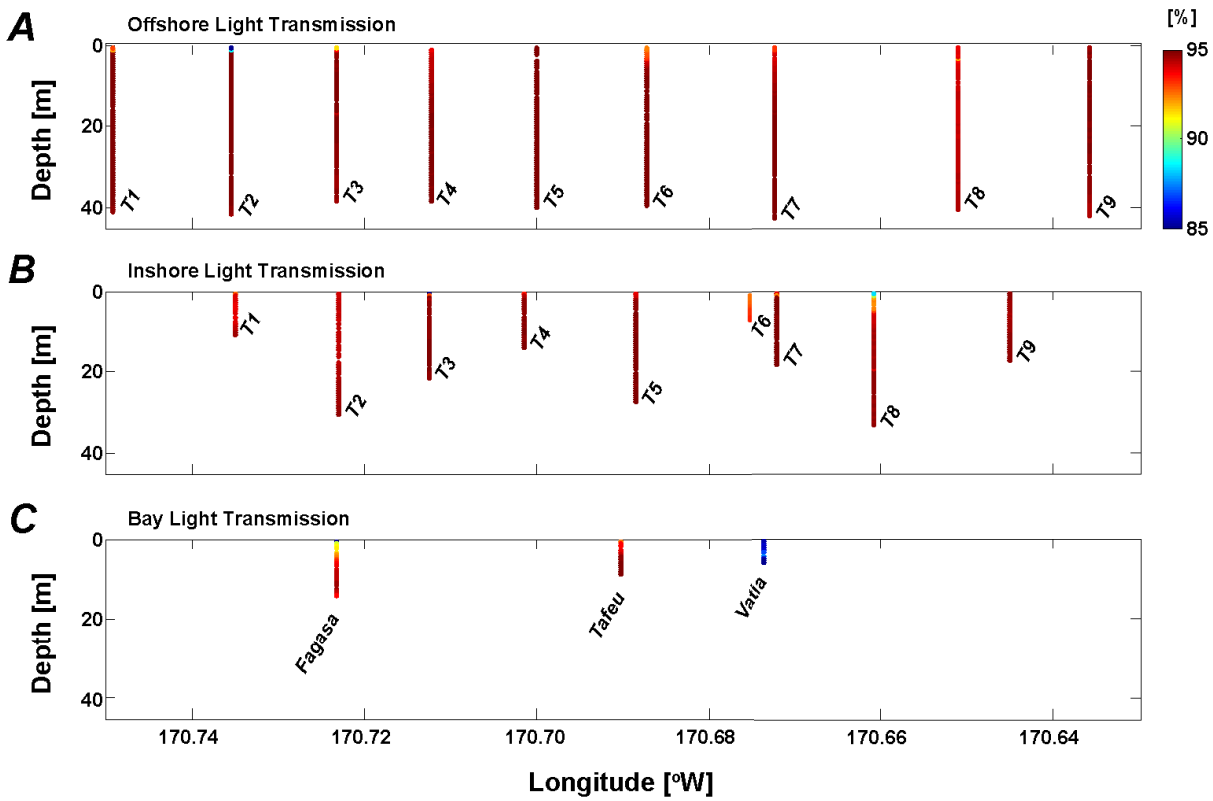

Figure 11–6. Individual vertical profiles by the water column profiler taken on Year Day 50 (18 February 2015), according to longitude in degrees west (left to right is west to east), with depth in meters (m) on y-axis. *A*, Offshore profiles of light transmission in percent (%). *B*, Inshore profiles of light transmission in percent (%). *C*, Bay profiles of light transmission in percent (%). Names of bays sampled are shown in panel *C*.

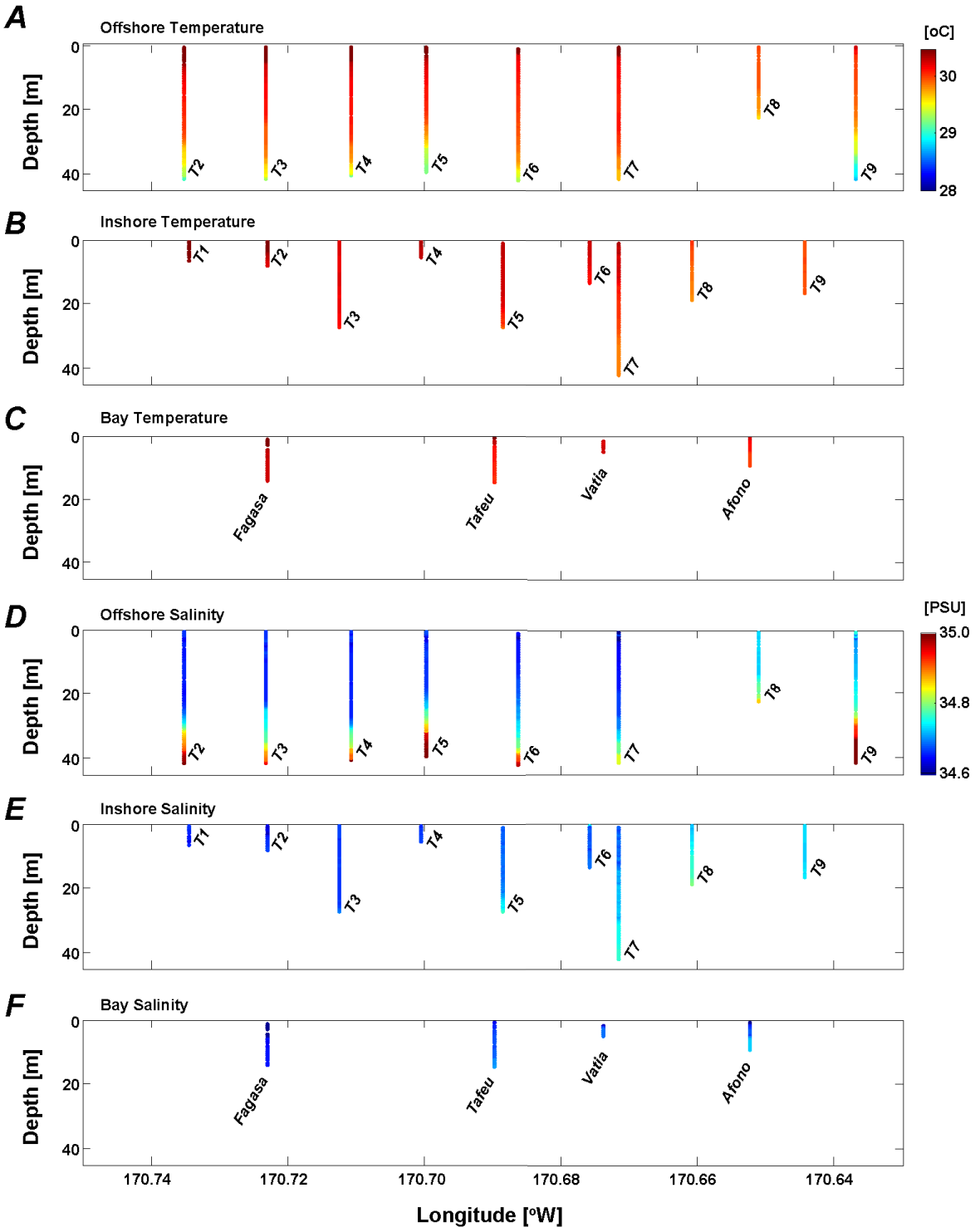

Figure 11–7. Individual vertical profiles by the water column profiler taken on Year Day 50 (19 February 2015), according to longitude in degrees west (left to right is west to east), with depth in meters (m) on y-axis. *A*, Offshore profiles of temperature in degrees Celsius (°C). *B*, Inshore profiles of temperature in degrees Celsius (°C). *C*, Bay profiles of temperature in degrees Celsius (°C). *D*, Offshore profiles of salinity in Practical Salinity Units (PSU). *E*, Inshore profiles of salinity in Practical Salinity Units (PSU). *F*, Bay profiles of salinity in Practical Salinity Units (PSU). Names of bays sampled are shown in panels *C* and *F*.

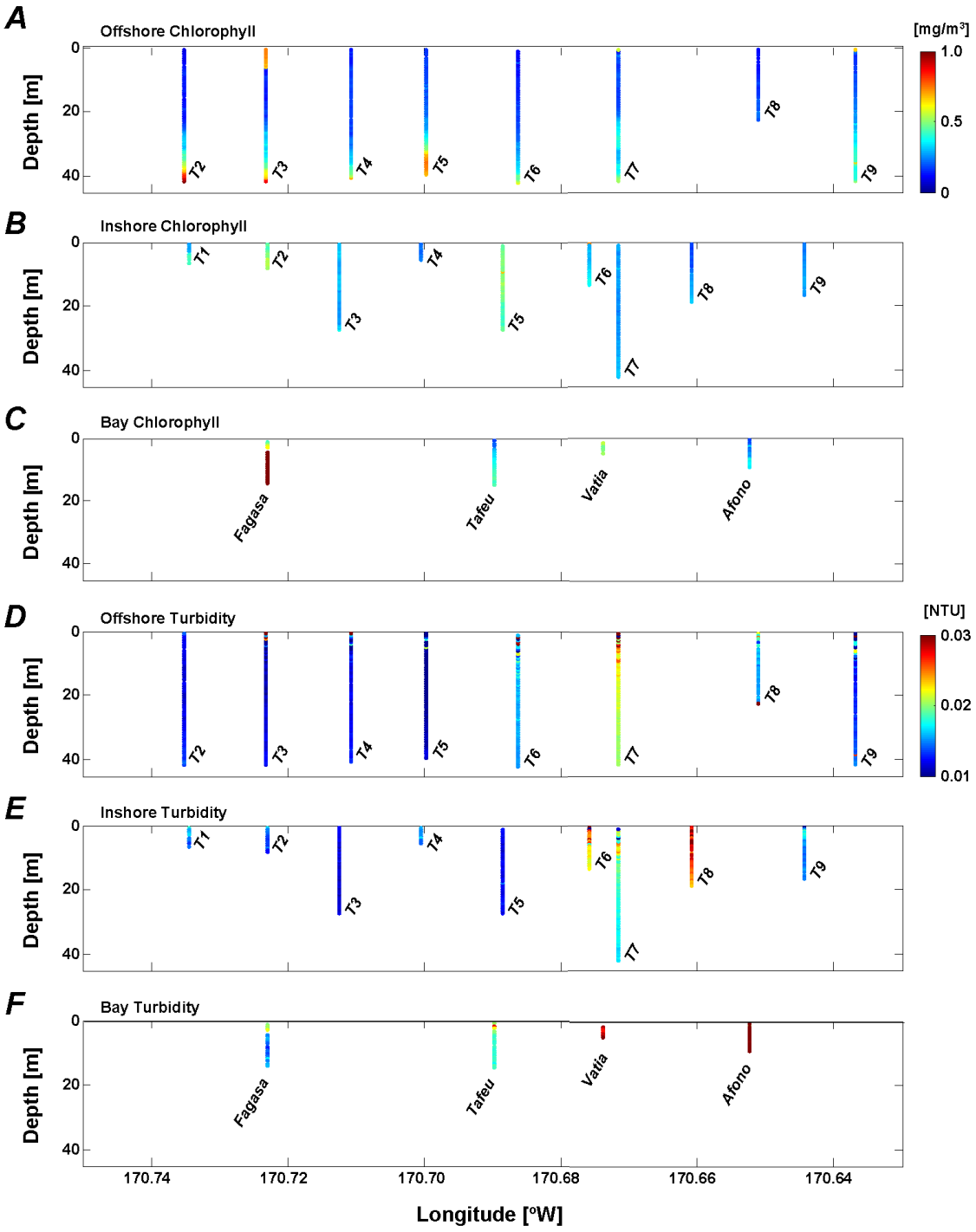

Figure 11–8. Individual vertical profiles by the water column profiler taken on Year Day 50 (19 February 2015), according to longitude in degrees west (left to right is west to east), with depth in meters (m) on y-axis. *A*, Offshore profiles of chlorophyll fluorescence in milligrams per cubic meter (mg/m^3). *B*, Inshore profiles of chlorophyll fluorescence in milligrams per cubic meter (mg/m^3). *C*, Bay profiles of chlorophyll fluorescence in milligrams per cubic meter (mg/m^3). *D*, Offshore profiles of turbidity in Nephelometric Turbidity Units (NTU). *E*, Inshore profiles of turbidity in Nephelometric Turbidity Units (NTU). *F*, Bay profiles of turbidity in Nephelometric Turbidity Units (NTU). Names of bays sampled are shown in panels *C* and *F*.

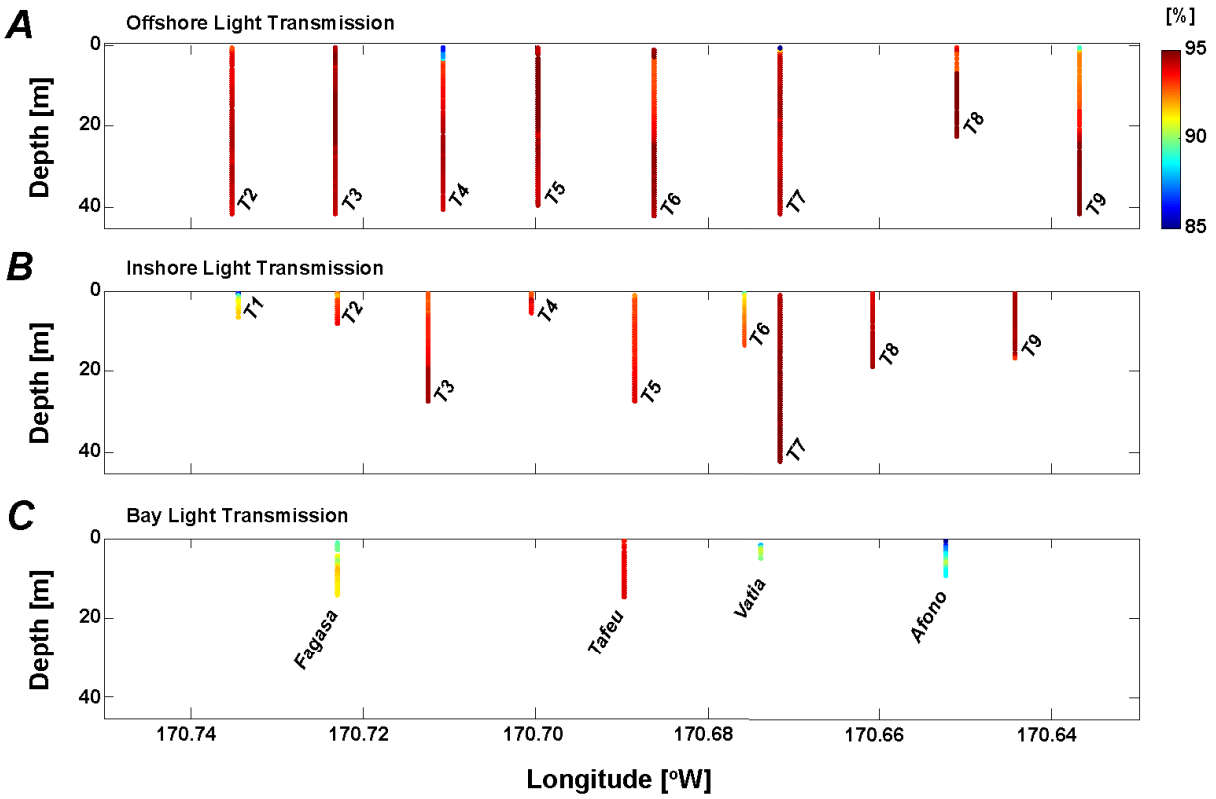

Figure 11–9. Individual vertical profiles by the water column profiler taken on Year Day 50 (19 February 2015), according to longitude in degrees west (left to right is west to east), with depth in meters (m) on y-axis. *A*, Offshore profiles of light transmission in percent (%). *B*, Inshore profiles of light transmission in percent (%). *C*, Bay profiles of light transmission in percent (%). Names of bays sampled are shown in panel *C*.

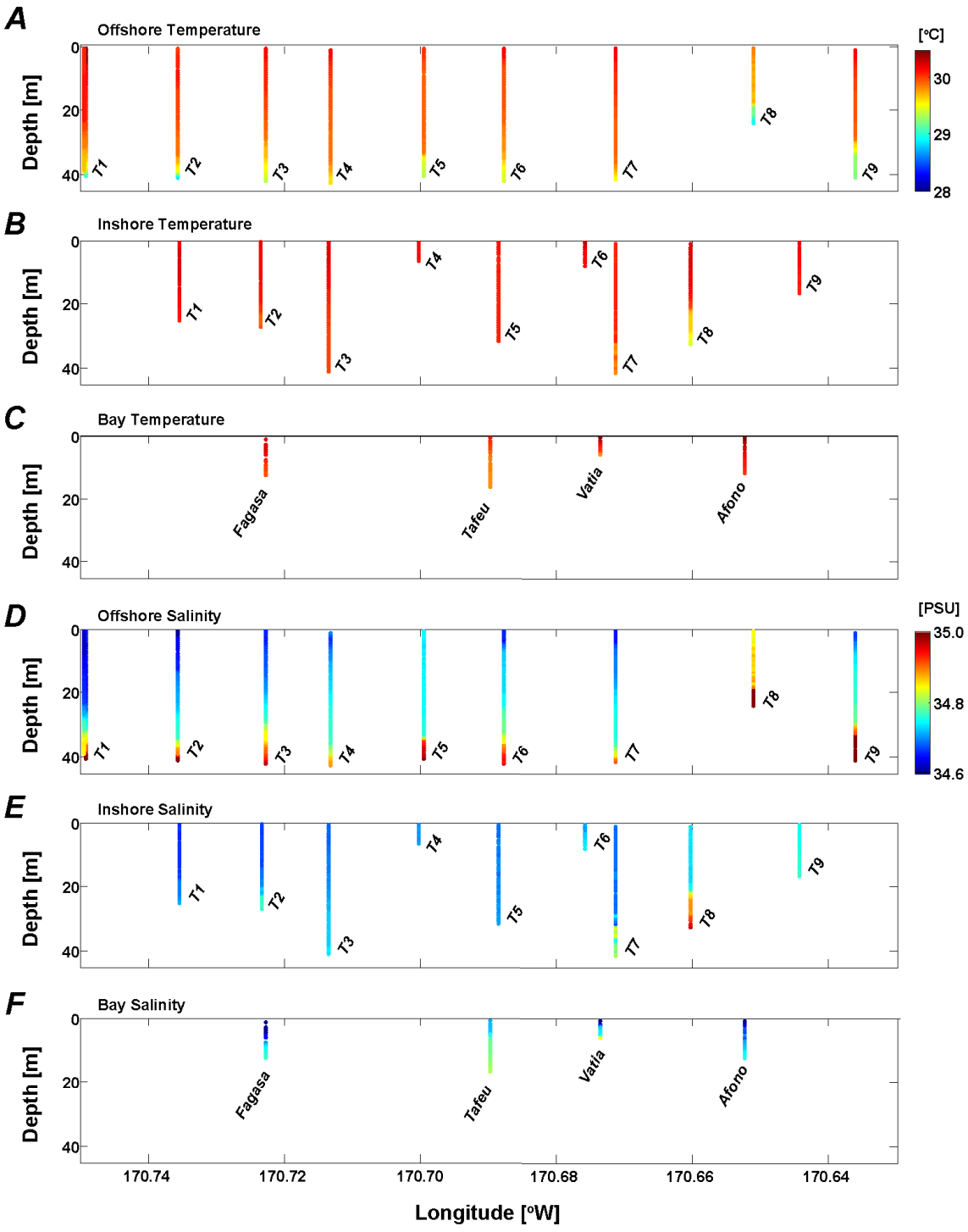

Figure 11–10. Individual vertical profiles by the water column profiler taken on Year Day 51 (20 February 2015), according to longitude in degrees west (left to right is west to east), with depth in meters (m) on y-axis. *A*, Offshore profiles of temperature in degrees Celsius (°C). *B*, Inshore profiles of temperature in degrees Celsius (°C). *C*, Bay profiles of temperature in degrees Celsius (°C). *D*, Offshore profiles of salinity in Practical Salinity Units (PSU). *E*, Inshore profiles of salinity in Practical Salinity Units (PSU). *F*, Bay profiles of salinity in Practical Salinity Units (PSU). Names of bays sampled are shown in panels *C* and *F*.

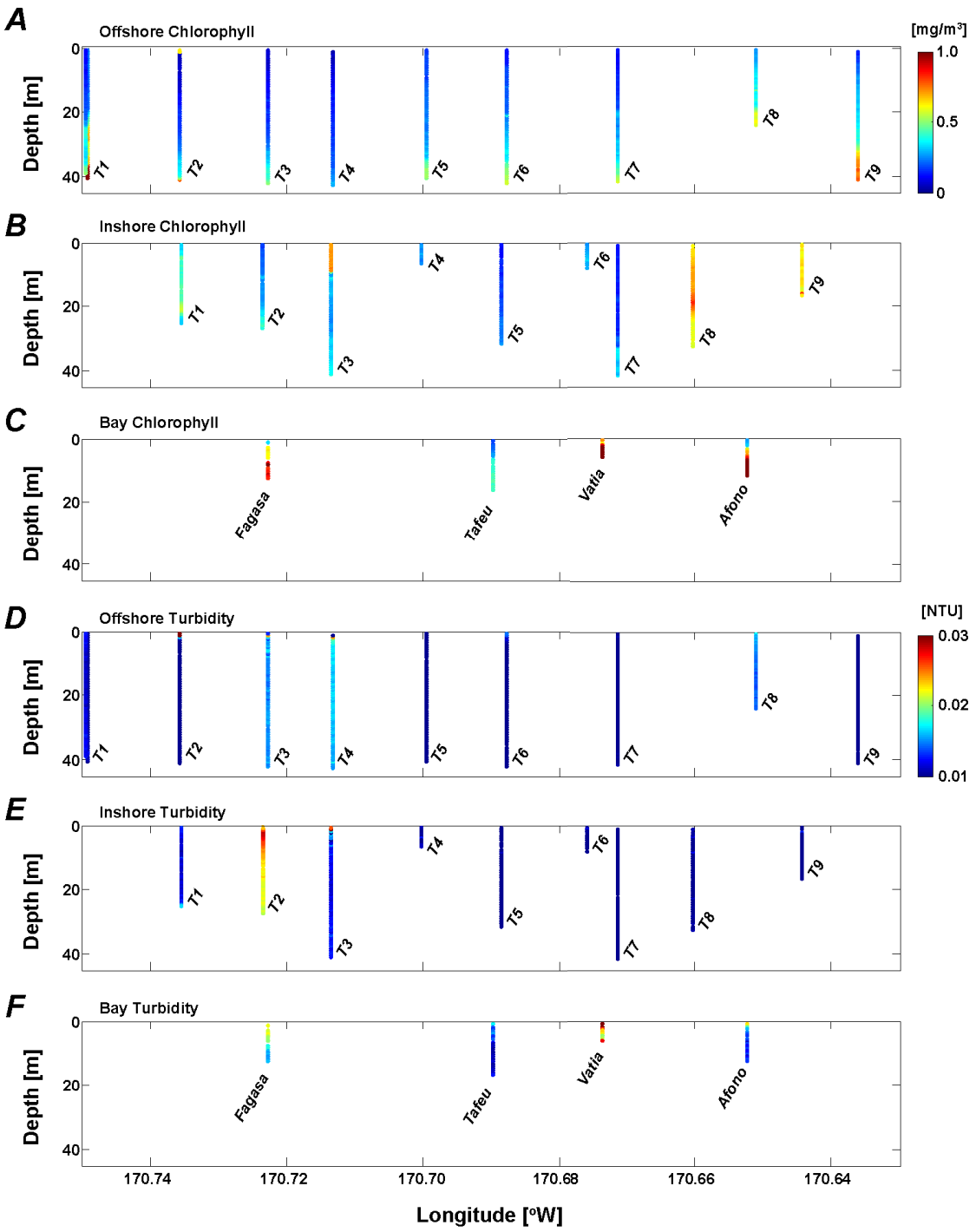

Figure 11–11. Individual vertical profiles by the water column profiler taken on Year Day 51 (20 February 2015), according to longitude in degrees west (left to right is west to east), with depth in meters (m) on y-axis. *A*, Offshore profiles of chlorophyll fluorescence in milligrams per cubic meter (mg/m^3). *B*, Inshore profiles of chlorophyll fluorescence in milligrams per cubic meter (mg/m^3). *C*, Bay profiles of chlorophyll fluorescence in milligrams per cubic meter (mg/m^3). *D*, Offshore profiles of turbidity in Nephelometric Turbidity Units (NTU). *E*, Inshore profiles of turbidity in Nephelometric Turbidity Units (NTU). *F*, Bay profiles of turbidity in Nephelometric Turbidity Units (NTU). Names of bays sampled are shown in panels *C* and *F*.

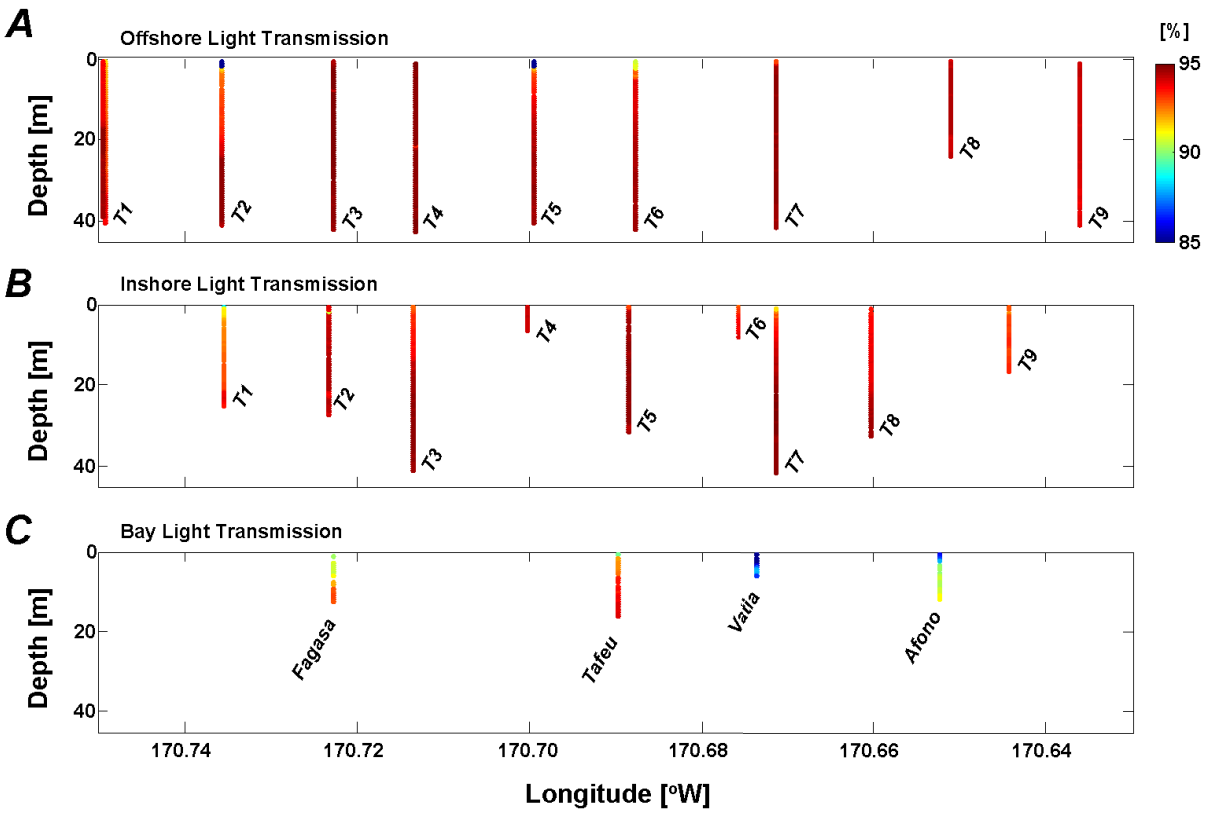

Figure 11–12. Individual vertical profiles by the water column profiler taken on Year Day 51 (20 February 2015), according to longitude in degrees west (left to right is west to east), with depth in meters (m) on y-axis. *A*, Offshore profiles of light transmission in percent (%). *B*, Inshore profiles of light transmission in percent (%). *C*, Bay profiles of light transmission in percent (%). Names of bays sampled are shown in panel *C*.

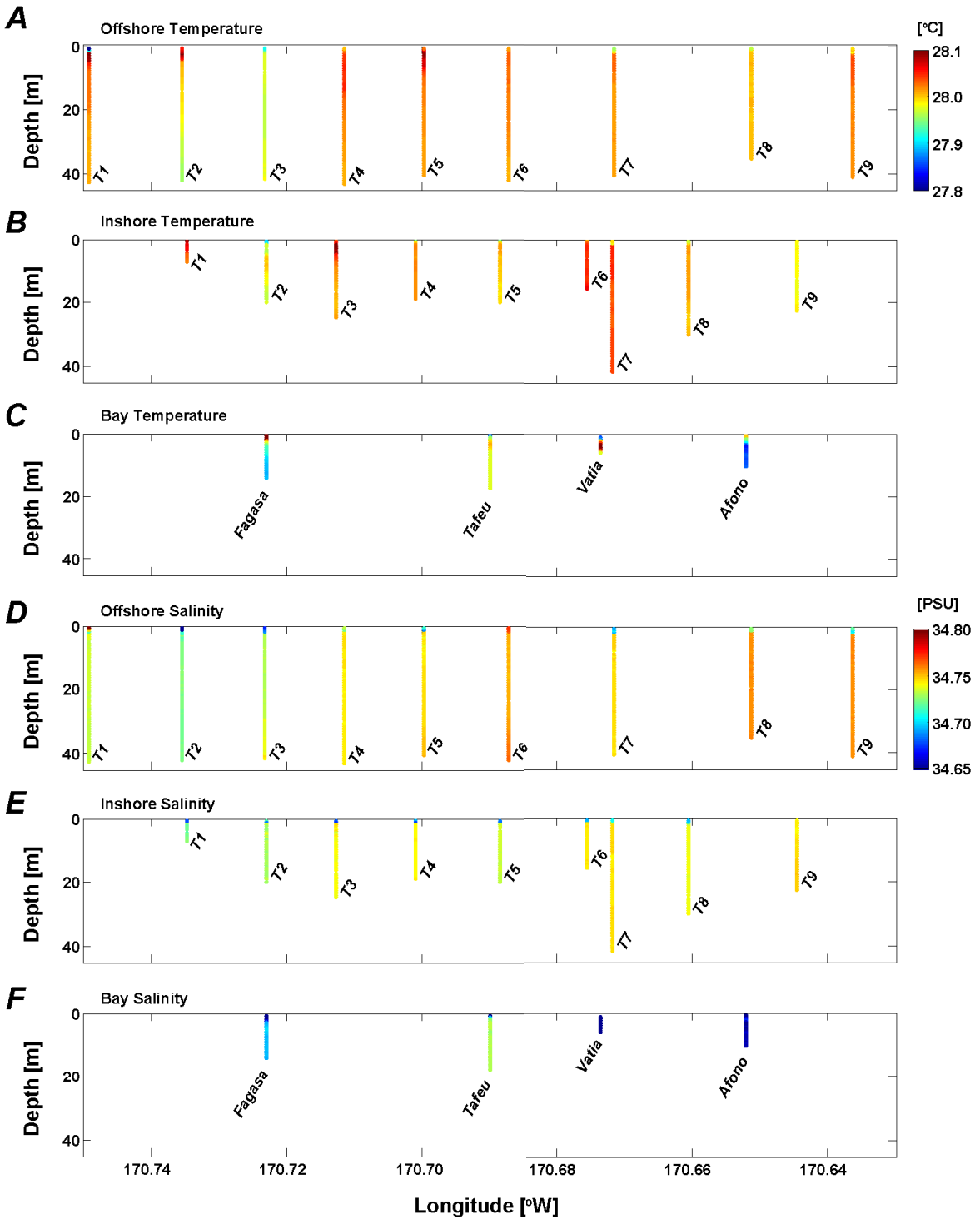

Figure 11–13. Individual vertical profiles by the water column profiler taken on Year Day 199(18 July 2015), according to longitude in degrees west (left to right is west to east), with depth in meters (m) on y-axis. *A*, Offshore profiles of temperature in degrees Celsius (°C). *B*, Inshore profiles of temperature in degrees Celsius (°C). *C*, Bay profiles of temperature in degrees Celsius (°C). *D*, Offshore profiles of salinity in Practical Salinity Units (PSU). *E*, Inshore profiles of salinity in Practical Salinity Units (PSU). *F*, Bay profiles of salinity in Practical Salinity Units (PSU). Names of bays sampled are shown in panels *C* and *F*.

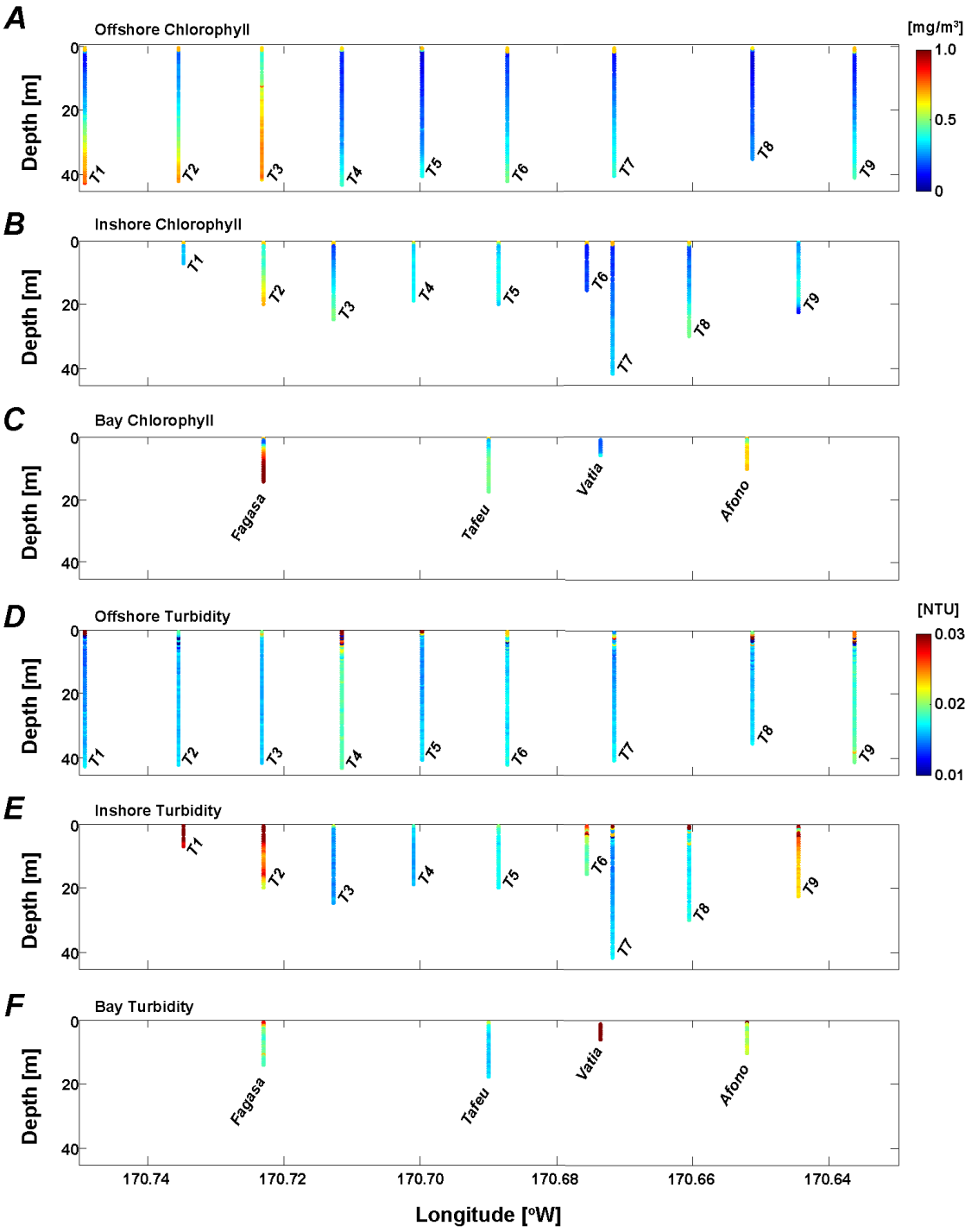

Figure 11–14. Individual vertical profiles by the water column profiler taken on Year Day 199 (18 July 2015), according to longitude in degrees west (left to right is west to east), with depth in meters (m) on y-axis. *A*, Offshore profiles of chlorophyll fluorescence in milligrams per cubic meter (mg/m^3). *B*, Inshore profiles of chlorophyll fluorescence in milligrams per cubic meter (mg/m^3). *C*, Bay profiles of chlorophyll fluorescence in milligrams per cubic meter (mg/m^3). *D*, Offshore profiles of turbidity in Nephelometric Turbidity Units (NTU). *E*, Inshore profiles of turbidity in Nephelometric Turbidity Units (NTU). *F*, Bay profiles of turbidity in Nephelometric Turbidity Units (NTU). Names of bays sampled are shown in panels *C* and *F*.

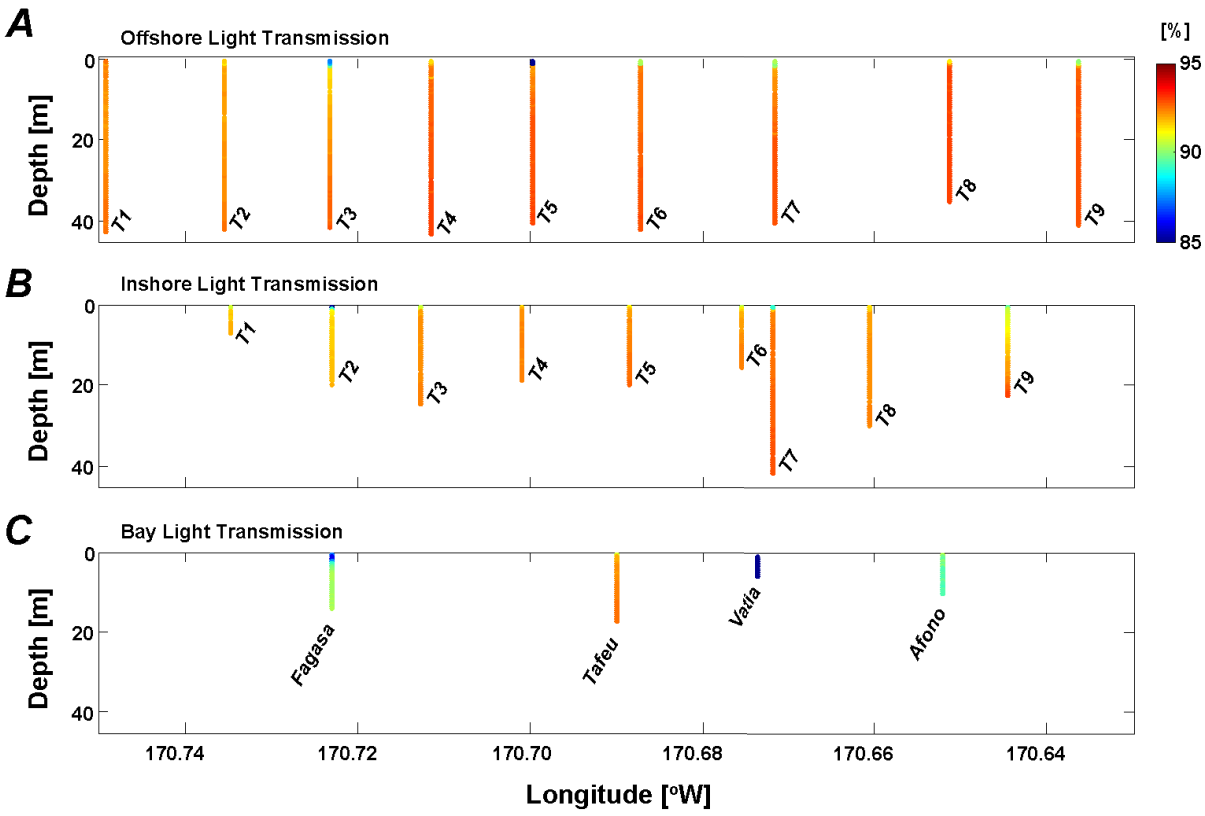

Figure 11–15. Individual vertical profiles by the water column profiler taken on Year Day 199 (18 July 2015), according to longitude in degrees west (left to right is west to east), with depth in meters (m) on y-axis. *A*, Offshore profiles of light transmission in percent (%). *B*, Inshore profiles of light transmission in percent (%). *C*, Bay profiles of light transmission in percent (%). Names of bays sampled are shown in panel *C*.